The effect of cytokinins on the metabolite secretome of *Giardia intestinalis* during trophozoite growth, nutrient deprivation, and encystation

A thesis submitted to the Committee of Graduate Studies

in partial fulfillment of the requirements

for the degree of

Master of Science

in the faculty of Arts and Science

Trent University

Peterborough, Ontario, Canada

Environmental & Life Sciences

M. Sc. Graduate Program

September 2023

ABSTRACT

The effect of cytokinins on the metabolite secretome of *Giardia intestinalis* during trophozoite growth, nutrient deprivation, and encystation

Vedanti Ghatwala

Giardia intestinalis is the causative agent of a diarrheal disease in mammals, but the mechanisms of disease pathogenesis are unclear. While proteins secreted by *Giardia* affect the host cells, the potential of hormone secretion has not been investigated to date. Cytokinins (CKs) are classified as phytohormones, but little is known about their role beyond plants. Mass spectrometry-based intracellular analysis revealed CKs typical of tRNA degradation, and extracellular analysis showed CK-riboside scavenging by *Giardia* with concurrent secretion of CK-free bases. Metabolomics profiling of culture supernatants showed similar trends where nucleosides were up taken, and nucleobases were secreted. The dynamics of amino acids, nucleosides and nucleobases were altered by CK-supplementation during encystation, along with inhibition of encystation. In summary, this is the first study to report CK synthesis and metabolism by Giardia along with the effects of CKs on the metabolite secretome of *Giardia*, while establishing a link between CK and nucleoside metabolism.

KEYWORDS: Giardia, cytokinins, beyond plants, nutrient deprivation, encystation, exogenous supplementation, synthesis, mass spectrometry, scavenging, secretion, metabolism, metabolites, secretome, tRNA degradation.

CONTRIBUTIONS

Dr. Anna Kisiala provided technical guidance and mentorship for experimental design, hormone and metabolite extractions, UHPLC-HRMS/MS analysis, along with editing of this thesis.

Ph.D. candidate Melanie Marlow provided technical help and guidance with reagent preparation and performing the western blot included in *Chapter 3*.

Dr. Erin Morrison provided guidance on BLAST search results included in *Chapter 2* and critical exchange of ideas that helped structure the discussion sections.

ACKNOWLEDGEMENTS

This M.Sc. was only possible with the help and support of many people, whom I would like to acknowledge. First of all, I want to sincerely thank my supervisors Dr. Janet Yee and Dr. Neil Emery for taking me on as a graduate student and providing this chance to pursue research. Janet, I owe you a big thank you for believing in my potential for this project when I reach out to you in undergrad. I still remember the day you asked if I was still interested in volunteering in your lab, since it was one of the happiest days of my life (I may have danced a little after you left!). I am filled with gratitude for your efforts in applying for the International Graduate Scholarship for me and making this M.Sc. financially possible. I greatly value your constant push and reminders to keep me motivated and on track to completion, along with your guidance and mentorship throughout the project. Thank you for also giving me multiple opportunities to attend conferences and boosting my confidence by your praises after a win. Neil, I cannot thank you enough for your humble support and understanding throughout my research career at Trent. The extent to which you recognize and aid the needs of international students of your lab is incredible. Your extra financial help throughout this degree not only kept me mentally at ease, but also made me into a better researcher by practicing technical skills. The amazing lab culture you have fostered, allowed me to develop invaluable friendships. Thank you for checking up on me in times of need and guiding me through life outside of research as well. The weekly lab meetings truly enhanced the research experience by inspiring me to think critically and continue learning. This leads me to thank all amazing lab members of both Yee and Emery labs for training, lending a helping hand, along with dulling my homesickness. I present my biggest thanks to my best friend first, science

buddy and committee member after, Dr. Anna Kisiala for being a backstage hero in this project. Your technical and intellectual contributions to this work have greatly promoted the success of this project. Everything I know to date, be it efficiency in lab work, critical thinking, way of learning, effective communication, being optimistic, and so much more, all have your foundational support. Without your involvement, the successful execution of the ambitious experimental plans would not have been possible.

I would also like to acknowledge the International Graduate Scholarship and Trent International bursaries for financial help during this thesis. Moreover, I thank Linda Cardwell from the ENLS office for many meetings to answer my numerous administrative questions and making the transition from an undergraduate to a graduate student, as smooth as possible.

Lastly but most importantly, I want to thank my mother Sheetal and my brother Himay for their countless sacrifices in support of my higher education. You have been through a lot, and you needed me the most these past few years but for my betterment, you suffered my absence. I cannot wait to reunite with you and hope for a peaceful and secure future, which I believe is within arm's reach.

TABLE OF CONTENTS

LIST OF FIGURES

LIST OF ABBRIVIATIONS

2-MeSiP	2-methylthio-N6-isopentenyladenine
aa	amino acid
ANOVA	analysis of variance
ATP	adenosine triphosphate
BA	N6-benzyladenine
BARP	N6-benzyladenosine-5'-monophosphate
BLAST	Basic local alignment search tool
C	celsius
CK	cytokinin
CRISPR/Cas9	clustered regularly interspaces short palindromic repeat/ CRISPR associated protein 9
cZ	cis-zeatin
DdLOG	*D. discoideum* Lonely Guy protein
DMAPP	dimethylallyl pyrophosphate
ENT	equilibrative nucleoside transporter
FB	free base
FS	full scan
h	hour
HPLC	high-performance liquid chromatography
HPLC-(ESI+)-HRMS/MS	high-performance liquid chromatography-positive electrospray ionization-high resolution tandem mass spectrometry
HPLC-(HRAM)-FS-MS	high performance liquid chromatography-high resolution accurate mass-full scan mass spectrometry
iP	N6-isopentenyladenine
IPP	isopentenyl pyrophosphate
iPR	N6-isopentenyladenine-9-riboside
iPRP	N6-isopentenyladenine-9-riboside-5'phosphate
IPT	adenylate isopentenyltransferase

m/z	mass-to-charge ratio
MEP	methylerythritol phosphate
MVA	mevalonate
n.d.	not detected
NO	nitric oxide
NT	nucleotide
PBS	phosphate buffered saline
pmol	picomole
ppm	parts per million
PRM	parallel reaction monitoring
PUP	purine uptake permease
SPE	solid phase extraction
TEM	transmission electron microscopy
tRNA	transfer RNA
tRNA-IPT	tRNA-isopentenyltransferase

CHAPTER 1

General Introduction

Giardia intestinalis is a protozoan parasite responsible for causing a food-water borne diarrheal disease called giardiasis in mammals (Adam, 2001; Einarsson et al., 2016). It is one of the most common diarrheal diseases worldwide with an estimated 280 million cases annually (Martínez-Gordillo et al., 2014). Moreover, the high prevalence of giardiasis in developing countries is a major cause of illness, stunted growth and even death in children under 5 years of age (Adam, 2021). Giardiasis comes with a wide variety of symptoms among infected individuals; however, the disease-causing factors (virulence factors) that are involved in symptom development are not well known (Carranza & Luján, 2010). Moreover, giardiasis can range from being asymptomatic to acute or manifest as chronic symptoms of the disease with post infection issues like irritable bowel syndrome (Singer et al., 2020). A widely used medication to treat giardiasis is metronidazole, which is an antibiotic and antiprotozoal drug (Adam, 2021). Although metronidazole is mostly effective, up to 10 – 20 % of cases have shown treatment failure (Tejman-Yarden et al., 2011). Thus, it is crucial to fill the gap of knowledge about the virulence factors used by Giardia to cause giardiasis, and to investigate potential new Giardia-specific drug targets.

Virulence factors are proteins or small molecules secreted by a pathogen that impact the host cell (Kaur et al., 2001). Proteins and enzymes secreted by Giardia in the presence and absence of mammalian intestinal epithelial cells have been previously identified (Ma'ayeh et al., 2017), but the secretion of other small signaling molecules like hormones have not been studied. Cytokinins (CKs) are one such group of small signaling molecules

first identified for their diverse roles in plant growth and development (Powell & Heyl, 2023). Subsequently, phytopathogens like bacteria and fungi were found to synthesize CKs to help establish infection within the host plant (Spallek et al., 2018). More recently, the presence and roles of CKs discovered in non-phytopathogenic bacteria and protists (Andrabi et al., 2018; Samanovic et al., 2018) prompted us to hypothesize that Giardia can synthesize and metabolize CKs and interact with the host through scavenging and secretion of these molecules.

Giardia intestinalis

Giardia is a unique, early branching eukaryote that lacks certain typical eukaryotic organelles like mitochondria, peroxisomes and a stacked Golgi complex (Carranza & Luján, 2010; Morrison et al., 2007). Giardia exists in two different life forms – a dormant and infectious cyst that can survive outside of a host; and a vegetative, tear drop shaped trophozoite cell found only in the digestive tract of mammals (*Figure 1.1*) (Einarsson et al., 2016; Luján & Svärd, 2011). In its trophozoite form, Giardia is flagellated, binucleated, and contains a distinct ventral disc that facilitates the attachment of trophozoites to the surface of intestinal epithelial cells (Rodríguez-Fuentes et al., 2006). In its cyst form, two trophozoites are encased within a thick cyst wall that provides protection against hostile external environments and enables its transmission into new hosts (Adam, 2021; Luján et al., 1997).

Giardia infection begins once a mammalian host ingests cysts through contaminated food or water. Proteases and the low pH in the stomach cause each cyst to break open and release two trophozoites (Boucher & Gillin, 1990; Schupp et al., 1988).

The proliferation of Giardia trophozoites in the intestinal tract, and their interaction and exchange of a range of proteins and enzymes with the intestinal epithelial cells contributes to disease symptom development (Dubourg et al., 2018; Kaur et al., 2001; Lee et al., 2012; Ma'ayeh et al., 2017; Rodríguez-Fuentes et al., 2006; Shant et al., 2002). Due to its parasitic lifestyle, Giardia is an auxotroph for many small molecules such as amino acids, nucleosides and nucleobases are needed as raw material for DNA synthesis, and thus, solely depends on scavenging these molecules (Adam, 2021; Morrison et al., 2007). During infection, some trophozoites detach and swim further down in the intestinal tract where exposure to a higher concentration of bile salts and alkaline pH lead to encystation – a crucial process that involved encasing the parasite in a thick cyst wall to enhance long term survival outside the host (Einarsson, Troell, et al., 2016; Frances D. Gillin et al., 1987; Kane et al., 1991).

Encystation of Giardia from trophozoites can be induced in axenic laboratory cultures and have been used for transcriptomics and proteomics analysis to study biochemical changes required for the differentiation of the parasite (Balan et al., 2021; Birkeland et al., 2010; Faghiri & Widmer, 2011; Faso et al., 2013; Rojas-López et al., 2021). However, the dynamics of extracellular metabolites including signaling molecules like CKs have not been studied during encystation of Giardia. This lack of knowledge is critical to address since encystation occurs inside infected hosts, the secreted small molecules during this differentiation process may affect physiology and response of host cells to the infection.

Cytokinins

Cytokinins (CKs) are a group of hormones initially referred to as phytohormones because of their initial identification as important factors in plant growth and development processes including cell division, senescence, organogenesis, and many others (Hluska et al., 2021; Kamada-Nobusada & Sakakibara, 2009). The investigation of the presence and role of CKs in species beyond plants began soon after their discovery in bacteria (Hughes & Sperandio, 2008). Since then, the presence of CKs has been documented in all domains of life except Archaea (Palberg et al., 2021); although recent research by our group suggest that some Archaea species may be capable of CK synthesis (unpublished).

Structurally, CKs are adenine derivatives that possess an isoprenoid or an aromatic side chain at the N^6 position (*Figure 1.2*) (Sakakibara, 2006). The biosynthesis pathway of isoprenoid CKs is well documented in model organisms of different phyla (Anand et al., 2022; Andrabi et al., 2018; Andreas et al., 2020; Aoki et al., 2019; Oslovsky et al., 2020; Othman et al., 2016; Rahman, 2019; Samanovic & Heran, 2015; Sarkar et al., 2023) but little is known about the origin of the aromatic CKs, like Benzyladenine (BA) and its derivatives (Aoki et al., 2019; Naseem et al., 2020; Sáenz et al., 2003). Isoprenoid CKs either arise from the isopentenyl transferase (IPT)-catalyzed N^6-prenylation of adenine mono-, di-, or tri-phosphate nucleotides (adenylate pathway) or the tRNA-IPT-catalyzed N^6-prenylation of the 37^{th} adenine nucleotide on the tRNA molecule (tRNA pathway) (*Figure 1.2*). The prenyl chain is donated by the isopentenyl pyrophosphate (IPP) or the isomer dimethylallyl pyrophosphate (DMAPP) which is a major intermediate for isoprenoid synthesis. The adenylate pathway is the primary CK source in plants whereas the tRNA-pathway is more prevalent pathway in non-plant species. In both pathways, the

prenylated nucleotide (NT) CKs are the precursor molecules that can be converted to their riboside (RB) derivatives by removal of the phosphate group catalyzed by ribonucleotide phosphohydrolases (Gibb et al., 2020) and subsequently, from the RB to the free base (FB) derivative by the removal of ribose by adenosine nucleosidases (*Figure 1.2*; Kamada-Nobusada & Sakakibara, 2009). The NTs can also be directly converted to FBs by a phosphoribohydrolase called the Lonely Guy (LOG), which is conserved among different classes of organisms including plant and animal pathogens (Naseem et al., 2020).

Research Objectives

To our knowledge, CKs in Giardia have never been reported nor studied. Since CKs are thought to be present in all forms of life, our group hypothesized that Giardia produces and metabolizes different forms of CKs either for its own growth and development or to influence its host. Preliminary experiments on CKs in Giardia and its culture medium (Hubert, 2020), demonstrated a need to optimize the detection of CKs in Giardia cultures. After modifications of the sample collection and extraction process, accurate and replicable detection of CKs within Giardia trophozoites and its complex culture medium was accomplished (Vedanti, 2021).

The aim of this thesis was to investigate Giardia's ability to produce and process CKs by the following objectives:

1. Determine ability of Giardia trophozoites to produce or process CKs and respond to various exogenously supplied benzyladenine (BA) type CK forms. BA-CKs were used as a marker since the complex growth medium TYI-S-33 used for in-vitro culturing of Giardia is already rich in natural isoprenoid CKs. Growth responses of

exogenously applied CKs were monitored as indicators of any beneficial or detrimental effects on trophozoite proliferation.

2. Examine if CKs are growth promoting factors for Giardia trophozoites. To address this, isopentenyl adenine (iP) type CKs was added to Giardia cultures in DMEM (Dulbecco's Modified Eagle Medium), where Giardia can remain viable for up to 24 hours, but they cannot grow and divide. Giardia cultured in DMEM with and without CK supplementation were compared for cellular motility and attachment as well as growth rate. To examine more subtle effects, metabolomics analysis of CK-rich growth medium (TYI-S-33) and CK-poor medium (DMEM) along with spent media after incubation with trophozoites were performed to characterize the metabolism pathways of Giardia that are based on exchange of small molecules between trophozoites and media.

3. Finally, to fully understand the extent of CK involvement in Giardia's life cycle, CK profiling along with metabolomics analysis was performed during differentiation of Giardia trophozoites into dormant cysts. Changes in metabolites help gain hints regarding the metabolism of encysting trophozoites and relationship to exogenously applied aromatic CKs.

FIGURES

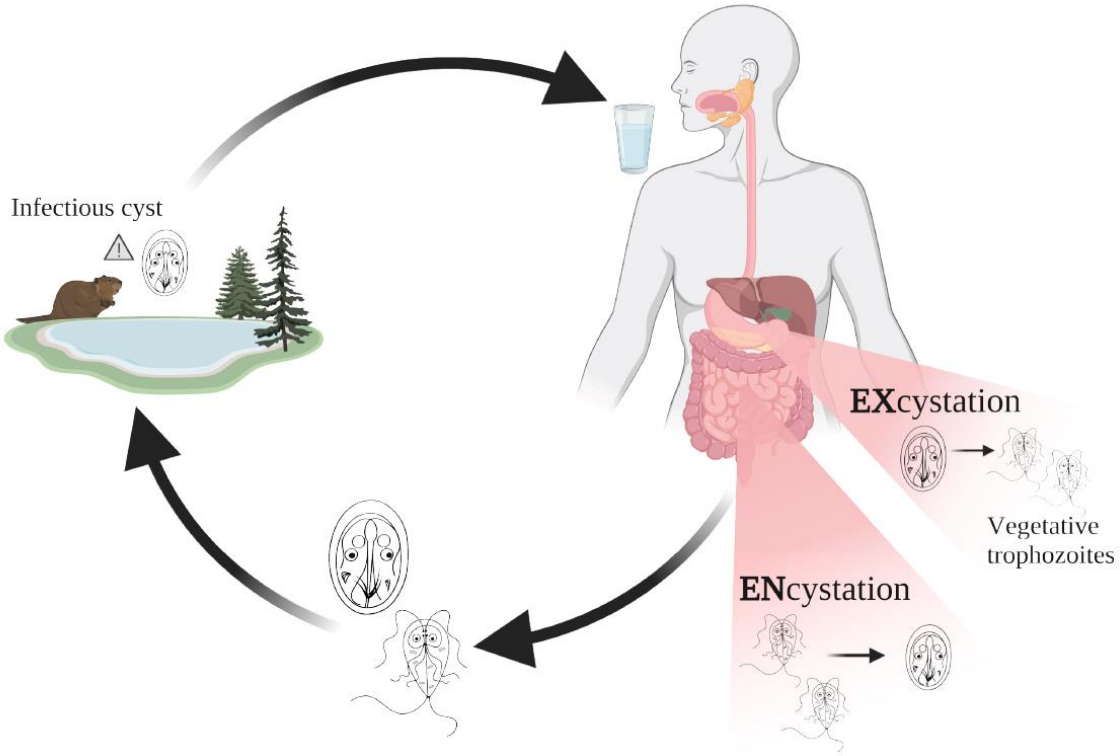

Figure 1.1: *Life cycle of Giardia intestinalis. Ingestion of dormant cysts initiates infection followed by disease establishment by motile trophozoites. Under adverse conditions, trophozoites differentiate back into dormant cysts and are excreted to continue the infectious cycle in another host. Figure created using Biorender.com.*

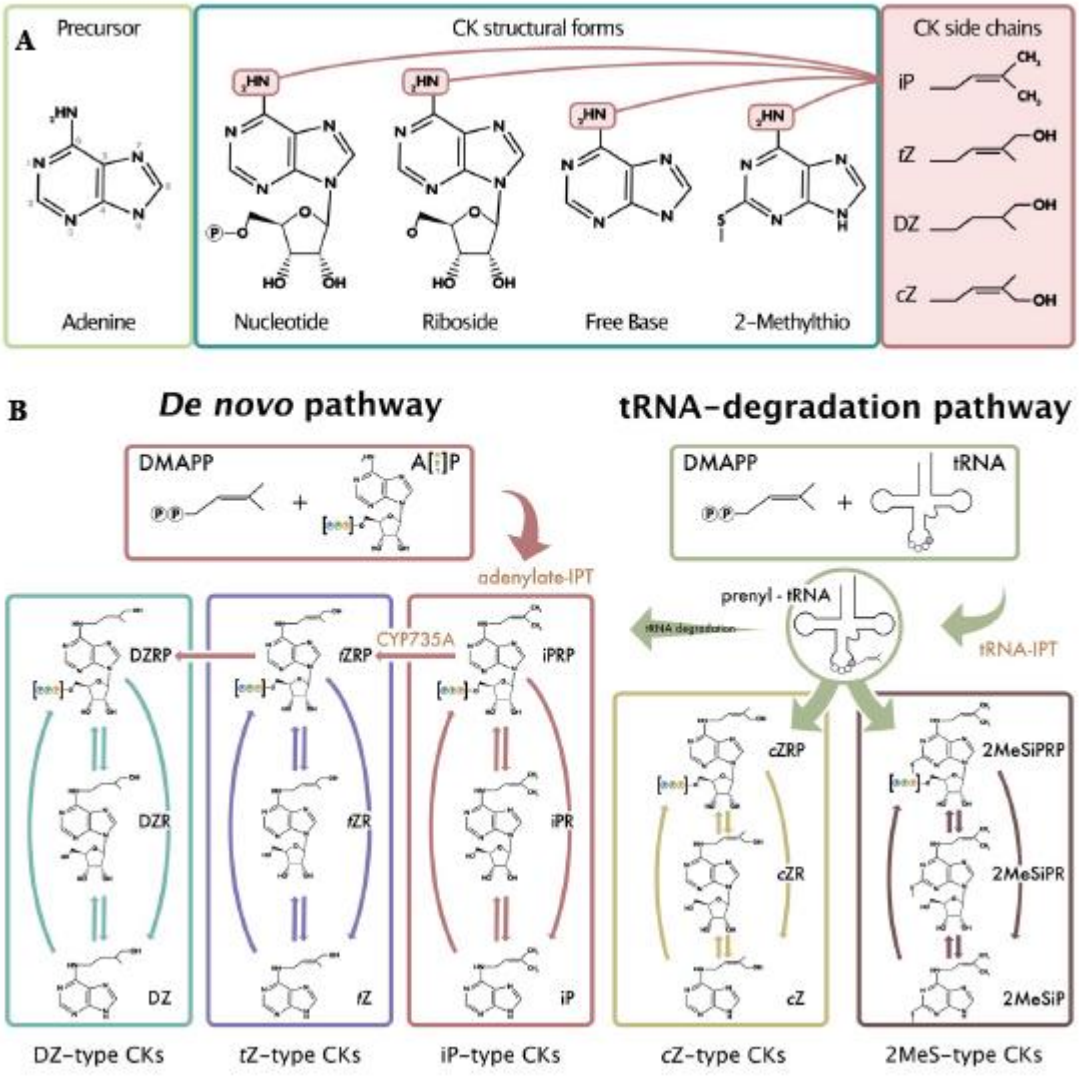

Figure 1.2*:Isoprenoid CK structures and simplified isoprenoid CK biosynthesis pathway based on plant, bacterial and fungal models* (Aoki, 2023). *(A) common CK forms and isoprenoid side chains. (B) two different CK pathways: de novo pathway that receives prenyl chain donor typically produced from methylerythritol phosphate pathway, and the tRNA degradation pathway that utilizes the prenyl chain donor dimethylallyl pyrophosphate (DMAPP) from the mevalonate pathway. Arrows represent enzymes responsible for interconversion of CK forms.*

CHAPTER 2

Cytokinin synthesis and metabolism by *Giardia intestinalis* during growth and nutrient deprivation

ABSTRACT

Giardia intestinalis is a protozoan parasite responsible for the diarrheal disease in mammals called ‘beaver fever’, but the mechanisms of disease pathogenesis are unclear. While proteins secreted by *Giardia* can affect the host cells, hormones produced or secreted by *Giardia* are unknown. Cytokinins (CKs) are adenine-derived signaling molecules classified as phytohormones. Recently, CKs were detected across multiple kingdoms due to the high conservation of the tRNA degradation pathway for CK synthesis. Moreover, Giardia's in-vivo and in-vitro environments are rich in CKs so it also possible that Giardia could metabolize extracellular CKs. Therefore, a metabolomics approach was used to gain biochemical insights into the role of CKs in Giardia. Liquid chromatography-high resolution mass spectrometry methods were developed to detect CKs at picomolar levels along with untargeted, abundant metabolites from a single sample. It was found that *Giardia* trophozoites can synthesize CKs likely originating from tRNA degradation. Moreover, they can convert extracellular CK ribosides into their presumed-active CK free base forms, irrespective of growth or nutrient deprivation conditions. However, exogenous CK supplementation of a minimal medium did not affect Giardia's growth, so it is unlikely that CK have a growth-regulating role in this protist. Finally, similarities were identified between the metabolism of CKs and other common small molecules which implied that Giardia must possess mechanisms for CK scavenging and secretion.

INTRODUCTION

Giardia intestinalis virulence

Giardia intestinalis is a parasitic protist that infects mammals by causing a diarrheal disease prevalent worldwide (Adam, 2021). Virulence factors responsible for disease establishment by Giardia trophozoites are not well understood (Dubourg et al., 2018). Unlike intracellular parasites such as those responsible for malaria and toxoplasmosis, Giardia attaches to the surface of the host's intestinal epithelium but does not enter the host cells (Kaur et al., 2001). Since Giardia lacks de-novo synthesis of most essential components needed for growth and differentiation, it relies on scavenging necessary nutrients from the host intestinal lumen (Morrison et al., 2007). Giardia also secretes molecules into the host environment, which could range from large proteins and enzymes for metabolism of extracellular nutrients for easier up-take (Ma'ayeh et al., 2017), to small molecules that are end products of cellular metabolism (Adam, 2021). Recent studies proposed that various secretory proteins act as virulence factors for disease establishment and host immune response modulation by Giardia (Dubourg et al., 2018; Kaur et al., 2001; Piña-Vázquez et al., 2012; Ringqvist et al., 2008), but little information exists on the secretion of small molecules that could act as effectors or hormones for host-parasite interaction (Hughes & Sperandio, 2008; Kendall & Sperandio, 2016; Sperandio et al., 2003).

Giardia was proposed to be incapable of hormone production due to absence of enzymes for cholesterol biosynthesis (Jarroll et al., 1981). Although a later study supported the inability of Giardia to synthesize cholesterol, the initial steps of sterol synthesis by

versatile intermediates called isoprenoids were identified (Lujan et al., 1995), and another study detected the transcriptional activity of genes involved in isoprenoid synthesis (Hernandez & Wasserman, 2006). Isoprenoids are indispensable for all organisms as they are essential for growth and development, along with roles in in diverse cellular processes such as: cholesterol and lipid synthesis for plasma membrane stability; protein isoprenylation for protein stability; or tRNA prenylation for enhanced translation fidelity (Hoshino & Gaucher, 2018; Lujan et al., 1995). For Giardia, cholesterol synthesis is still questionable but limited lipid synthesis is possible (Yichoy, 2009) along with proven protein isoprenylation (Lujan et al., 1995). Although tRNA prenylation was never reported for Giardia, the genome possesses a transcriptionally active gene for tRNA-isopentenyl transferase (tRNA-IPT; Giardia DB: GL50803_0017480), an enzyme that catalyzes the N^6 prenylation of the 37^{th} adenine nucleotide on the tRNA within the parasite (Rojas-López et al., 2021). The presence of tRNA-IPT in Giardia strongly suggests that it can synthesize CKs (*Figure 2.1*). In most organisms, the degradation of prenyl-tRNA leads to free N^6-prenyl adenine-based small hormone-like molecules called isoprenoid cytokinins (CKs) (Dabravolski, 2020). When mammalian tissues were screened for CK presence, the small intestine containing bile secretions was one of the three major CK-containing regions (Seegobin et al., 2018). The CK profile of the in-vitro growth medium of Giardia (TYI-S-33) had a CK profile resembling the CK profile of the mammalian small intestine, which is also the in-vivo environment of Giardia (Aoki et al., 2021; Hubert, 2020; Vedanti, 2021). This suggests that Giardia must have the ability to process extracellularly available CKs.

Cytokinins beyond plants

The role of CKs in plant systems is extensively documented but information about roles in organisms outside of the plant kingdom is limited. There is evidence of a highly conserved gene encoding the enzyme tRNA-IPT that is involved in the first step of production of CKs among a large variety of organisms; from microbes to humans (Nishii et al., 2018). Thus, many recent studies have highlighted the presence and potential roles of CKs in organisms of different kingdoms, for instance:

1) A soil dwelling, free-living protist with plant-like features *Dictyostelium discoideum* is known to produce CKs mainly through the adenylate pathway. When an adenylate-IPT knockout mutant was produced, subtle phenotypes were observed with circular, reduced mitochondria resulting in an altered energy-related metabolome (Aoki, 2023). On the other hand, parasitic protists *T. gondii* and *P. berghei* that infect mammal and rodents respectively, produce CKs for cell cycle progression and plastid replication within their plant-like apicoplast organelle (Andrabi et al., 2018).

2) Within non-phytopathogenic bacteria, the presence, and roles of CKs have recently been highlighted. An exclusive human-infecting bacterial pathogen *M. tuberculosis* seems to have a conserved tRNA degradation pathway for CK production, even though it has no close evolutionary relationship with plants (Samanovic & Heran, 2015). The initial products of tRNA degradation are CK-NTs, which are known substrates of the LOG enzyme found to be highly conserved through evolution. The LOG enzyme directly converts CK-NTs to CK-FBs, resulting in abundant CK-FB degradation products called aldehydes in *M. tuberculosis* (Zhu & Javid, 2015). Aldehyde abundance in the bacterium provides protection against oxidative stress caused by the host cells (Samanovic et al.,

2015). This function of LOG was characterized by a proteasome mutant which regulates LOG levels and subsequent aldehyde levels, eventually affecting oxidative stress response of the pathogen (Samanovic et al., 2015). Another human bacterial pathogen *B. pertussis* is also known to contain a LOG-like protein with involvement in oxidative stress response, which suggests that a similar mechanism to *M. tuberculosis* might be present in *B. pertussis* (Moramarco et al., 2019).

3) Human cells (HeLa) seem to produce CKs with unknown mechanisms while metabolizing extracellular CKs to their structural derivatives (Aoki et al., 2019) Specifically, iPRP, iPR, iP, 2MeS-iPR, 2Me-SiP, 2MeS-ZR, 2MeS-Z are produced, and all except iPRP are secreted. Moreover, an exogenously supplied aromatic CK – BAR was scavenged from the extracellular medium throughout a time course experiment while the respective FB form, BA, was secreted into the medium over time. In addition to HeLa cells, many other mammalian tissues and fluids were also reported to produce CKs (Seegobin et al., 2018). Beyond the discovery of CKs in non-plant organisms, there is limited understanding about the effects of CKs on animal cells. Animal cells and tissues have a biphasic response to exogenously supplied CKs, for instance, low doses of CKs (Kinetin; <100 nM) provide protection against oxidative stress in many mammalian cells (Othman et al., 2016), while high doses cause DNA damage and cytotoxicity (Voller et al., 2019).

Research objectives

Based on the above-mentioned lines of evidence it can be hypothesized that CKs may possess a biological role in Giardia or its pathogenesis. With no previous reports about

CKs within Giardia, the aim of this work was to confirm the CK biosynthetic ability of Giardia trophozoites and propose a putative CK production pathway. Moreover, to fully understand the involvement of CKs within Giardia's biology and its interaction with the host cells, we investigated its ability to scavenge, process and secrete any CKs supplied to the in-vitro environment during trophozoite growth. In addition, this chapter explored the growth promoting potential of CKs in Giardia by adding CKs to a CK- and nutrient-poor culture medium. The latter was assessed by metabolomics analysis of the medium incubated with or without Giardia to understand the metabolism of trophozoites along with metabolite-level evidence about CK-induced metabolism by Giardia trophozoites in nutrient rich and nutrient limiting conditions in two separate experiments referred herein to as "growth condition" and "nutrient deprivation condition" respectively.

MATERIALS AND METHODS

Cell culture conditions

Giardia intestinalis trophozoites from the WB C6 clone (Assemblage A, ATCC 50803) were used in all experiments. Routine cultures were grown in modified TYI-S-33 medium supplemented with 10% equine serum (Keister, 1983) along with 11.4 mM L-cysteine and 0.57 mM L-ascorbic acid at 37°C within 16 mL screw-cap glass culture tubes. Cell counts were taken at various time points during the culture using an automated cell counter (ViCell XR cell viability analyzer, Beckman-Coulter) to construct growth curves. To test the effect of CKs as growth regulators, Giardia trophozoites were incubated in Dulbecco's Modified Eagle Medium (DMEM; 10564-011, Gibco) supplemented with 11.4 mM L-cysteine and 0.57 mM L-ascorbic acid for up to 21-h. DMEM is referred to as a 'maintenance medium' since trophozoites incubated in this medium stay motile, intact and at the same cell density for up to 24 hours before cell viability is affected. Trophozoites cultured in TYI-S-33 were washed and approximately 2.8×10^6 cells were inoculated in 7 mL screw-cap plastic culture tubes containing supplemented DMEM.

Cytokinin supplementation

For the trophozoite growth condition, the Giardia growth medium (TYI-S-33) was supplemented separately with three synthetic cytokinins (CKs; 1 μM each) – N^6-benzyladenine (BA), N^6-benzyladenine riboside (BAR) or N^6-benzyladenine-9-riboside-5' monophosphate (BARP) (OlChemIm Ltd.). The absence of endogenous BA, BAR and BARP in the TYI-S-33 medium facilitates clear tracking of these CKs and their

modifications over time. Moreover, since BA-type CKs are known to be active in a variety of biological systems (Aoki et al., 2019; Doležal et al., 2007; Ishii et al., 2003; Sáenz et al., 2003), they could also be tested as supplements for their effect on growth of Giardia trophozoites. To prepare stock solutions, CKs were solubilized in a minimal volume of 1 M NaOH and diluted with HPLC-grade methanol (CH_3OH) to obtain a stock solution (320 μM). Solutions were filter sterilized (Midi 0.2 μm PVDF centrifugal filter, Canadian Life Science) by centrifugation (3724 × g, 4°C, 4 minutes; Allegra X-14R, Beckman Coulter). To obtain a working concentration of 1 μM, 50 μL of each CK solution was added to respectively labeled 16 mL culture tubes containing trophozoites and to the medium never incubated with trophozoites (referred to as "medium-blank" from now on), at the 0-h time point. In the unsupplemented culture tubes 50 μL of methanol was added as the solvent control.

For the nutrient deprivation condition, the Giardia trophozoites were cultured in maintenance medium (DMEM) without CK supplementation and with supplementation with one of the iP-types CKs (iP, iPR, iPRP; OlChemIm Ltd.) at 1 μM inal concentration. The negligible level of iP-type CKs in DMEM facilitates the clear tracking of their modifications over time. Moreover, the TYI-S-33 CK profile is dominated by iP-type CKs. Therefore, supplementing the DMEM with iP-type CKs provide trophozoites with CKs found commonly in the growth medium (TYI-S-33). The iP-type CK solutions for DMEM supplementation were prepared similar to BA-type CKs.

Sample collection

The TYI-S-33 growth medium of Giardia contains organic components like casein peptone digest, yeast extract and equine serum that might contribute to background CKs (Aoki et al., 2021). Therefore, to determine the CK content of TYI-S-33 and the components that contribute to background CKs, 5 mL aliquots of TYI-S-33 with reducing equine serum concentrations from the normal 10% to 5, 3.75, 2.5, 1.25 and 0% were collected. In addition, 5 mL aliquots of TYI-S-33 with reducing peptone (casein peptone digest:yeast extract = 13:7 w/w) concentrations from the normal 30 g/L to 20, 10 and 0 g/L. Aliquots of these modified media were frozen in liquid nitrogen, lyophilized, and stored at -80°C until further analysis.

To examine the extracellular CK changes during trophozoite growth along with the fate of exogenously supplied BA-type CKs, three replicates of supernatants were collected at various time points from each of the unsupplemented TYI-S-33, and BA-, BAR- and BARP-supplemented cultures. All tubes were chilled on ice for 15 minutes to detach the trophozoites, and centrifuged (2200 × g, 4°C, 15 minutes) for collection of 5 mL of supernatant from each sample. Medium-blanks (medium never exposed to trophozoites) were collected as negative controls for extracellular CK levels at the beginning and end of the time course study. All samples were frozen in liquid nitrogen, lyophilized, and stored at -80°C until further processing.

The above-mentioned experiment was repeated for 1 μM BAR supplementation of TYI-S-33 to measure intracellular CKs. Cell pellets were collected at the early stationary phase of growth (1×10^6 cells/mL). Ten 16-mL culture tubes were pooled to produce a single pellet sample ($9.8 \pm 3.5 \times 10^7$ cells) for hormone extraction. The resulting pellets

were washed three times in phosphate-buffered saline (PBS) to remove any residual culture medium. After the final wash, triplicate cell counts were performed for each cell resuspension before centrifuging again to remove residual PBS. The weights of semi-dry pellets were recorded before storage at -80°C. The collection was repeated thrice to obtain three cell pellet replicates from both unsupplemented and BAR-supplemented cultures.

To examine the extracellular CK changes during nutrient deprivation of trophozoites along with the fate of replenished iP-type CKs, three replicates of supernatants were collected at various time points from each of the unsupplemented TYI-S-33), unsupplemented DMEM, and DMEM supplemented with a 1 µM mix of iP, iPR and iPRP were collected as previously mentioned with the following difference: 7 mL supernatant was collected from cultures incubated in DMEM containing cultures whereas 5 mL was collected for cultures incubated in TYI-S-33.

Cytokinin extraction and purification

A hormone extraction and purification protocol (Aoki et al., 2021) was used for CK extraction from TYI-S-33 medium with varying composition, medium-blanks, supernatants (unsupplemented and BA, BAR and BARP-supplemented TYI-S-33 cultures) and cell pellet samples (unsupplemented and BAR-supplemented TYI-S-33 cultures). Cold (-20^{o}C) Bieleski #2 extraction solvent (1mL; CH_3OH:H_2O:HCO_2H = 15:4:1, v/v/v) was added along with 10 ng of ^{2}H-labeled CK internal standards. Samples were homogenized by vortexing, and cell pellets were grinded using 2 mm ZrO_2 beads (Comeau Technique Ltd.) and tissue homogenizer (MM300 Retsch; 5 min at 25 Hz). All samples were allowed to further extract passively at -20°C overnight.

The following day, extracts were removed by centrifugation (10 min, 11,180 × g; Sorvall ST 16, Thermo Scientific) and residue was re-extracted using 1 mL of Bieleski #2 solvent for 30 minutes at -20°C. The combined 2 mL samples were dried overnight in a speed vacuum concentrator (Savant SPD111V, Thermo Fisher Scientific). Dried residues were reconstituted in 1 mL of 1 M HCO_2H to ensure complete CK protonation and centrifuged at 11,180 × g for 10 min. Isolation and purification of CK forms out of the sample matrix was performed on mixed-mode, cation-exchange, solid phase extraction (SPE) columns (MCX 6cc/500mg, Canadian Life Sciences) using a vacuum manifold. The MCX columns were activated with 10 mL of analytical grade CH_3OH and equilibrated with 10 mL of 1 M HCO_2H. Crude samples were allowed to pass through by gravity followed by a wash step with 10 mL of 1 M HCO_2H and 10 mL of CH_3OH.

Cytokinins were eluted based on their charge and hydrophobicity. Cytokinin nucleotides (NTs) were eluted first using 5 mL 0.35 M NH_4OH, followed by elution of the ribosides (RBs) along with freebases (FBs) using 5 mL 0.35 M NH_4OH in 60% CH_3OH. MCX fractions were evaporated in a speed vacuum concentrator to dryness. The NTs were further processed by redissolving dried residues in 1 mL of 0.1 M ethanolamine (pH 10.8) and adding 3 units of alkaline phosphatase (calf intestine alkaline phosphatase; New England Biolabs) to catalyze NT dephosphorylation into their respective RB forms. The samples were incubated at 37°C overnight followed by drying in a speed vacuum concentrator. The dried residues were reconstituted in 1.5 mL Milli-Q H_2O and centrifuged for 10 min at 11,180 × g. The resulting RBs were further purified on C18 columns (C18 6cc/500mg; Canadian Life Sciences)**.** The C18 columns were activated using 3 mL CH_3OH and equilibrated with 6 mL Milli-Q H_2O. Samples were allowed to pass through the column

resin by gravity, followed by a wash with 3 mL Milli-Q H_2O. The purified RB derivatives were eluted using 1.25 mL CH_3OH:H_2O (80:20 v/v) and dried in a speed vacuum concentrator overnight. All residues were redissolved in 1.5 mL of initial mobile phase conditions (H_2O:C_2H_3CN:CH_3CO_2H = 95:5:0.08, v/v/v). Sample vials were stored at -20^oC until mass spectrometry analysis.

Cytokinin profiles of the TYI-S-33 samples with varying composition, medium-blanks, supernatants, and cell pellets were analyzed by the Ultimate3000 UHPLC system (Thermo Scientific) coupled with the Orbitrap QExactive mass spectrometer (Thermo Scientific) (Kisiala et al., 2019). Separation of CKs was achieved by using Kinetex C18 HPLC column (2.1 x 50 mm, 2.6 µm; Phenomenex). This included: 28 CKs [cis-zeatin (cZ), cis-zeatin riboside (cZR), cis-zeatin-9-glucoside (cZ9G), cis-zeatin nucleotide (cZRP), cis-zeatin O-glucoside (cZOG), cis-zeatin riboside-O-glucoside (cZROG), dihydrozeatin (DZ), dihydrozeatin nucleotide (DZRP), dihydrozeatin-O-glucoside (DZOG), dihydrozeatin riboside (DZR), dihydrozeatin riboside-O-glucoside (DZROG), dihydrozeatin-9-N-glucoside (DZ9G), isopentenyladenine (iP), isopentenyladenine nucleotide (iPRP), isopentenyladenine-7-glucoside (iP7G), isopentenyladenine-9-glucoside (iP9G), isopentenyladenosine (iPR), 2-methylthio-isopentenyladenine (2MeSiP), 2-methylthio-isopentenyladenosine (2MeSiPR), 2-methylthio-zeatin (2MeSZ), 2-methylthio-zeatin riboside (2MeSZR), trans-zeatin (tZ), trans-zeatin riboside (tZR), trans-zeatin-7-glucoside (tZ7G), trans-zeatin-9-glucoside (tZ9G), trans-zeatin nucleotide (tZRP), trans-zeatin O-glucoside (tZOG), and trans-zeatin riboside-O-glucoside (tZROG)]. A 25 µL sample aliquot was injected and all CKs were analysed in a single 8.2 min run (Kisiala et al., 2019) with a gradient of mobile phase A (0.08% CH_3CO_2H in H_2O) and

mobile phase B (0.08% $CH3CO_2H$ in C_2H_3OH) at a flow rate of 0.5 mL/min. The gradient was initiated at 5% B for 0.5 min, linearly increasing to 45% B over 4.5 min with a subsequent increase to 95% B over 0.1 min, a hold for 1 min, followed by an instantaneous drop to initial conditions (5% B) and a hold for 2 minutes for column re-equilibration. All CK analytes were detected in positive ionization mode using parallel reaction monitoring (PRM) mode. The HESI-II capillary temperature and auxiliary gas heater temperature were 250℃ and 450℃, respectively. Sheath, auxiliary and sweep gasses were operated at 30, 8 and 0 (arbitrary units), respectively, with a maximum spray current of 100 µA, spray voltage of 3.9 kV and S-lens RF level of 60. Data were acquired at a resolution of 35,000 at *m/z* 200 and precursor ions were isolated at m/z 1.2 window width, with automatic gain unsupplemented of 1×10^6 and maximum injection time of 128 ms.

Metabolite extraction and purification

Metabolomics was performed for the supernatants of the trophozoite nutrient deprivation condition for the unsupplemented TYI-S-33, unsupplemented DMEM and iP-type CK-supplemented DMEM. Metabolites from all lyophilized supernatants were extracted using cold 50% acetonitrile (ACN) and purified by SPE using HLB (hydrophilic lipophilic balance) cartridges as previously described with modifications (Šimura et al., 2018)**.** HLB extracts were evaporated to dryness and reconstituted in 500 µL of 90% ACN, 300 µL of which was transferred to insert equipped MS glass vials. Prior to ultra high-performance liquid chromatography-high resolution accurate mass-full scan mass spectrometry (UHPLC-(HRAM)-FS-MS) analysis, 20 µL of a stable isotope labeled canonical amino acid mix (0.25 µM; Cambridge Isotope Laboratories) was added to all

samples. Additionally, pooled mixtures containing 10-15 µL of each sample type (TYI-S-33, DMEM, DMEM+CK) were used to generate MS/MS for compound identification in data-dependent MS2 (ddMS2) mode. Samples were resolved with a Kinetex C18 column (2.1 × 50 mm, 2.6 µm). A volume of 25 µL of each sample was injected into a Dionex UltiMate 3000 HPLC (ThermoFisher) coupled to a QExactive Orbitrap mass spectrometer (ThermoFisher). A flow rate of 0.2 mL/min was used with a mobile phase of 0.08% acetic acid in water (A) and 0.08% acetic acid in acetonitrile (B). The following gradient was used to elute the analytes: mobile phase B was held at 0% for 1.25 min to retain the compounds on the column and avoid the metabolite elution in the void volume, before increasing to 50% over 2.75 min and to 100% over the next 0.5 min. Solvent B was then held at 100% for 2 min before returning to 0% over 0.5 min for 4 minutes of column re-equilibration. The Orbitrap QExactive was operated with a heated electrospray ionization (HESI) probe in positive and negative mode. Each sample was analyzed using a mass range of *m/z* 70−900, and data were acquired at 70,000 resolution, automatic gain unsupplemented (AGC) target of 1×10^6, and maximum injection time (IT) of 100 ms.

Since this was the first study evaluating the effects of CKs on the metabolite secretome of Giardia trophozoites during starvation, a global metabolomics approach was focused on a customized processing method that was used to query a list of over 100 exact metabolite masses as either $[M+H]^+$ or $[M-H]^-$ ions (*Table S 2.1*). Compound identification was based on the levels of confidence. Level 1 is highest confidence according to Schrimpe-Rutledge et al., (2016), obtained using comparison of retention times of compounds to authentic and labeled internal standards (authentic standards were a mix of unlabeled, high purity compounds for HPLC analysis including sugars, organic acids, and

amino acids; additionally, labeled internal standards included the mix of labeled amino acids as specified above). Level 2 is accurate precursor mass (10 ppm error) and comparison of fragmentation to MS/MS database (METLIN, PubChem). Level 3 is accurate precursor mass match to databases mentioned earlier. The relative normalized levels of metabolites were calculated based on the median recoveries of the labeled amino acid standards in each sample.

Data analysis

Cytokinin identification and quantification was done using Xcalibur software (ThermoFisher v.3.0.63). Quantification of CKs was performed by isotope dilution analysis based on the recovery of ^{2}H-labeled internal standards. Cytokinin concentrations for supernatant and medium-blank samples are expressed as pmol/mL, whereas for the cell pellet samples, CK concentrations are indicated as pmol/10^6 cells. Statistical significance of the data was assessed by one of the following: Multiple comparison t-test with FDR correction and two-way ANOVA, followed by Tukey's post hoc test (growth assays); one-way ANOVA, followed by Duncan's post hoc test (CK content in TYI-S-33 with varying serum or peptone concentrations), one-way ANOVA, followed by Dunnett's post hoc test (CK content in supernatants); or t-test (CK content in medium-blanks, CK content in cell pellets) using PRISM software (GraphPad Inc. v.9.5.1; p values < 0.05; n=3). All data points represent a mean of triplicate values with error range shown by standard error.

RESULTS

CK supplementation does not affect trophozoite growth

To test the effect of aromatic CK supplementation on Giardia growth, cell densities of Giardia trophozoites cultured in unsupplemented TYI-S-33 were compared to BA-, BAR- and BARP-supplemented (1 μM each) TYI-S-33 cultures. No significant differences were observed between cell densities of the unsupplemented and each of BA-, BAR- and BARP-supplemented cultures at any of the time points (0-, 10-, 30- and 50-h; *Figure 2.2 A; P>0.05;* Multiple comparison t-test with FDR correction). In all four culture types, similar growth phases were observed with trophozoite doubling time of 10-11 hours.

To determine if adding iP-type CKs to a low CK and low nutrient medium has beneficial or detrimental effect on cell growth, cell densities of trophozoites incubated in unsupplemented TYI-S-33, unsupplemented DMEM and CK-supplemented DMEM (iP, iPR, iPRP mixture; 1 μM) were compared. While trophozoites in the CK and nutrient rich TYI-S-33 medium showed increasing cell densities over time, the cell densities of trophozoites in DMEM and DMEM + CK cultures remained constant across the incubation period without any significant changes at any time points. These results suggest that CK-supplementation of DMEM with iP-type CKs did not promote or inhibit growth of trophozoites (*Figure 2.2 B*).

TYI-S-33 is CK-rich while DMEM is CK-poor, and profiles are stable in medium-blanks

Cytokinin levels of TYI-S-33 medium containing varying concentrations of either equine serum (0, 1.25, 2.5, 3.75, 5, and 10 %) or peptone (0, 10, 20 and 30 g/L) were analyzed to examine how the medium components contribute to the background CKs. Although not significant, increasing levels of total CKs were observed in TYI-S-33 with increasing concentrations of serum (*Supp. figure 2.1 A*). In contrast, TYI-S-33 containing peptone at varying concentrations showed significant increases in total CKs with increasing peptone concentrations (*Supp. figure 2.1 B*). Due to the relatively high abundance of CKs present in TYI-S-33, medium-blanks were analyzed at the 0-h and 50-h to ensure that the CK levels in the medium-blanks remained consistent throughout incubation.

In the TYI-S-33 medium-blanks, a total of eight CKs were detected, including three iP-type CKs: iP, iPR, and iPRP), four 2MeS-type CKs: 2MeSiP, 2MeSiPR, 2MeSZ and 2MeSZR, and one cZ-type CK: cZR (*Supp. table 2.2*). No significant differences were observed in the levels of CKs detected in the medium-blanks between 0 h and 50 h (t-test, $p > 0.05$). The CK profile of the medium-blank was dominated by iP-type CKs (iPR~iPRP>iP), followed by cZR (< 2.5 pmol/mL) and trace levels of four 2MeS-type CKs (< 0.2 pmol/mL) (*Supp. table 2.2*).

The BA-type CK-supplemented TYI-S-33 medium-blanks had a CK profile comparable to the unsupplemented TYI-S-33 medium-blanks. Additionally, the three aromatic CKs (BA, BAR and BARP) were detected in their respective supplemented media in highest abundance, while their derivatives were detected at considerably lower levels in BAR and BARP-supplemented samples (*Supp. table 2.3*). In the BAR-supplemented

medium-blanks, low levels of BA were detected at the 0-h time point, which remained constant over time (*Supp. table 2.3*). In the BARP-supplemented medium-blanks, trace levels of both derivatives, BA, and BAR, were detected at the 0-h time point. Notably, at the 50-h time point, the BAR concentration increased significantly while BA concentration did not change (*Supp. table 2.3*). This, along with the significantly decreased BARP level at the 50-h time point indicated that there was some non-biological degradation of BARP into its riboside (BAR) derivative over time likely due to instability of NT form (Martínez-García et al., 2002). The level of BA also increased significantly over time in the BA-supplemented medium-blanks. Although significant, the changes observed in the two supplemented CKs (BA and BARP) at the 50-h time point were no more than 25% of their respective original concentrations.

Compared to the TYI-S-33, unsupplemented DMEM contained negligible CKs, even with 10% serum addition. This was apparent by the presence of only three iP-type CKs (iP, iPR, iPRP) at relatively low concentrations (< 4 pmol/mL) (*Supp. table 2.4*). No other CKs were detected in this medium. In the unsupplemented and the iP-type CK-supplemented DMEM medium-blanks analyzed at 0- and 21-h, CK levels remained constant over the incubation period. In the unsupplemented DMEM, the three iP-types CKs (iP, iPR, iPRP) that were detected at low concentrations did not change over 21-h (*Supp. table 2.4; P> 0.05*). The iP-type CKs (iP, iPR and iPRP) supplemented to the DMEM medium-blanks were detected at the expected level (1 µM each) and remained constant over time (*Supp. table 2.4*).

CK-RBs are scavenged while CK-FBs are secreted by Giardia trophozoites during growth

To profile extracellular CKs, supernatants were collected from unsupplemented TYI-S-33 incubated with Giardia trophozoites at 10-, 30- and 50-h. Analysis of culture supernatants revealed that the presence of Giardia resulted in significant changes of most CKs that are normally present in TYI-S-33. The most prominent extracellular CK changes were the decrease of iPR, and the increase of its respective FB derivative, iP. The levels of iPR decreased from over 50 pmol/mL to below 0.5 pmol/mL after 50 hours of incubation with Giardia trophozoites. Inversely, iP levels increased from under 35 pmol/mL up to 100 pmol/mL during the same time course (*Figure 2.3 A*). In parallel, 2MeSiPR and 2MeSZR decreased from over 0.05 and 0.1 pmol/mL, respectively, to undetectable levels at the end of the time course, while the levels of their corresponding FBs, 2MeSiP and 2MeSZ, increased from under 0.06 pmol/mL up to 0.16 pmol/mL for both CKs (data not shown). A similar decreasing pattern was observed for cZR (2.48 ± 0.15 pmol/mL to 0.79 ± 0.06 pmol/mL); however, the FB derivative (cZ) was not detected. Levels of all CKs detected in the supernatants were significantly different between the 0-h and the end of the time course (One-way ANOVA, Dunnett's post hoc test; $p < 0.05$, n=3) except for iPRP which fluctuated insignificantly between 48 and 71 pmol/mL throughout the incubation period (*Supp. figure 2.2 A*).

Analyses of BA-type CK-supplemented culture supernatants revealed that the changes in isoprenoid CKs (iP-type, 2MeS-type and cZR) were similar to changes observed in unsupplemented trophozoite cultures (data not shown). In the BAR-supplemented culture, the most prominent change detected for the BA-type CKs was the decrease of BAR

with a simultaneous increase in BA concentration throughout the 50-h incubation period (*Figure 2.3 B*). The concentration of BAR detected at the 0-h time point and the concentration of BA detected at the 50-h time point did not differ statistically indicating that nearly 100% of BAR was converted to BA during the time course (t-test, $p < 0.05$, n=3). This transition between derivatives (RB to FB) mirrors the iPR and iP change observed in the unsupplemented culture. The BARP level in the BARP-supplemented culture supernatants fluctuated insignificantly throughout the time course with no more than 20% change at any time-point compared to the 0-h time point (*Supp. figure 2.2 D*). Some degradation of BARP to BAR was observed in the supernatants of this culture resulting in a significant increase of BAR at the 10-h and 30-h time points compared to the 0-h time point (*Figure 2.3 C*). At the 50-h time point, the BAR concentration dropped to a negligible level (< 0.7 pmol/mL). Inversely, BA concentration gradually increased with significant accumulation by 30 and 50 hours (*Figure 2.3 C*). Notably, at the 50-h time point, the level of BA detected in the BARP-supplemented culture supernatants (*Figure 2.3 C*) was not significantly different (t-test, $p > 0.05$, n=3) than the level of BAR detected in the BARP-supplemented medium-blank (*Supp. table 2.3*). This suggests that degradation of BARP to BAR must have been the same over time in the medium-blanks and supernatants; however, in the supernatants, the presence of Giardia resulted in the decrease of BAR and in turn, an increase of BA. This indicates a biological mechanism for the accumulation of BA observed in the BAR- and BARP-supplemented culture supernatants.

The BA concentration in the supernatants of BA-supplemented culture increased significantly by 15%, 34% and 17% at the 10-, 30- and 50-h time points, respectively, compared to the 0-h time point (*Supp. figure 2.2 C*). Although significant, BA changes in

the supernatants did not seem to be of biological origin because BA concentration also increased by 21% in the medium-blanks at the 50-h time point (*Supp. table 2.3*) and no other derivatives (BAR or BARP) were detected in the culture supernatants throughout the time course.

Giardia synthesizes nucleotide and free base CKs

Since BAR was the only supplemented CK that changed markedly over time in the presence of Giardia, cell pellets were collected from unsupplemented and BAR-supplementated TYI-S-33 cultures to profile CKs produced by Giardia. The cell pellet collection time corresponded to an early stationary growth phase of cultured trophozoites (1×10^6 cells/mL). Two iP-type CKs (iP and iPRP) detected extracellularly, were also detected within cell pellets from cultures with and without BAR-supplementation. It is notable that, while no dynamic change was observed in extracellular iPRP over time (*Supp. figure 2.2 A*), high concentration of iPRP was detected in cell pellets from both unsupplemented (4.68 ± 0.27 pmol/10^8 cells) and BAR-supplemented cultures (5.50 ± 0.63 pmol/10^8 cells). The FB form, iP, was detected at low concentrations (0.33 ± 0.04 pmol/10^8 cells and 0.65 ± 0.04 pmol/10^8 cells in the unsupplemented and BAR-supplemented cultures, respectively) and iPR was not detected. The levels of iP-type CKs (iP and iPRP) found intracellularly were not significantly different between the cell pellets collected from unsupplemented and BAR-supplemented cultures (t-test, $p < 0.05$, n=3). Additionally, two aromatic CKs - BA and BAR were detected in cell pellets from the BAR-supplemented cultures at 13.99 ± 4.92 pmol/10^8 cells and 6.67 ± 2.41 pmol/10^8 cells, respectively (*Supp. figure 2.3*).

CK-RBs are scavenged while CK-FBs are secreted by Giardia during nutrient deprivation

To profile extracellular CKs during trophozoite growth, supernatants were collected from cultures grown in unsupplemented TYI-S-33 as the nutrient-rich condition, while extracellular CK changes in nutrient deprivation condition were tested using supernatants from unsupplemented DMEM and iP-type CK-supplemented DMEM cultures. The CK dynamics observed during trophozoite growth were consistent with earlier observations (*Figure 2.4 A*).

In unsupplemented DMEM culture supernatants, minimal iP-type CKs were present as mentioned earlier for medium-blanks (*Supp. table 2.4*). Dynamics of iPR and iP observed during Giardia growth in TYI-S-33, were not observed for the unsupplemented DMEM culture. All changes in iP, iPR and iPRP were insignificant over the incubation period (*Figure 2.4 B*).

In the iP-type CK-supplemented DMEM culture supernatants (iP, iPR, and iPRP; 1 µM each), revealed iPR and iP dynamics that resembled observations of the growth condition. A gradual decrease in the RB form (iPR) from approximately 1000 pmol/mL at the 0-h time point to negligible level by 21-h, with concurrent increase in the FB form (iP) from approximately 1000 pmol/mL to approximately 2000 pmol/mL by the end of the time course (*Figure 2.4 C*). While dramatic changes in the RB and FB forms were observed in this culture, the nucleotide form (iPRP) remained relatively unchanged over time (*Supp. figure 2.2 B*), and this was similar to observations in growth condition (*Supp. figure 2.2 A, D*). Although trophozoite growth was not affected by the addition of CKs to DMEM (*Figure 2.2 B*), it is apparent that Giardia trophozoites are metabolizing extracellularly

available iPR and secreting iP when grown in a nutrient deprived condition. Moreover, comparing the iPR and iP concentrations at 0- and 21-h, revealed that the CK-RB to FB conversion efficiency of trophozoites is close to 100%, and this was comparable to iPR and iP changes in TYI-S-33 supernatants (*Figure 2.3 A, Figure 2.4 A*). This also suggests that the extracellular CK-riboside to freebase metabolism performed by Giardia seems to be dependent on the high extracellular CK concentrations.

Differential metabolite profile of unsupplemented media: TYI-S-33 vs DMEM

The metabolite profile of the TYI-S-33 compared to the DMEM has never been reported before. Since TYI-S-33 is a nutrient rich environment while DMEM has limited nutrients, it was expected that fewer metabolites be detected in DMEM compared to TYI-S-33. This is evident with greater abundance of metabolites in TYI-S-33 compared to DMEM (*Supp. figure 2.4*). Interestingly, some metabolites such as vitamins (*Supp. figure 2.4 D*) were in higher relative abundance in DMEM compared to TYI-S-33. Out of the 130 metabolites that we screened for, a total of 63 metabolites were detected in the TYI-S-33, and 37 metabolites in DMEM and DMEM supplemented with CKs. The number and relative abundances of metabolites detected in the unsupplemented and CK-supplemented DMEM did not differ (*Supp. figure 2.5*).

In the TYI-S-33 medium-blanks, levels of most metabolites were stable during the 21-h incubation period, while some metabolite levels changed (data not shown). We noticed that guanine and guanosine, two components in yeast extract, changed considerably during incubation even in the absence of cells, suggesting that these components are easily

degraded (Jameson & Morris, 1989). Therefore, these and other unstable components in the yeast extract are excluded from the analysis.

Metabolite dynamics during trophozoite growth in the TYI-S-33 supernatants

To profile extracellular metabolites during trophozoite growth, supernatants were collected from TYI-S-33 culture at 0-, 3-, 6-, 9-, and 21-h timepoints. Most metabolites in this study were identified using their unfragmented compound mass which represents compound identification level 3 except the amino acids which were identified using level 1 accuracy using labeled internal standards available for quantification (see methods).

Most metabolites detected in the supernatants showed changes over time suggesting that Giardia depends heavily on the availability of a diversity of molecules in its extracellular environment for its nutritional needs. Of the detected metabolites, molecules of the amino acid and DNA related metabolite groups showed a meaningful trend. In the first group, arginine decreased while citrulline and ornithine increased (*Figure 2.5 A*). Moreover, serine decreased rapidly, and alanine increased, while valine, asparagine and threonine remained relatively stable (*Figure 2.5 B*).

The second group that changed was comprised of the DNA related metabolites - specifically nucleosides and nucleobases. All detected nucleosides (deoxy-methylthio adenosine (dMTA), adenosine, inosine, thymidine, and uridine) decreased gradually over time while some corresponding nucleobases (adenine, hypoxanthine, uracil) increased except guanine (*Figure 2.6*). Within the detected nucleosides, purines (dMTA, adenosine, inosine) decreased to negligible levels by the end of the time course while the decrease of the pyrimidines (thymidine, uridine) plateaued between 9 – 21h. Within nucleobases, the

increase of adenine was almost linear over the 21-h incubation period while other nucleobases increased more sporadically. The pyrimidine nucleoside, cytidine, was not detected, but its base, cytosine, increased like the other nucleobases. On the other hand, with the observed decrease of the pyrimidine nucleoside, thymidine, the increase of nucleobase thymine was expected; however, thymine was not detected.

DISCUSSION

This is the first study that aimed to characterize the CK synthesis and metabolism ability of Giardia trophozoites. Moreover, using exogenous CKs, the experiments aimed to monitor the exchange of CKs with the extracellular medium during cell proliferation in nutrient rich and nutrient poor conditions. During nutrient deprivation, a metabolomics investigation of the extracellular medium led us to obtain a correlation between CK metabolism and other metabolites.

The growth medium, TYI-S-33, used to routinely culture Giardia trophozoites in-vitro is rich in organic components from yeast extract and serum. The majority of CKs within TYI-S-33 originated from the yeast extract and the profile of CKs detected in the medium is consistent with previous reports of yeast extract CK profiling (Jameson & Morris, 1989). These results are also consistent with the findings of a recent survey of various inorganic and organic culture media used in laboratories for CK presence and their origin (Aoki et al., 2021) where organic components like yeast extract and peptone were considered to be the source of CKs. This study also confirmed some nutritional needs of the trophozoites by the metabolomic comparison of the nutrient rich TYI-S-33 medium to the nutrient poor DMEM, which is one of the common culture medium for mammalian epithelial cells (Aoki et al., 2021). To study co-culture of Giardia with its host epithelial cells, many attempts have been made to sustain a Giardia culture in DMEM with or without host cells (Hubert, 2020; Ma'ayeh et al., 2017; Ringqvist et al., 2008; Rodríguez-Fuentes et al., 2006). However, the consensus is that Giardia does not survive for long time periods in DMEM when they are not co-incubated with mammalian cells (Fisher et al., 2013). These observations are confirmed by this study that highlights the scarce nutrient profile

of DMEM along with the absence of any purine and pyrimidine nucleosides needed for DNA replication even with serum supplementation.

Intracellular CK analysis revealed the presence of two endogenous CKs in Giardia trophozoites – iPRP and iP. Giardia is a parasite that lacks *de novo* biosynthesis of most metabolites needed for growth and cell division (Morrison et al., 2007). However, Giardia seems to turn to *de novo* biosynthesis of certain structurally indispensable compounds like isoprenoids through a highly conserved MVA pathway, when it experiences scarcity of these molecules in the extracellular environment (Hernandez & Wasserman, 2006). The transcriptionally regulated MVA pathway results in the production of isopentenyl pyrophosphate (IPP) which is an important intermediate for isoprenoid biosynthesis used for numerous downstream applications in Giardia including: plasma membrane synthesis and stability (Romano et al., 2015); prenylation of proteins for growth (Lujan et al., 1995)**;** and tRNA modifications for correct base selection at the anticodon loop hence promoting translation fidelity (Lamichhane et al., 2011). One of the tRNA modifications involves a prenyl chain addition at the N^6 position of the 37^{th} adenosine nucleotide by the prenyl donor IPP, catalyzed by tRNA-IPT enzyme, which is highly conserved among all organisms (Nishii et al., 2018). This results in a tRNA bound CK, iPRP. The degradation of the tRNA leads to availability of free unmodified nucleotides for re-use in nucleic acid assembly, and free modified nucleotides including iPRP. This is likely the route for iPRP production within Giardia since the genome contains a tRNA-IPT (Giardia DB: GL50803_17480) enzyme, and ribonucleases that cleave RNA (Giardia DB: GL50803_3279, 9155, 34134, 9912) (Einarsson, Troell, et al., 2016). The tRNA-derived iPRP is likely converted directly to the free base iP by the highly conserved Lonely Guy (LOG)-like phosphoribohydrolase

enzyme. Although a LOG-like protein was not found in the Giardia genome based on homology search against LOG enzymes of *D. discoidium*, *M. tuberculosis*, and *A. thaliana*, it is likely that LOG-like activity is the result of one or more hypothetical proteins since approximately 40% of the Giardia genome remains unannotated (Xu et al., 2020). Moreover, Giardia possess an adenine phosphoribosyltransferase that catalyzes the addition of phosphoribose to adenine. Although Giardia contains both 5'-nucleotidase (Giardia DB: GL50803_0017205) for CK-NT to CK-RB conversion and purine nucleoside phosphorylase (Giardia DB: GL50803_91348), the presence of iP instead of iPR detected within the cell pellets indicates that there is a higher probability of LOG-like activity present. *Figure 2.7* summarizes the proposed CK synthesis pathway in Giardia considering the current knowledge of the MVA pathway genes experimentally identified (Hernandez & Wasserman, 2006), or putatively present (Hoshino & Gaucher, 2018), along with potential presence of the CK synthesis genes tRNA-IPT and LOG-like phorphoribohydrolase which is supported by the CK forms detected intracellularly. The downstream purpose of iPRP or iP production within the Giardia trophozoites remains unknown. However, some possible roles can be speculated based on: (i) non-plant organisms with plant-like features such as the free-living protist *Dictyostelium discoidium* (Aoki et al., 2020) and the parasitic protist *Toxoplasma gondii* (Andrabi et al., 2018) synthesize and utilize CKs for diverse cellular functions; (ii) organisms of various phyla that interact with plants, specifically plant pathogens like insects, nematodes, bacteria, fungi, or protists developed an ability to regulate their CK production to establish infection by interfering with CK biosynthesis of the host plant (Anand et al., 2022; Andreas et al., 2020; Rahman, 2019; Sarkar et al., 2023; Spallek et al., 2018); (iii) CK are produced by

organisms that do not interact with plants including insects, nematodes, fungi, protists, and bacteria. Of these species, some pathogens of mammals seem to have a conserved ability for CK production along with potential crucial cellular functions such as nitric oxide (NO) resistance in *Mycobacterium tuberculosis*, (Samanovic & Heran, 2015) or cell cycle progression in *Toxoplasma gondii* (Andrabi et al., 2018). Therefore, it is highly probable that the CKs produced by Giardia have a role in some aspect of cell biology or pathogenesis that is yet undetermined.

Giardia is an extracellular parasite that depends on scavenging nutrients from the host's intestinal tract, and it secretes a variety of molecules that can adversely affect the host intestinal epithelium. The set of molecules secreted by an organism is referred to as the secretome, and the identification of these molecules is an important conceptual tool to gain insights into the disease-causing mechanisms of pathogens including Giardia (Shant et al., 2002). For this reason, most analyses in this study were focused on the extracellular medium collected from cultures incubated with trophozoites. In routine growth condition or during nutrient deprivation of trophozoites, all riboside CKs (BAR, iPR, cZR, MeSZR, MeSiPR) present in varying concentrations in the medium, decreased, either when the cell density increased (TYI-S-33) or remained constant (DMEM). Meanwhile, most corresponding free base CK derivatives (BA, iP, MeSZ, MeSiP), except cZ, increased approximately to a concentration similar to the initial CK-RB levels in the culture medium. Moreover, detection of the exogenously supplied synthetic CKs - BAR and BA, within the cell pellets suggests that ribosides are taken up and hydrolyzed to their free base form within the cell followed by secretion of the freebase. This CK-RB uptake and secretion of CK-FB can be correlated to previous reports on the common nucleoside salvage and

metabolism by Giardia for its purine and pyrimidine needs for DNA and RNA synthesis (Aldritt et al., 1985; Baum et al., 1989; Wang & Aldritt, 1983). Due to its parasitic lifestyle, Giardia lacks *de novo* purine and pyrimidine synthesis and solely depends on salvage of these molecules from the extracellular medium. Firstly, Giardia scavenges purine and pyrimidine nucleosides (Baum et al., 1993; Davey et al., 1992), secondly, it hydrolyzes the ribose group through nucleoside hydrolases (Aldritt et al., 1985; Baum et al., 1989; Wang & Aldritt, 1983), and finally, it adds a phosphoribose to the free base using phosphoribosyltransferase enzymes (Munagala & Wang, 2002; Sarver & Wang, 2002). The excess nucleobases are discarded by the trophozoite through nucleobase transporters (Ey et al., 1992). It is likely that Giardia trophozoites use a similar route (*Figure 2.8*) for processing the extracellular CK ribosides and exporting the resultant CK free bases. Once CK-RBs are imported into the cells through the nucleoside transporter and the ribose cleaved, there must be an unknown recognition mechanism within Giardia that prevents the phosphoribosylation and subsequent incorporation of the modified adenine bases (CKs) into the genetic material (*Figure 2.8*). The cell may identify these modified adenines as 'faulty bases' which lead to their secretion. This hypothesis was supported by the metabolomics analysis of the culture supernatants, for which all detected nucleosides decreased in a pattern similar to CK-RBs while many nucleobases were secreted into the culture medium like the CK-FBs. Specifically, the CK-RB and CK-FB changes resembled the decreases of non-modified and modified adenine nucleosides (adenosine, dMTA) and increase of the free base adenine respectively, suggesting similar metabolic processing due to structural similarity. This possibility of the up-take of a structurally similar purine-based molecule is also highlighted in Giardia where a membrane transporter was found to have

broad nucleoside specificity to drive import of many common nucleosides by detection of the 3’ OH on the ribose moiety, irrespective of the base structure or modifications (*Figure 2.9*) (Davey et al., 1992). A similar mechanism for secretion of a wide range of nucleobases was reported for Giardia that could lead to the export of CK-FBs (Ey et al., 1992). These transporters are analogous to the sugar (SWEET) and nucleoside/nucleobase transporters (PUP and ENTs) present in plants and humans that are recently discovered to participate in transport of CKs across the cell membrane (Hluska et al., 2021).

For the exogenously supplied CKs in the growth and nutrient deprivation condition, the changes in extracellular concentrations of ribosides, BAR in the growing culture and iPR in the nutrient deprived culture, and their respective free bases, BA and iP, were most pronounced. However, their respective nucleotide derivatives BARP and iPRP did not change within the culture supernatants over time. This result is supported by previous reports of nucleotide impermeability through the plasma membrane because of their charge (Pinheiro et al., 2008a). Instead, the common purine and pyrimidine nucleotides present in the extracellular environment are catabolized by phosphatases like ATPases, ADPases and ecto-5`-nucleotidase enzymes that are located on the exterior surface of the cell (Pinheiro et al., 2008b; Russo-Abrahão et al., 2011; Sansom et al., 2008) to produce nucleosides or nucleobases for easy uptake by the cell. Since the potential substrate specificity of these ecto-enzymes towards CKs is unknown, the results of this study suggest that BARP and iPRP might not be suitable substrates, as no substantial change was observed in the extracellular levels of both nucleotides during trophozoite growth or nutrient deprivation conditions.

Initial studies on Giardia metabolism used enzyme assays on crude protein lysates (Adam, 2001). Some of these enzyme activities were later confirmed by transcriptomics and proteomics reports (Birkeland et al., 2010; Faso et al., 2013), however, the end products of the most basic metabolism pathways that depend on the exchange of molecules between Giardia and the extracellular medium have only recently been confirmed by metabolomics (Vermathen et al., 2018). Although scarce, most metabolomic profiling of Giardia has focused on intracellular metabolites (Müller et al., 2020; Popruk et al., 2023). Therefore, this study focused on the extracellular metabolites to confirm some basic pathways like the arginine dihydrolase pathway for energy production (Adam, 2021). Within this time-course based metabolomic MS analysis of free amino acids, the consumption of arginine along with secretion of citrulline and ornithine were observed, indicating arginine dihydrolase activity while other another amino acid alanine was exported to facilitate the import of serine, threonine, and asparagine. These observations are in agreement with the previous NMR-based report of extracellular amino acid changes of a proliferating trophozoite culture (Vermathen et al., 2018). Moreover, the WB C6 isolate of Giardia used in our study seems to prefer the exchange of serine for alanine since threonine and asparagine remained relatively constant in the culture supernatants over time.

FIGURES

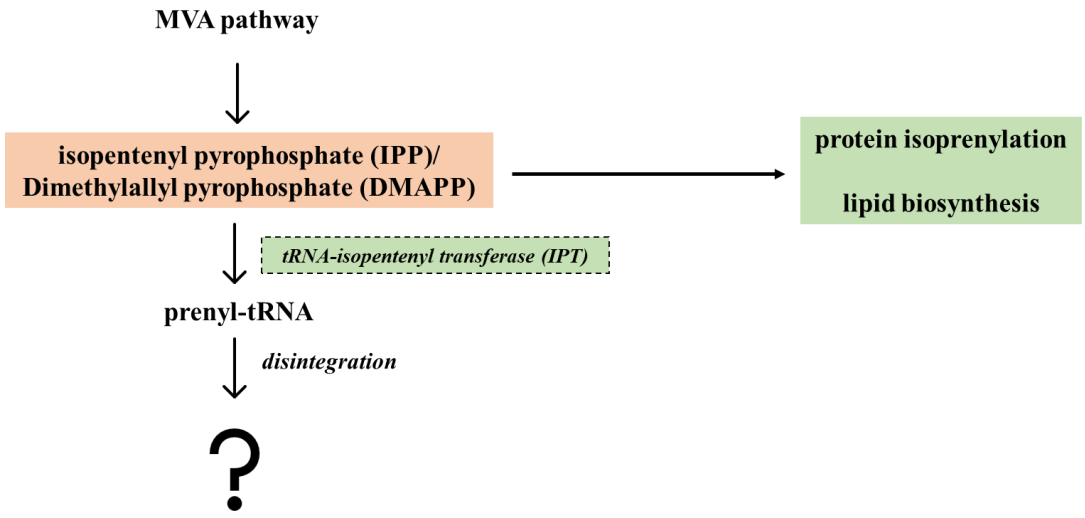

Figure 2.1: *Origin of the prenyl chain donor IPP/ DMAPP in Giardia intestinalis and potential for tRNA prenylation and resultant cytokinin synthesis (Einarsson et al., 2016; Hernandez & Wasserman, 2006)*

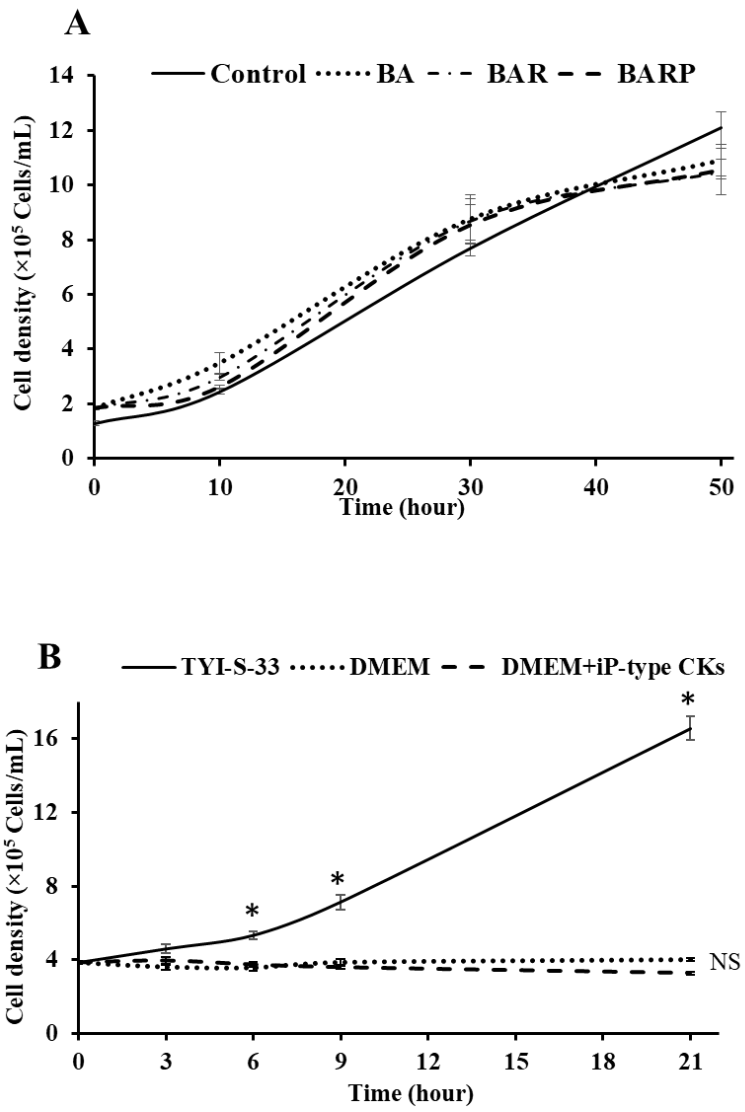

Figure 2.2*:Growth of Giardia intestinalis trophozoites is not unaffected by CK supplementation: (A) cell density in unsupplemented (control) and BA-, BAR- and BARP-supplemented TYI-S-33 medium (1 μM each) measured at 0, 10, 30 and 50 hours (multiple comparison t-test, FDR correction; $p < 0.05$) and (B) cell density in unsupplemented TYI-S-33, unsupplemented DMEM and iP-type CK-supplemented DMEM (iP, iPR, iPRP; 1 μM) measured at 0, 3, 6, 9, and 21 hours (Two-way ANOVA, Tukey's post hoc test; $p < 0.05$). NS beside the cell densities of DMEM and DMEM + CKs indicate no significant change in the density of cells with CK-supplementation of DMEM compared to unsupplemented DMEM. Error bars represent standard error (n=3).*

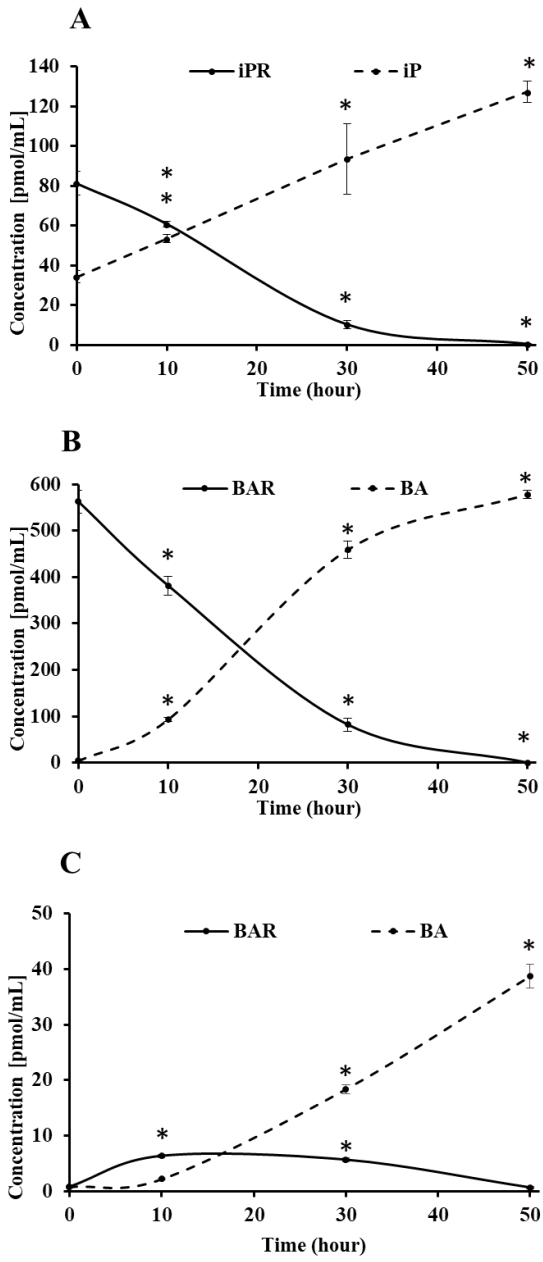

Figure 2.3: *Concentration changes of iP-type CKs (iPR and iP) detected in the unsupplemented TYI-S-33 culture supernatants. (A) Concentration changes of BA-type CKs (BAR and BA) detected in the BAR-supplemented culture supernatants, (B) concentration changes of BA-type CKs (BAR and BA) detected in BARP-supplemented culture (C) over a 50-h incubation period. Asterisks show significantly different CK concentrations at each time point (10-, 30-, and 50-h) compared to the respective CK concentration at the beginning of the time-course (0-h) (One-way ANOVA, Dunnett's post hoc test; $p < 0.05$). Error bars represent standard error (n=3).*

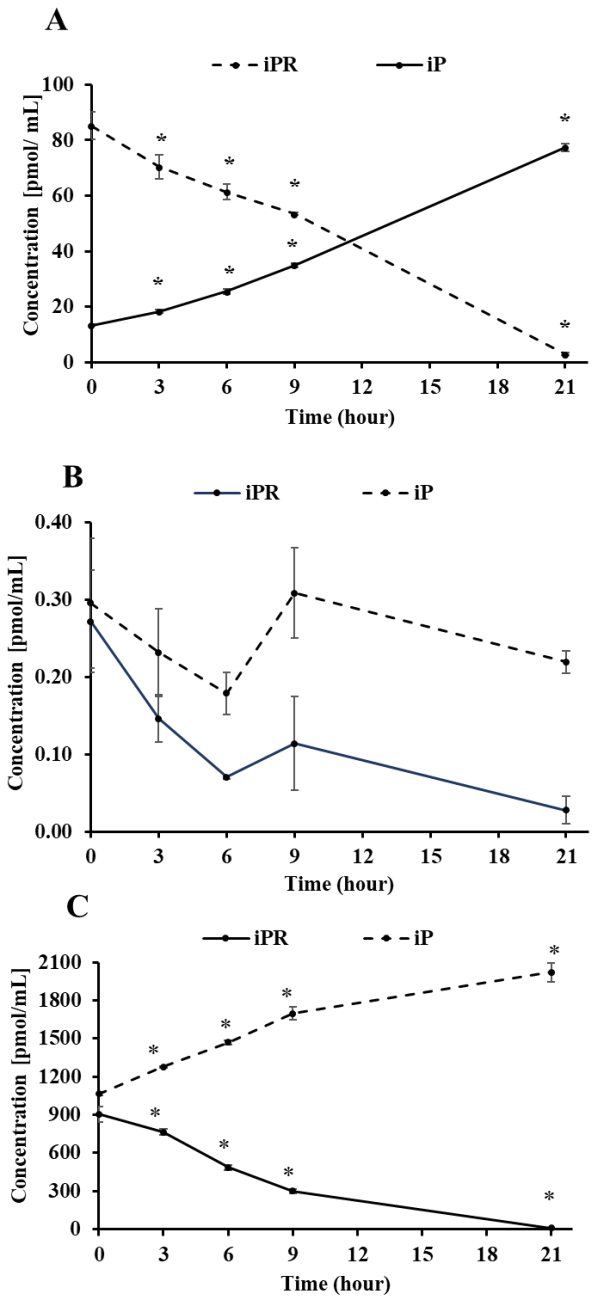

Figure 2.4: *Concentration changes of iP-type CKs (iPR and iP) detected in: (A) unsupplemented TYI-S-33 culture supernatants (B) unsupplemented DMEM culture supernatants of and (C) the iP-type CK-supplemented DMEM culture supernatants of over a 21-h incubation period. Asterisks indicate significantly different CK concentrations at each time point (3-, 6-, 9- and 21-h) compared to the respective CK concentration at the beginning of the time-course (0-h) (One-way ANOVA, Dunnett's post hoc test; $p < 0.05$). Error bars represent standard error (n=3).*

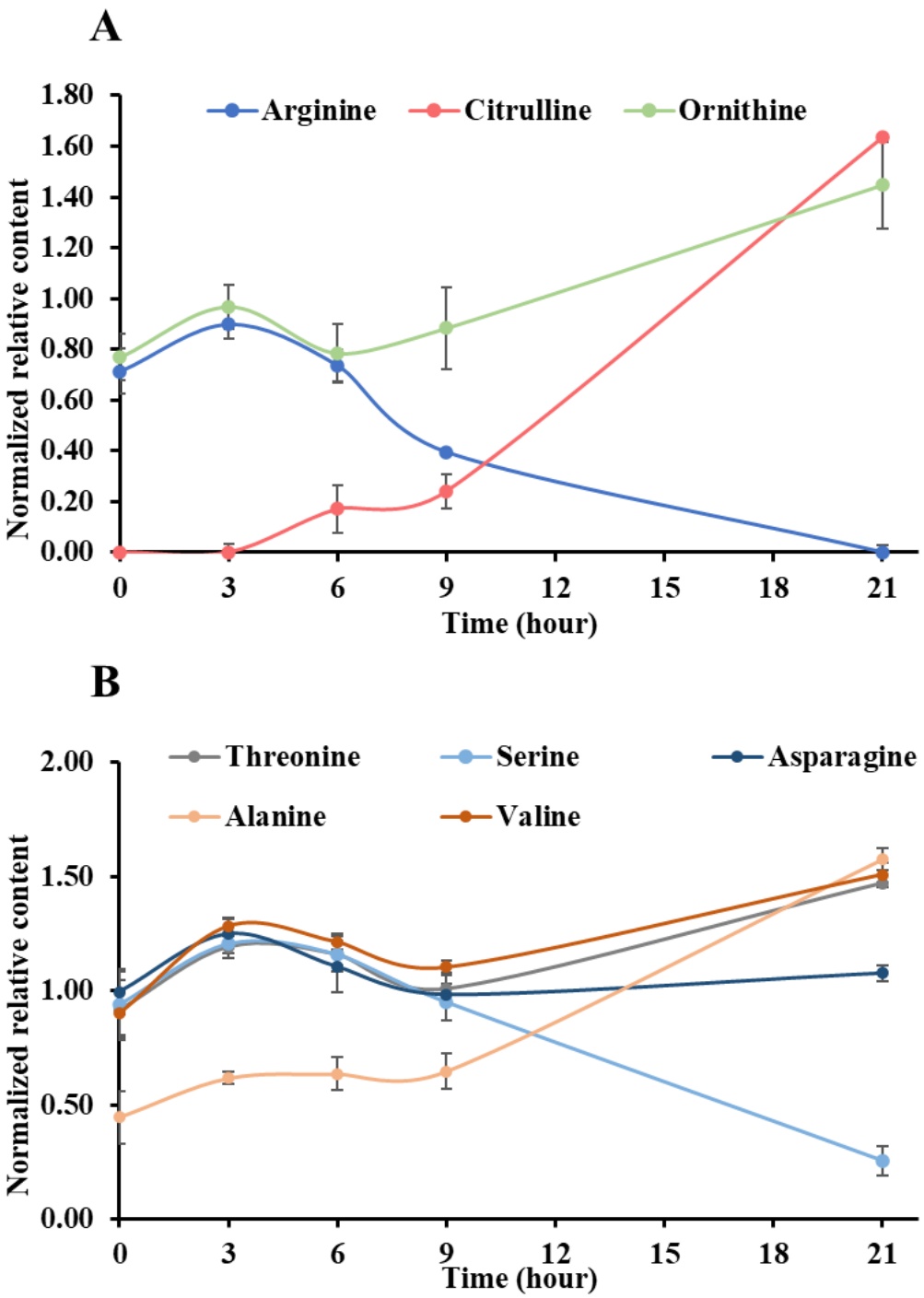

Figure 2.5: *Extracellular dynamics of: (A) Arginine dihydrolase-related amino acids (arginine, citrulline, ornithine) and (B) other free amino acids (reported earlier to be metabolized by Giardia; Adam, 2001b) detected in the unsupplemented TYI-S-33 culture supernatants over a 21-h incubation period. Error bars represent standard error (n=3).*

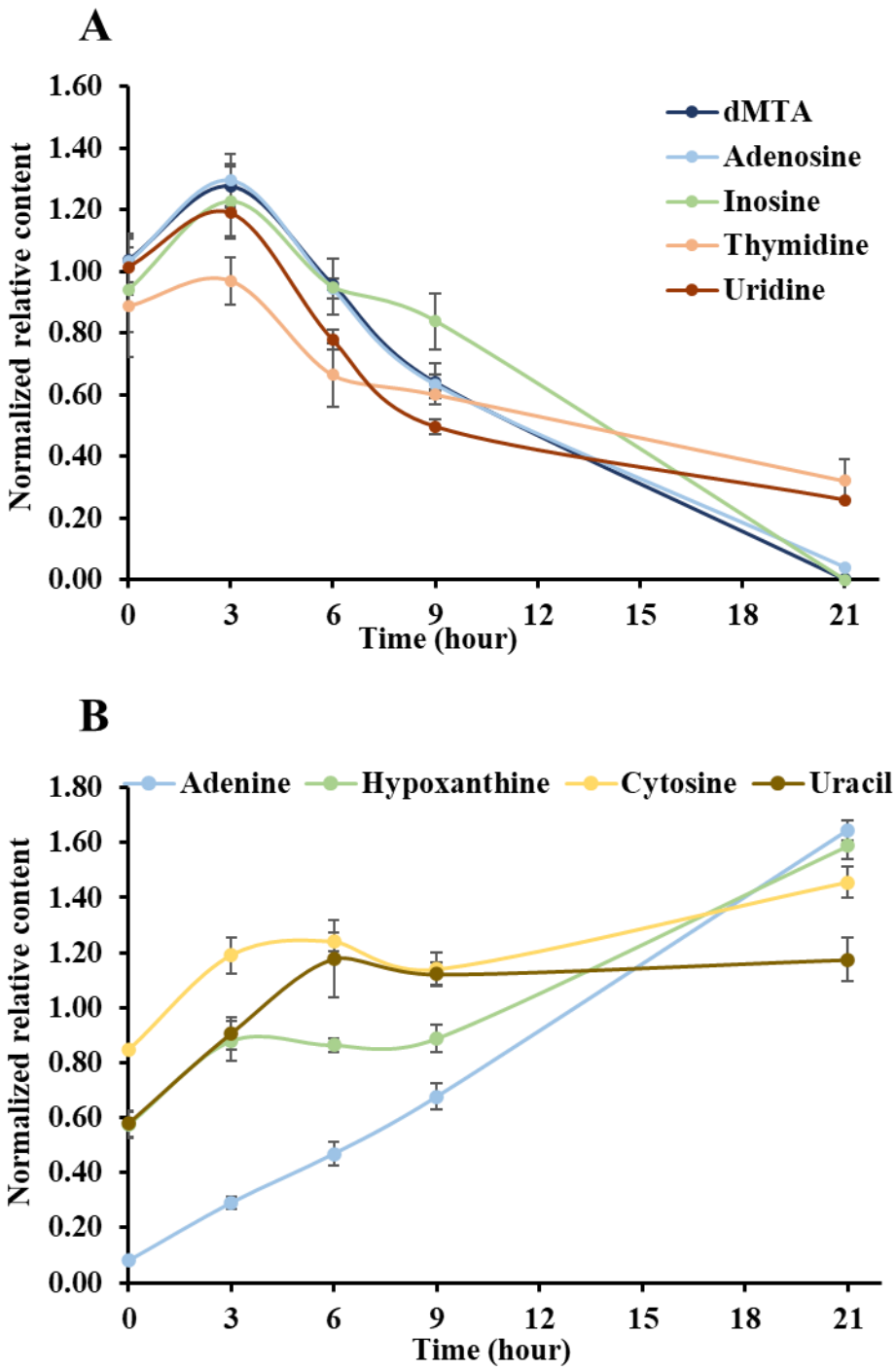

Figure 2.6: *Dynamics of (A) nucleosides and (B) nucleobases detected in the unsupplemented TYI-S-33 culture supernatants over a 21-h incubation period. Respective nucleoside-nucleobase pairs are color-coded. Error bars represent standard error (n=3).*

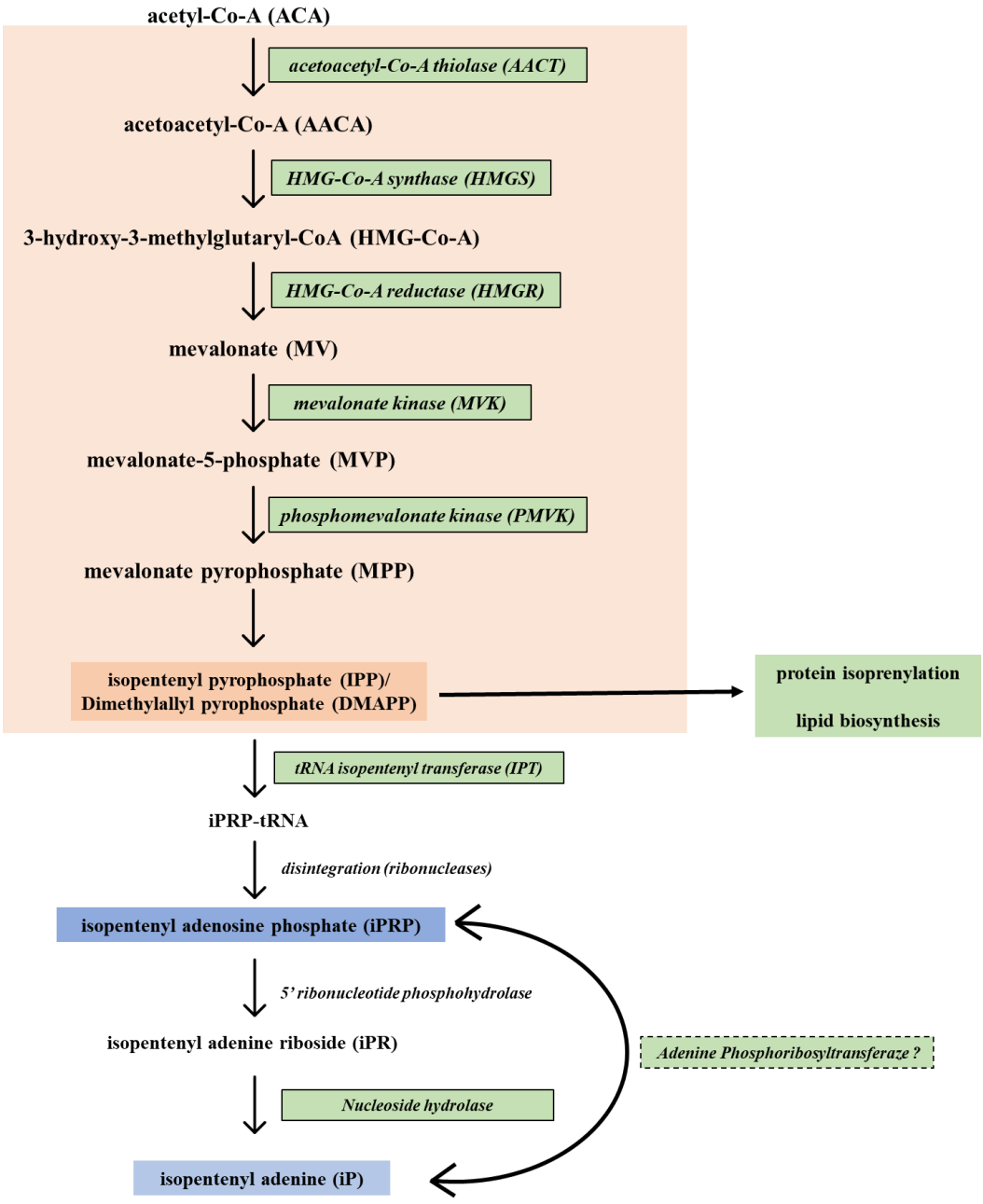

Figure 2.7: *Proposed CK synthesis pathway in Giardia based on reports of transcribed genes, active enzyme activity, or protein search in the Giardia genome. Legend: solid line green boxes - experimentally confirmed gene expression, orange boxes - mevalonate (MVA) pathway for isoprenoid synthesis and blue boxes - detected cytokinins. Dotted line box represents putative enzyme based on observed CKs (Adam, 2001; Davey et al., 1992; Gibb et al., 2020; Hernandez & Wasserman, 2006; Luján et al., 1996; Romano et al., 2015).*

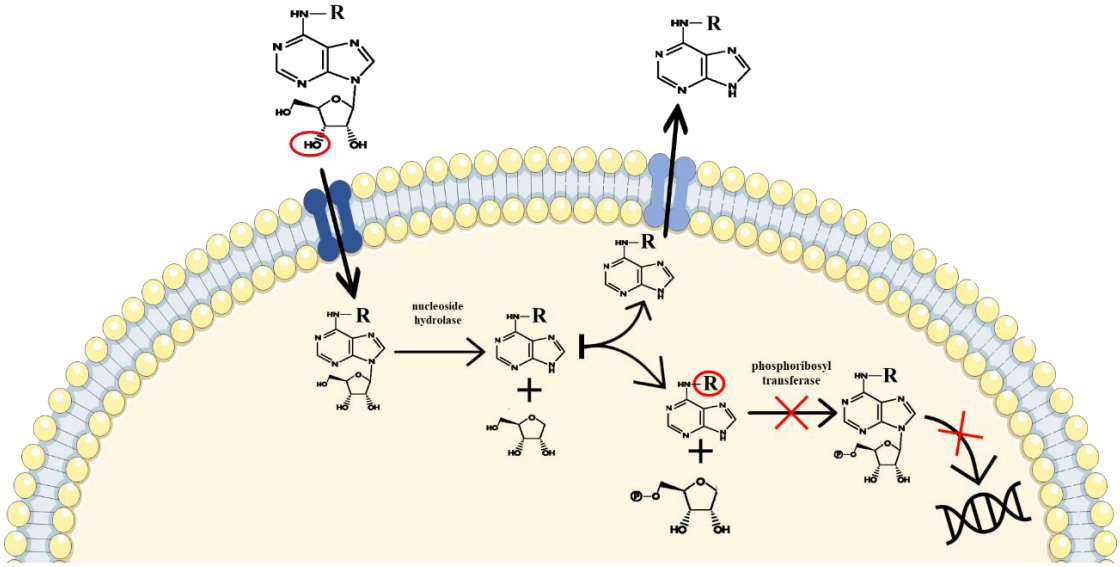

Figure 2.8: *Proposed CK metabolism by Giardia trophozoites. Legend: dark blue - broad specificity nucleoside transporter, light blue - broad specificity nucleobase transporter, red circles - the structural feature recognized for further processing. RBs (CK and others) are uptaken based on the recognition of the 3'OH of the ribose moiety and catabolized into CK-FBs and ribose by an adenosine hydrolase. The CK-FBs are prevented from phosphoribosylation by phosphoriboslytransferase due to the recognition of* N^6 *modification by an unknown mechanism. In consequence, FBs (CK and others) are discarded by Giardia using a broad specificity nucleobase transporter (Baum et al., 1993; Campagnaro & de Koning, 2020; Davey et al., 1992; Ey et al., 1992) (created through modification of Servier.com figures*

.

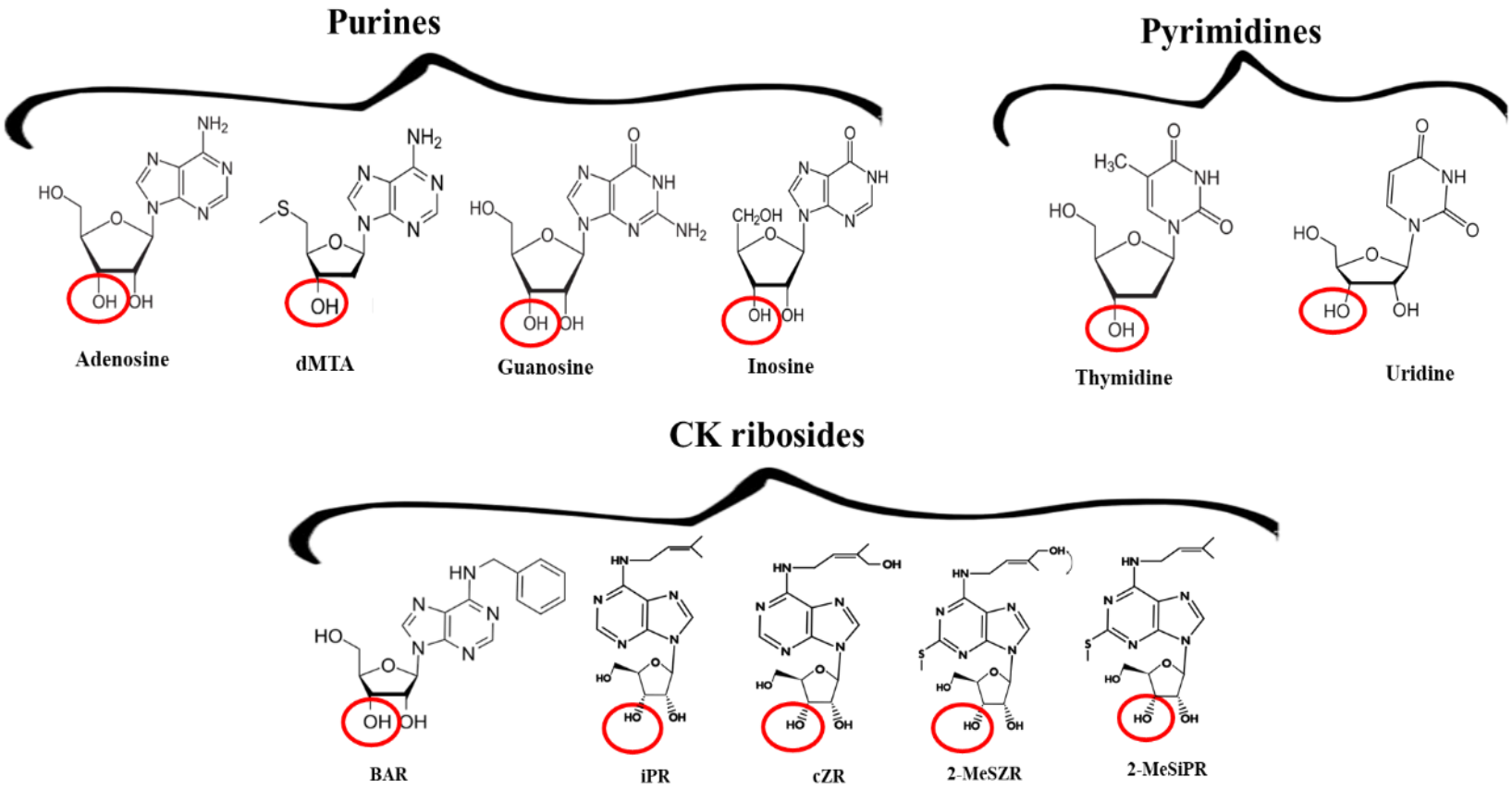

Figure 2.9: *Structural similarity between the detected nucleosides uptaken by Giardia trophozoite using the broad specificity nucleoside transporter that recognizes the 3'OH (red circle) on the ribose moiety* (Davey et al., 1992). *Some purines and pyrimidines have specific transporters* (Baum et al., 1989, 1993).

SUPPLEMENTARY INFORMATION

Supplementary table 2.1: *Metabolites profiled in metabolomics samples. Bolded amino acids indicate the contents of the labeled canonical internal standard mix used for data normalization.*

Amino Acids and Derivatives	DNA related metabolites	Organic Acids	Sugars and sugar phosphates	Vitamins and co-enzymes	Other
Alanine (Ala)/ Sarcosine (Sar)	Adenine (Ade)	cis-Aconitate (cis-Aco)	Adenosine diphosphate glucose (ADPG)	B1 Thiamine	3-aminoisobutanoate
Arginine (Arg)	Cytosine	Citrate (Cit)/Isocitrate (Iso)	Adenosine diphosphate ribose (ADPR)	B2 Riboflavin	3-hydroxybutanoic acid
Asparagine (Asn)	Guanine (Gnin)	Fumerate (Fum)	Glyceraldehyde 3-phosphate (GAP)	B3 Nicotinic acid (niacin)	2-aminophenol
Aspartate (Asp)	Hypoxanthine	Gluconate (GA)	Erythritol	B5 Pntothenic acid	3-hydroxybenzaldehyde
Cysteine	Thymine	Glycerate	Fructose 1,6-bisphosphate (FBP)	B6 Pyridoxine	Salicylamide
Glutamine (Gln)	Uracil	Glycolate	Glucose (Glu)/ Gal/ Fru/ Man	B7 Biotin	Indole-3-acetate
Glutamic acid (Glu)/ O-acetylserine	Adenosine (Asin)	Glyoxylate	Glucose-6-phosphate (G6P)/G1P/ F6P/ M6P	B9 Folic acid	10-hydroxydecanoate
Glycine (Gly)	Cytidine	Hydroxyglutarate (2-HG)	Mannitol (Man-Ol)	Choline (CHOL)	Ll-2-6-diaminoheptanedioate
Histidine (His)	Guanosine (Gsin)	Ketoglutarate (AKG)	Phosphoenolpyruvic acid (PEP)	Nicotinamide mononucleotide (NMN)	Omega-hydroxydodecanoic acid
Isoleucine (Ile)	Inosine (Isin)	Lactate (Lac)	2-Phosphoglycerate (2PGA)	Nicotinamide adenine dinucleotide, oxidised (NAD+)	2-acetamido-2-deoxy-beta-d-glucosylamine
Leucine (Leu)	Thymidine	Malate (Mal)	2-phosphoglycolate (2-PG)	Nicotinamide adenine dinucleotide, reduced (NADH)	Docosahexaenoic acid
Lysine (Lys)	Uridine (Uri)/Pseudouridine (Psi)	Oxalate	6-Phosphogluconate (6PGA)	Nicotinamide adenine dinucleotide phosphate, oxidized (NADP+)	Glycocholate
Methionine (Met)	Adenosine monophosphate (AMP)	Pyruvate (Pyr)	Raffinose	Nicotinamide adenine dinucleotide phosphate, reduced(NADPH)	Taurine
Phenylalanine (Phe)	Adenosine diphosphate (ADP)	Shikimate	Ribose (RIB)		Glycerol phosphate
Proline (Pro)	Adenosine triphosphate (ATP)	Succinate (Suc)	Ribose-5-phosphate (R5P)		GABA
Serine (Ser)	Cytidine monophosphate (CMP)	Tartatic acid	Ribotol		Indole-3-carboxyaldehyde
Threonine (Thr)/ Homoserine (Hse)	Cytidine diphosphate (CDP)	Uric acid	Ribulose 1,5-biphosphate (RuBP)		3-indoleacetaldehyde
Tryptophan (Trp)	Cytidine triphosphate (CTP)		Sedoheptulose-7-phosphate (S7P)		Phosphoric acid
Tyrosine (Tyr)	Guanosine monophosphate (GMP)		Stachyose		Acetyl-CoA
Valine (Val)/Betaine (BET)	Guanosine diphosphate (GDP)		Sucrose/Trehalose (TRE)/Galactinol		Quinic acid
Acetyl-l-cysteine	Guanosine triphosphate (GTP)		Uridine diphosphate glucose (UDPG)		Mevalonate (MVA)
L-alanyl-glutamine	Inosine monophosphate (IMP)				(±)-Mevalonic acid 5-phosphate (MVAP)
Aminoadipate (AAD)	Thymidine 5-monophosphate (TMP)				Ispoentely pyrophosphate (IPP)
Argininosuccinate (ASA)	Uridine monophosphate (UMP)				Mevalonic acid 5-pyrophosphate (MVAPP)
Citruline (Citu)	Uridine diphosphate (UDP)				Geranyl phyrophosphate (GPP)
Cysthationine (CYS)	Uridine triphosphate (UTP)				Farnesyl pyrophosphate (FPP)
Cystine	Cyclic adenosine monophosphate (cAMP)				Geranylgeranyl pyrophosphate (GGPP)
Dihydroxyisovalerate (DIHV)	Cyclic guanosine monophosphate (cGMP)				4,6-dihydroxyquinoline
Glutamylcysteine (Glu-Cys)	5-deoxyadenosine				S-methylmethionine
Guanidinoacetate (GAA)	5'-Deoxy-5'-Methylthioadenosine (dMTA)				Glutathione, reduced (GSH)
(+/-)-3methyl-2-oxovalerate (K-IVal)	Deoxyadenosine monophosphate (dAMP)				S-adenosylhomocysteine (SAH)
Ketoisovalerate (KIV)	5-Methyluridine (m5U)				S-adenosylmethionine (SAM)
Kynurenine (KYN)					Glutathione, oxidized (GSSG)

Supplementary table 2.2: *Levels of CKs detected in TYI-S-33 medium-blanks (medium incubated without trophozoites). No significant differences were observed in the levels of CKs detected in the medium-blanks between 0-h and 50-h time points (t-test, $p < 0.05$, n=3 ± SE).*

Cytokinin	**TYI-S-33 medium-blank level [pmol/mL]**	
	0 h	**50 h**
iP	28.58 ± 1.18	28.86 ± 1.59
iPR	53.86 ± 4.05	63.62 ± 2.57
iPRP	65.62 ± 9.94	48.66 ± 1.40
cZR	2.48 ± 0.15	1.70 ± 0.19
MeSZ	0.05 ± 0.01	0.03 ± 0.00
MeSZR	0.13 ± 0.01	0.04 ± 0.02
MeSiP	0.04 ± 0.01	0.02 ± 0.00
MeSiPR	0.07 ± 0.00	0.06 ± 0.00

Supplementary table 2.3: *Levels of aromatic CKs detected in BA-type CK supplemented TYI-S-33 medium-blanks. Asterisks indicate significant differences between each of the CKs detected at 0-h and 50-h (t-test, $p < 0.05$, n=3 ± SE); n.d. = not detected.*

Supplementation (1 µM)	**Aromatic CKs**	**Medium-blank level [pmol/mL]**	
		0-h	**50-h**
BA	BA	409.87 ± 0.19	495.55 ± 27.74*
	BAR	n.d.	n.d.
	BARP	n.d.	n.d.
BAR	BA	4.23 ± 0.23	5.92 ± 1.06
	BAR	562.75 ± 25.15	568.50 ± 50.83
	BARP	n.d.	n.d.
BARP	BA	0.88 ± 0.07	1.14 ± 0.08
	BAR	0.82 ± 0.10	29.25 ± 2.01*
	BARP	500.35 ± 21.99	373.01 ± 21.73*

Supplementary table 2.4: *Levels of CKs detected in unsupplemented and in iP-type CK supplemented DMEM medium-blanks. No significant differences were observed in the levels of CKs detected in the medium-blanks between 0-h and 21-h (t-test, $p < 0.05$, $n=3 \pm SE$).*

Cytokinin	**Unsupplemented DMEM medium-blank level [pmol/mL]**		**iP-type CK-supplemented DMEM medium-blank level [pmol/mL]**	
	0 h	**21 h**	**0 h**	**21 h**
iP	0.30 ± 0.08	0.09 ± 0.00	1064.34 ± 62.31	993.38 ± 25.83
iPR	0.27 ± 0.07	0.09 ± 0.00	905.03 ± 13.73	949.10 ± 22.56
iPRP	3.42 ± 0.40	0.69 ± 0.11	1547.92 ± 19.63	1494.32 ± 45.28

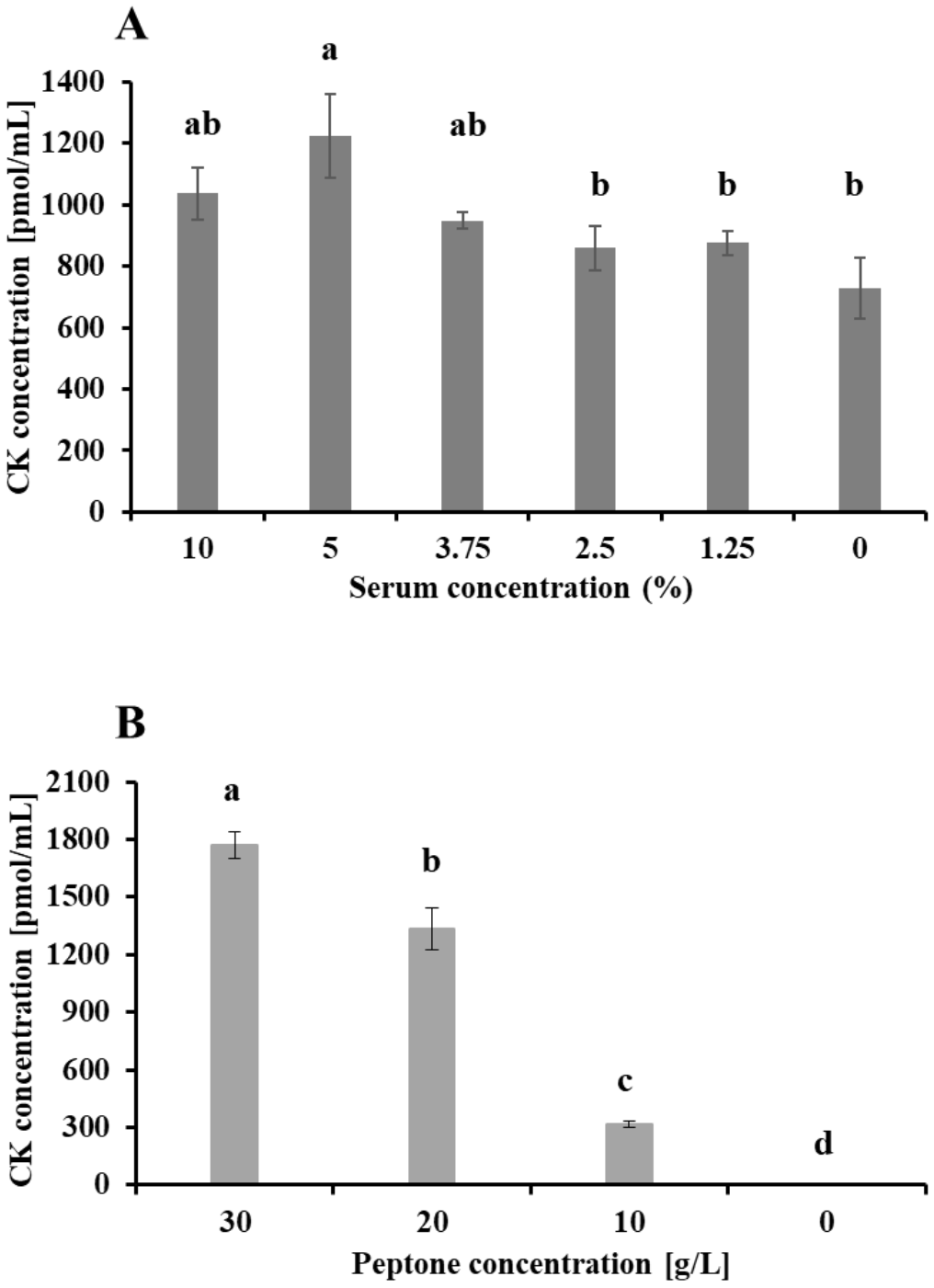

Supplementary figure 2.1: *Total Cytokinin levels [pmol/mL] in TYI-S-33 containing decreasing concentrations of equine serum (A) or peptone-yeast extract mix (B). Different letters (a, b, c, d) represent significant differences between groups (One-way ANOVA, Duncan's post hoc test, $p < 0.05$). Error bars represent standard error (n=4).*

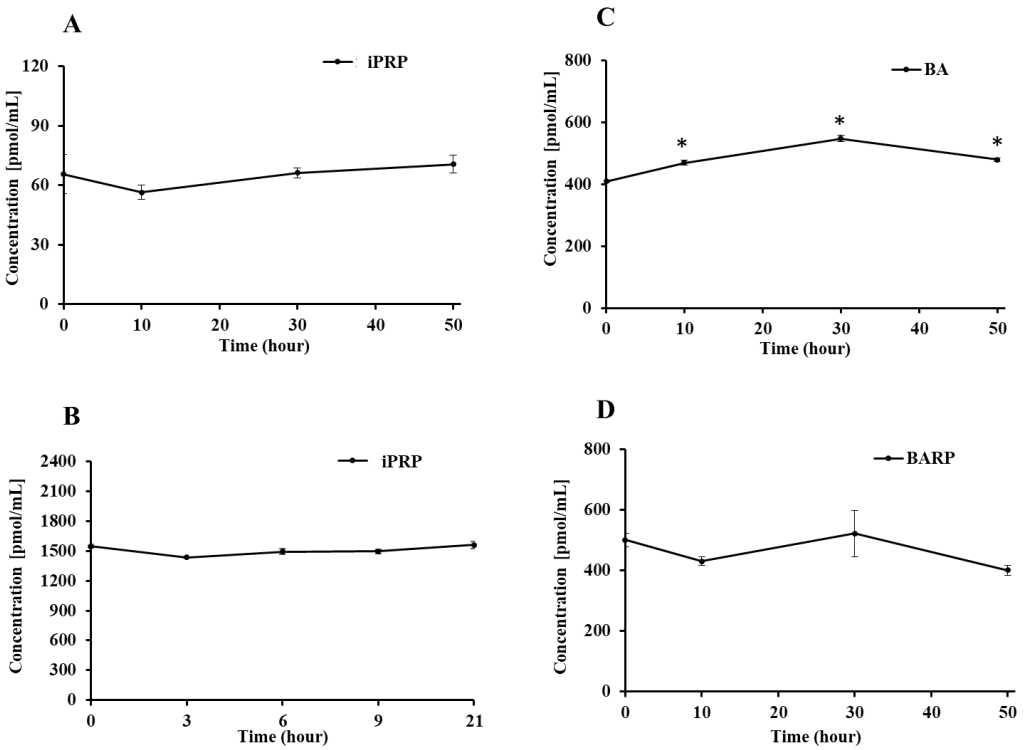

Supplementary figure 2.2: *Dynamics of iPRP detected in (A) TYI-S-33 culture supernatants (B) CK-supplemented DMEM culture supernatants. (C) BA dynamics in the BA-supplemented TYI-S-33 supernatants and BARP dynamics in the BARP-supplemented TYI-S-33 supernatants over time. CK levels at each time point were compared to the 0h time point (One-way ANOVA, Dunnett's post hoc test, $p < 0.05$). Error bars represent standard error (n=3).*

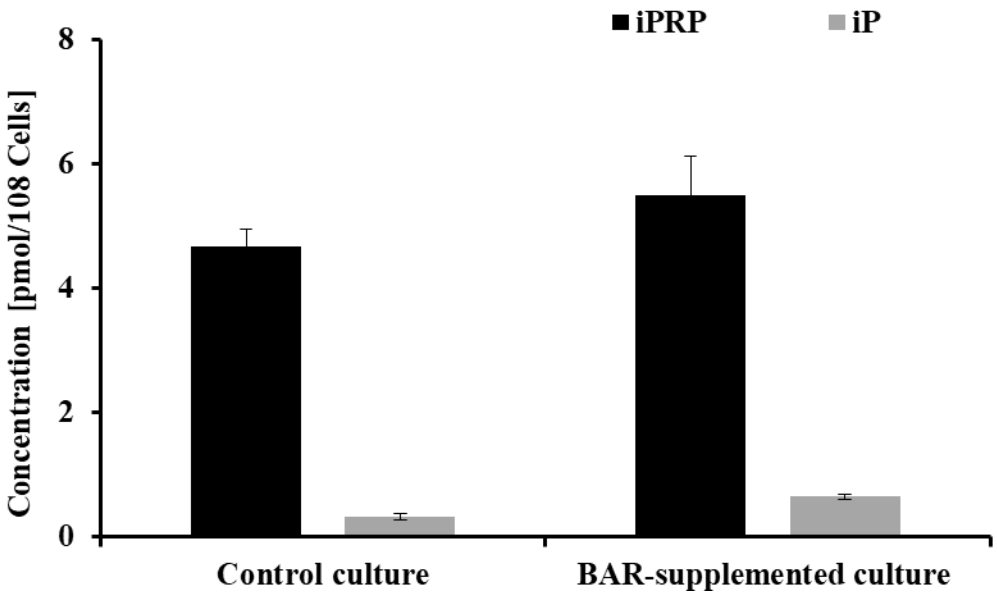

Supplementary figure 2.3: *Endogenous CKs (iPRP and iP) detected in the cell pellets of unsupplemented and BAR-supplemented TYI-S-33 cultures collected at the early stationary growth phase (1 x 106 cells/mL). No significant differences were found in iPRP and iP levels between the pellets from unsupplemented and BAR-supplemented cultures (t-test, p-value<0.05). Error bars represent standard error (n=3).*

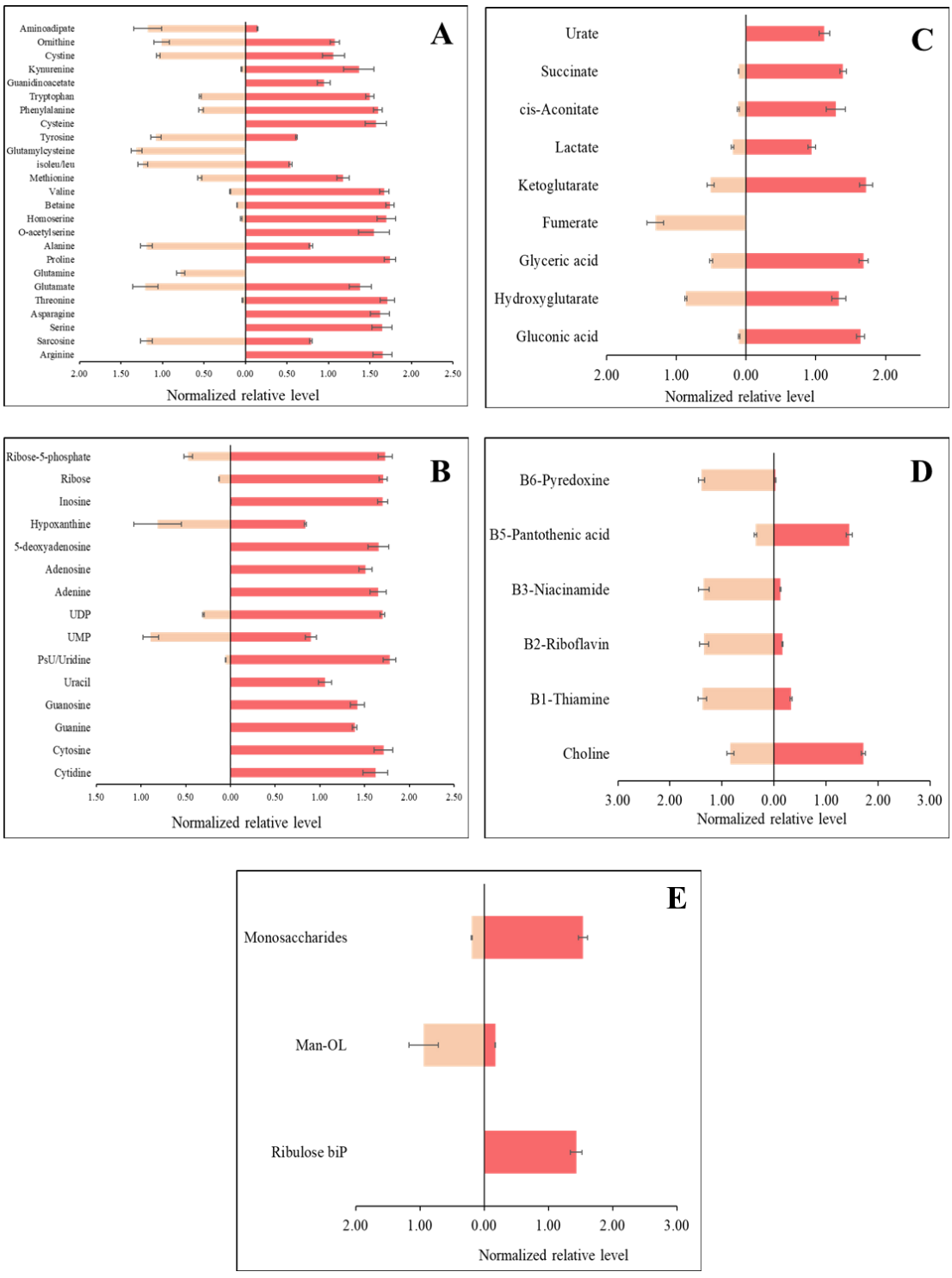

Supplementary figure 2.4: *Metabolite profile of the DMEM (■) and TYI-S-33 (■) media. A = amino acids and derivatives, B = DNA related metabolites, C = organic acids, D = vitamins, and E = sugars. Error bars represent standard error (n=3)*

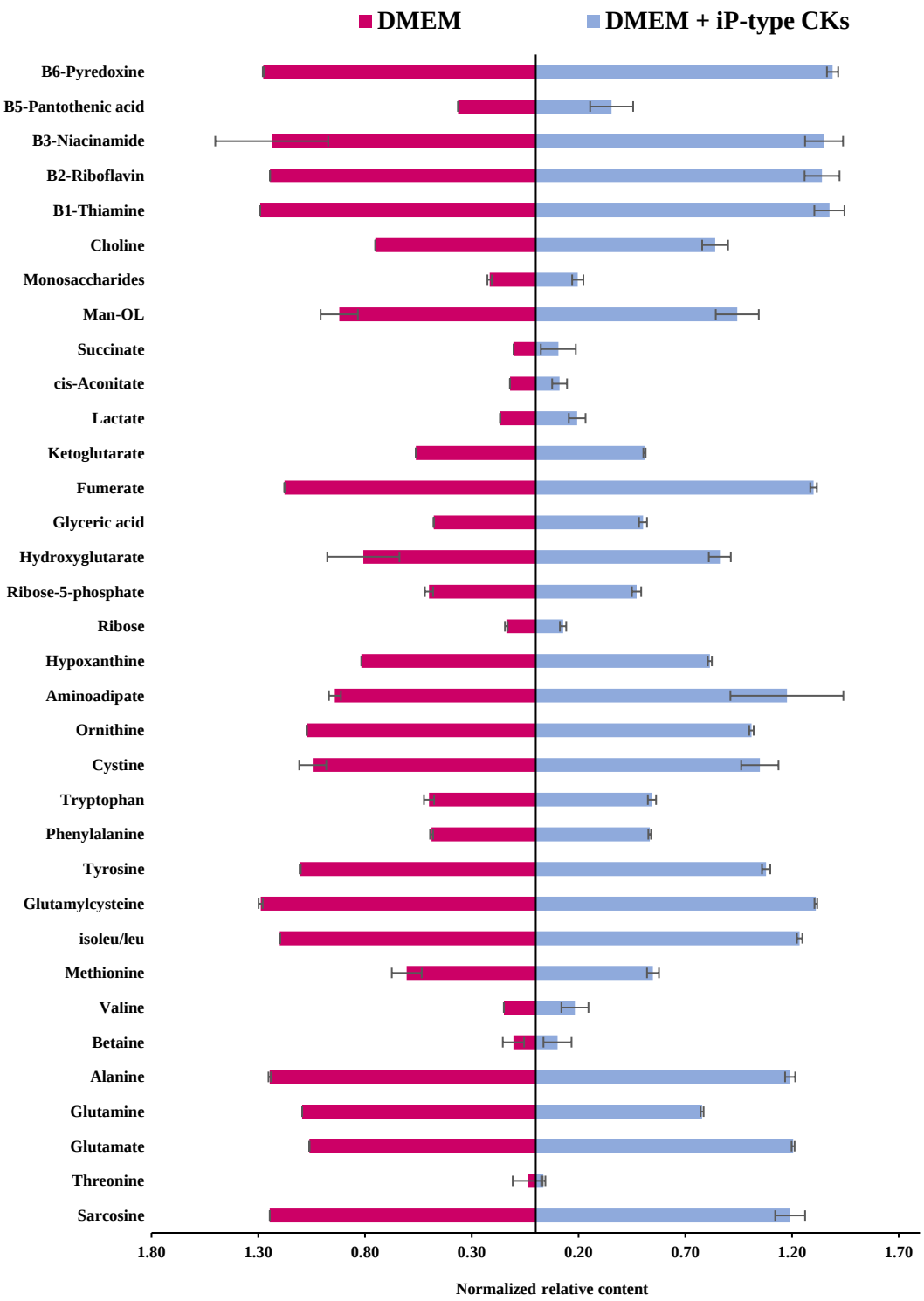

Supplementary figure 2.5: *The iP-type CK supplementation of DMEM did not interfere with detection of any metabolites. Error bars represent standard error (n=3).*

CHAPTER 3

Cytokinin and metabolic profiling during encystation of *Giardia intestinalis*

ABSTRACT

Giardia intestinalis is a protozoan parasite responsible for a diarrheal disease in mammals, but the mechanisms of disease pathogenesis are unclear. While proteins secreted by *Giardia* can affect the host cells, the presence or secretion of hormones by *Giardia* is understudied. Recently, the plant growth regulating cytokinins (CKs) were discovered in protists; however, their roles beyond plants are not well known. To investigate the involvement of CKs in the life cycle of *Giardia*, an exogenous CK was added to trophozoites induced to undergo encystation. To identify the impacts of exogenous CKs on the uptake or secretion of CKs and other metabolites during encystation, culture supernatants were analyzed by liquid chromatography-high resolution mass spectrometry. Results suggest that CK-supplementation inhibits encystation and impacts the metabolism of amino acids (e.g., dynamics of arginine decrease and increase of citrulline and ornithine) and nucleoside salvage (e.g., rate of adenosine decrease and the increase of adenine) in the culture medium across encystation stages. The up-take of CK ribosides, their catabolism into CK free bases (CK-FBs) followed by secretion of CK-FBs by encysting trophozoites, was not affected by CK-supplementation although encystation may be slightly inhibited. Overall, this is the first study to establish a link between extracellular CKs and the nucleoside salvage mechanisms of Giardia. This novel layer of cellular metabolism coincides with previous transcriptome and proteome observations.

INTRODUCTION

Giardia intestinalis encystation

Giardia intestinalis is a protozoan parasite responsible for causing one of the most common diarrheal diseases in mammals called giardiasis or "beaver fever". Annually, more than 280 million cases in humans and numerous livestock infections have made Giardia a global burden (Singer et al., 2020). Giardiasis ranges from asymptomatic cases to severe malabsorption and the reason for these differences are unclear (Adam, 2021). Giardia is an extracellular parasite, and it secretes virulence factors to affect host cells and for disease establishment (Ma'ayeh et al., 2017). Previous studies on the Giardia secretome have been restricted to proteins secreted by Giardia (Dubourg et al., 2018; Kaur et al., 2001; Lee et al., 2012; Rodríguez-Fuentes et al., 2006; Shant et al., 2002), but secretion of non-protein molecules including small signaling compounds like hormones, has not been investigated. Cytokinins (CKs) are a group of small molecules that act as signaling molecules in plants and plant-pathogen interactions (Spallek et al., 2018). Phytopathogens like bacteria and fungi synthesize CKs to establish infection within the host plant by hindering plant growth, development, and differentiation (Sarkar et al., 2023; Seng et al., 2023). Recently, the presence and roles of CKs were discovered in non-phytopathogenic bacteria and protists (Andrabi et al., 2018; Aoki, 2023; Samanovic et al., 2018), which leads us to hypothesize that Giardia can produce and utilize CKs. Chapter 2 of this thesis presented results that support this hypothesis by showing Giardia trophozoites synthesize CKs as well as take-up and metabolize endogenous and exogenous CKs during growth and nutrient deprivation conditions. This chapter extends our study by examining CK changes during the process of encystation, which is a crucial differentiation process of the parasite for its infectivity

and survival outside its host. Several transcriptome and proteome-based studies have been performed on Giardia encystation (Balan et al., 2021; Birkeland et al., 2010; Einarsson et al., 2016; Faghiri & Widmer, 2011; Faso et al., 2013; Morf et al., 2010; Rojas-López et al., 2021). However, one can only infer that the terminal products or metabolites of proteome activity are also affected, as there are no prior studies investigating any metabolites change during the encystation, except for oxygen consumption patterns (Paget et al., 1998). By uncovering the changes in metabolites during encystation, we can obtain a more complete picture of Giardia's metabolism and the changes in its extracellular environment during this process. This chapter addresses the knowledge gap regarding CK and other small metabolite exchange between Giardia and its in-vitro culture medium using an emerging approach for the study of small metabolites called metabolomics.

Giardia has a biphasic life cycle – a dormant cyst that initiates infection by entering hosts through contaminated food and water, and a vegetative trophozoite that causes disease symptoms by proliferating inside the intestinal tract of infected mammals (Faghiri & Widmer, 2011). Ingested cysts are triggered to excyst into two motile trophozoites by the acidic pH of the stomach and pancreatic proteases (Boucher & Gillin, 1990). When motile trophozoites swim down the gastrointestinal tract, some proliferate, and some undergo differentiation into a cyst – a process referred to as encystation (Adam, 2021). Factors that induce encystation include an increase in pH, an increase in bile, and changes in lipid composition of the upper intestinal tract of mammals (Barash et al., 2017; Pham et al., 2017). This differentiation process is characterized by the formation of a protective cyst wall made of proteins and carbohydrates which allow the parasite to withstand environmental stressors outside the host and continue its infectious cycle (Ebneter et al.,

2016). Therefore, characterizing the encystation process can help discern potential drug targets that can interrupt the life cycle of Giardia and reduce its global incidence.

Encystation stages

Numerous studies have highlighted distinct stages of encystation based on changes in RNA (Rojas-López et al., 2021) and protein abundance (Faso et al., 2013). During the early stage, encystation stimuli lead to initiation of components for the cyst wall. The cyst wall is composed of cyst wall protein 1 (Mowatt et al., 1995), cyst wall protein 2 (Lujan et al., 1995), and cyst wall protein 3 (Sun et al., 2003) arranged in conjunction with the carbohydrate β-1-3-galactosamine [GalNac] homopolymer (Gerwig et al., 2002). Initially, cyst wall protein 1 (CWP1) is synthesized in the endoplasmic reticulum and secreted in small vesicles called the encystation specific vesicles (ESVs), which are then transported towards the cell periphery (Faso et al., 2013). Since ESVs are membrane bound, genes and proteins related to lipid metabolism are also upregulated to encase the cyst wall material (Morf et al., 2010; Rojas-López et al., 2021). Moreover, during early encystation, genes related to cytoskeleton assembly are downregulated to promote rounding of the cell and initiate the transition to an oval shaped cyst (Kim et al., 2022).

The mid-late stage of encystation is when changes to the regulation of many metabolic pathways are detected, specifically, upregulation of energy metabolism and downregulation of amino acid and nucleoside salvage and catabolism pathways (Rojas-López et al., 2021). Moreover, the cyst wall formation progresses by the sequential arrangement of the cyst wall proteins followed by wall maturation through polymerization

using the GalNac polymer (Gerwig et al., 2002; Lujan et al., 1995; Mowatt et al., 1995; Sun et al., 2003).

During late encystation, DNA replication and recombination occurs in Giardia trophozoites by upregulation of meiosis-related genes and proteins (Balan et al., 2021; Rojas-López et al., 2021). When cyst maturation is complete, the transcriptome and proteome are drastically different than trophozoite form; although not metabolically inactive, the cyst has very little energy requirements, so all metabolic pathways are severely downregulated and protein synthesis is minimal (Rojas-López et al., 2021). However, it is important to note that more than 50% of the up or downregulation of genes are observed only in water resistant cysts compared to trophozoites. Metabolism remains active at even late encystation since the transformation of trophozoite to cyst requires maintaining or enhancing function of most cellular metabolic pathways (Morf et al., 2010).

Research objectives

From all existing knowledge of the encystation process, metabolic changes occurring during mid to late encystation are underreported (Balan et al., 2021; Paget et al., 2013). Speculations are made based on transcriptomics and proteomics but have only recently been confirmed by a global metabolism by-product screening of intracellular metabolites (Müller et al., 2020; Paget et al., 1998; Popruk et al., 2023; Vermathen et al., 2018). However, Giardia is a parasite that lacks *de novo* synthesis of many crucial molecules of basic cellular metabolism and depends on exchange of molecules with its extracellular medium for its nutritional needs along with establishment of disease and communication with the host (Dubourg et al., 2018). Therefore, studying the metabolites

of the spent medium during encystation can further confirm the findings of the transcriptomics and proteomics studies and obtain new insights into the post translational changes in cell metabolism. Along with examining the common small molecules involved in the basic metabolic processes of the parasite that are dependent on the exchange of metabolites with the host intestinal lumen, this work also aims to study the fate of CKs which are small molecules with a potential signaling role. Apart from their signaling role, CKs are well known inducers of cell differentiation in plants (Powell & Heyl, 2023). More recently, a similar dormancy promoting-role of CKs was discovered in a free-living protist *Dictyostelium discoideum* (Aoki, 2023). In addition, the knockdown of a CK synthesis gene in *Dictyostelum* by CRISPR/Cas9, resulted in subtle subcellular and metabolic pathway changes which were apparent through a global metabolomics approach (Aoki, 2023). Therefore, one aim of the work in this chapter is to examine the effect of adding an exogenous CK to Giardia cells induced to encyst and determine if this will have effects on its growth and ability to encyst. Furthermore, metabolite profiling of spent medium from these cultures will be performed, which is an indicator of the uptake and secretion of these molecules by Giardia during encystation. These results will give us a better picture of metabolic needs of this parasite and understand the potential role of CKs during its life cycle.

MATERIALS AND METHODS

Cell culture conditions

Giardia intestinalis trophozoites from the WB C6 clonal line (Assemblage A, ATCC 50803) were used in all experiments. Giardia encystation was achieved by implementing the Uppsala protocol (Einarsson et al., 2016). Briefly, trophozoites were grown to confluence in modified TYDK medium containing a bovine bile concentration of 0.1 g/L and a pH of 6.8, within 16 mL screw-cap glass culture tubes at 37°C. The medium and unattached trophozoites were decanted and the tubes were refilled with 'encystation medium' which is TYKD medium with a 12.5-fold higher bile concentration (1.25 g/L) and an elevated pH of 7.8. Post-induction of encystation timepoints (0-, 7-, 14-, 21-, and 28-h) were selected to coincide with previous transcriptomics and proteomics data (Balan et al., 2021; Rojas-López et al., 2021). Cell counts were taken at each timepoint using an automated cell counter (ViCell XR cell viability analyzer, Beckman-Coulter) to determine cell density.

Cytokinin supplementation

The Giardia growth medium (TYDK) was supplemented with a synthetic cytokinin (N^6-benzyladenine riboside (BAR) at 1 μM (OlChemIm Ltd.). The absence of endogenous BAR in the TYDK medium facilitates clear tracking of its modifications over time. Moreover, since BA-type CKs are known to be active in a variety of biological systems (Ishii et al., 2003; Doležal et al., 2007; Aoki et al., 2019), they could also be tested for their effect on the differentiation of Giardia trophozoites. In addition, as evident in Chapter 1,

BAR or other CK-ribosides are readily utilized by trophozoites and converted to their respective freebase derivative, we can expect BAR to be processed similarly by encysting trophozoites. To prepare hormone stock solutions, CKs were solubilized in a minimal volume of 1 M NaOH and diluted with HPLC-grade methanol (CH_3OH) to obtain a stock solution (320 μM). Solutions were filter sterilized (Midi 0.2 μm PVDF centrifugal filter, Canadian Life Science) by centrifugation (3724 × g, 4℃, 4 minutes; Allegra X-14R, Beckman Coulter). To obtain a working concentration of 1 μM, 50 μL of each CK solution were added to respectively labeled 16 mL culture tubes containing trophozoites and to the cell-free medium (medium-blank) at the 0-h time point. Control culture tubes were supplemented with 50 μL of methanol.

Immunofluorescence Assay (IFA)

The successful induction of encystation was assessed by tracking the appearance and localization of a cyst wall protein in Giardia cells by immunofluorescence microscopy assays (IFA). Briefly, trophozoites were harvested from control and BAR-supplemented cultures at 0-, 7-, 14-, 21-, and 28-h post induction of encystation (PIE) and attached to 0.1% polyethylenimine coated coverslips followed by methanol fixation, cellular permeabilization, and blocking. The coverslips were then hybridized with a monoclonal clonal antibody against cyst wall protein 1 (CWP1) conjugated to CY3 fluorophore (Waterborne Inc) diluted 1:60 and incubated for 1 h at 37℃. The coverslips were affixed onto glass slides with a mounting medium containing 4’,6-diamidino-2-phenylindole (DAPI) (Vector Laboratories catalog no. H-1200)

Slides were visualized on an upright fluorescence microscopy (Leica microsystems; DM6000 B) as described in (Horlock-Roberts et al., 2017)**.** All images were viewed at either 40x or 100x magnification under oil immersion. Images were analysed using Leica Application Systems suite X (LAS-X).

Western blot

The induction of encystation was also assessed by determining the level of CWP1 in cells harvested at 0-, 7-, 14-, 21-, and 28-h PIE, by using western blotting**.** Approximately 2.5×10^7 cells were resuspended in 195 µL of RIPA lysis buffer (150 mM NaCl, 75 mM NaOH, 80 mM glycine, 1% IGEPAL CA-630 [Sigma-Aldrich], 0.1% SDS, 1x protease inhibitor cocktail [BioShop Canada Inc.], 10 mM DTT, 1 µg/mL leupeptin; 10.6 pH) and incubated at 4°C for 15 minutes on a rotisserie. The samples were then centrifuged at 4°C for 15 min at 10,000×g and the supernatants were analyzed on a 14% polyacrylamide gel. The proteins on the gel were then transferred to a nitrocellulose membrane at a constant 25 V for 25 min, at RT (BioRad Trans-Blot Turbo Transfer System). The blot was stained with Ponceau (BioShop Canada Inc.) to determine the relative amount of protein loaded into each lane. The blot was then hybridized with a monoclonal clonal antibody against cyst wall protein 1 (CWP1) conjugated to Alexa647 (Waterborne Inc.) at 1:1000 dilution and incubated at 4°C overnight. The direct immunostaining of CWP1 on the blot was visualized under the red LED epifluorescent in a gel imager (Biorad ChemiDoc MP). The fold change in CWP1 over the time course was determined as follows. The intensity of the CWP1 band and the Ponceau staining in each lane of the blot was captured in the gel imager (Biorad Chemidoc MP) and analyzed by the

BioRad ImageLab software. The densitometry value of each CWP1 band was normalized by dividing it by the value for the Ponceau staining that represents the relative total protein in each lane. This normalized value for CWP1 at each time point was then divided by the normalized CWP1 value for the 0-h PIE sample that is used as the calibrator to determine the relative CWP1 expression value.

Supernatant collection

Based on chapter 1, it is expected that the peptone, yeast extract, bile and serum can contribute to background CKs and numerous other metabolites in the TYDK encystation medium. To examine the dynamics of extracellular CKs during encystation, three replicates of supernatants were collected at each time point from control and BAR-supplemented cultures. Culture tubes were chilled on ice for 15 minutes to help detach the trophozoites, and then centrifuged (2200 × g, 4℃, 15 minutes) so that 5 mL of cell-free supernatant could be collected from each sample for immediate freezing in liquid nitrogen. Additionally, medium-blanks (medium never exposed to trophozoites) were collected as negative controls for extracellular CK and metabolite levels at the beginning and end of the time course for the control culture and at all time points for the BAR-supplemented culture. All samples were frozen, lyophilized and stored at -80℃ until further processing.

Cytokinin and metabolite extraction and purification

A highly efficient cytokinins and metabolite extraction from control and BAR-supplemented medium-blanks and culture supernatants was achieved from a single sample by slight modifications to previously published hormone and metabolite extraction

protocols (Sarkar et al., 2023). Briefly, after passive extraction of analytes (CKs and metabolites), along with 10 ng of ^{2}H-labeled CK internal standards (Kisiala et al., 2019) from homogenized samples using ice-cold 50% acetonitrile, a mixture of the HLB cartridge flow-through and 30% acetonitrile extract was collected (Šimura et al., 2018). The resulting extract was divided into two equal parts for separated downstream processing of CKs and metabolites. The metabolite fraction was reconstituted in 90% acetonitrile and transferred to insert-equipped glass MS vials, while the CK fraction was reconstituted in 1M HCO_2H to ensure complete CK protonation. CKs were isolated and further purified out of the sample matrix through mixed-mode, cation-exchange, solid phase extraction (SPE) cartridges (MCX 6cc/500mg, Canadian Life Sciences) using a vacuum manifold followed by derivatization of NTs into RBs and further purification on C18 cartridges (C18 6cc/500mg; Canadian Life Sciences). Resultant CK residues were redissolved in 0.5 mL of initial mobile phase conditions (H_2O:C_2H_3CN:CH_3CO_2H = 95:5:0.08, v/v/v). Sample vials were stored at -20°C until mass spectrometry analysis.

Cytokinin profiles of the encystation medium-blanks, control and BAR-supplemented culture supernatants were analyzed by the Ultimate3000 UHPLC system (Thermo Scientific) coupled with the Orbitrap QExactive mass spectrometer (Thermo Scientific) (Kisiala, et al., 2019). A 25 µL aliquot was injected onto the reversed phase C_{18} column (Kinetex, 2.6 µm particle size, 2.1 × 50 mm, Phenomenex). A gradient of mobile phase A (0.08% CH_3CO_2H in H_2O) and mobile phase B (0.08% CH3CO_2H in C_2H_3OH) was used to separate and elute CKs at a flow rate of 0.5 mL/min. The gradient was initiated at 5% B for 0.5 min, linearly increasing to 45% B over 4.5 min with a subsequent increase to 95% B over 0.1 min, a hold for 1 min, followed by an instantaneous drop to initial conditions (5% B) and a hold for 2 minutes for column re-equilibration. Total run time was

8.2 minutes. All CK analytes were detected and quantified in positive ionization mode using parallel reaction monitoring (PRM) mode. The HESI-II capillary temperature and auxiliary gas heater temperature were 250℃ and 450℃, respectively. Sheath, auxiliary and sweep gasses were operated at 30, 8 and 0 (arbitrary units), respectively, with a maximum spray current of 100 μA, spray voltage of 3.9 kV and S-lens RF level of 60. Data were acquired at a resolution of 35,000 at *m/z* 200 and precursor ions were isolated at m/z 1.2 window width, with automatic gain control of 1×10^6 and maximum injection time of 128 ms.

Metabolite profiles of the encystation medium blanks, control and BAR-supplemented culture supernatants were analyzed. Prior to ultra high-performance liquid chromatography-high resolution accurate mass-full scan mass spectrometry (UHPLC-(HRAM)-FS-MS) analysis, a mixture of stable isotope labeled canonical amino acids (0.25 μM; Cambridge Isotope Laboratories) was added to all samples for normalization. Moreover, 10-15 μL all control samples (medium-blanks and culture supernatants) were mixed together to make a pooled sample while same volume of all BAR-supplemented samples (medium-blanks and culture supernatants) were mixed to create another pooled sample mixture to perform data dependent acquisition experiments. Metabolites were resolved with a Kinetex C18 column (2.1 × 50 mm, 2.6 μm). Total 25 μL of each sample was injected into a Dionex UltiMate 3000 HPLC (ThermoFisher) coupled to a QExactive Orbitrap mass spectrometer (ThermoFisher). A flow rate of 0.2 mL/min was used with a mobile phase of 0.08% acetic acid in water (A) and 0.08% acetic acid in acetonitrile (B). The following gradient was used to elute the analytes: mobile phase B was held at 0% for 1.25 min to retain the compounds on the column and avoid the metabolite elution in the void volume before increasing to 50% over 2.75 min and to 100% over the next 0.5 min.

Solvent B was then held at 100% for 2 min before returning to 0% over 0.5 min for 4 minutes of column re-equilibration. Orbitrap QExactive was operated with a heated electrospray ionization (HESI) probe in positive and negative mode (Kisiala et al., 2019). Each sample was analyzed using a mass range of *m/z* 70−900, and data were acquired at 70,000 resolution, automatic gain control (AGC) target of 1×106, and maximum injection time (IT) of 100 ms.

Data analysis

Cytokinin identification and quantification was done using Xcalibur software (ThermoFisher v.3.0.63). Quantification of CKs was performed by isotope dilution analysis based on the recovery of ^{2}H-labeled internal standards (Kisiala et al., 2019). Cytokinin concentrations for supernatant and medium-blank samples are expressed as pmol/mL. All data points represent an average of three replicate samples and error bars show standard error.

Since this was the first study evaluating the extracellular metabolite profile of Giardia trophozoites during encystation, we used a global metabolomics approach with a customized processing method containing the following groups of analytes: free amino acids and derivatives, DNA metabolism related, organic acids, vitamins (*Chapter 2: Supp. table 2.1*). However, only the free amino acids and DNA metabolism related compounds were analysed in this experiment since previous results (*Chapter 2: Figure 2.5 and 2.6*) showed that these two groups of metabolites have the most relevant changes. Metabolite identification was based on accurate mass (10 ppm mass error) and comparison of retention times to labeled internal standards (canonical amino acids). Free amino acids were

identified by comparison of retention times to internal standards while DNA related metabolites were identified using accurate precursor mass (unfragmented compound mass/charge) matched to databases (PubChem, MET) (Schrimpe-Rutledge et al., 2016). For compound quantification, relative concentration of metabolites found in the samples were calculated by normalizing the peak area of each metabolite in each sample to the median recovery of the labeled amino acids in that sample. Therefore, the relative change in content of a metabolite can only be compared to itself over time.

RESULTS

Encystation induction verification

To verify successful induction of encystation in-vitro, trophozoites collected from control and BAR-supplemented cultures were subjected to immunofluorescence assay (IFA) to visualize cell shape, nuclei number per cell, and the appearance and localization of the Cyst Wall Protein 1 (CWP1) at various time points post induction of encystation (*Figure 3.1*). At 0 h PIE, trophozoites are tear drop in shape with visible flagella, have two nuclei per cell, and do not show CWP1 staining. At 7-h PIE, cells showing diffuse CWP1 staining in the cytosol start to appear. At 14-h PIE, cells showing punctate staining of CWP1 appear and these cells are rounder in shape. By 21-h PIE, CWP1 is found in a structure enclosing the cell surface. By 28-h, cells appeared refractile (DIC mode) and contained a complete cyst wall. Some cells encased in a partial or complete cyst wall at 21- and 28-h PIE showed more than 2 nuclei as shown in 21-h PIE DAPI column, indicating cell division during or after cyst wall formation.

Western blot analysis of CWP1 expression in the control and BAR-supplemented cultures showed that it increased over time PIE (Figure 3.2). For the control culture, the relative CWP1 protein expression increased from 2.9-fold at 7-h, to 8.6 fold at 14-h, 10.5 fold at 21-h and 9.7 fold at 28-h PIE, whereas for the BAR-supplemented culture, the increase in relative CWP1 expression was only 1.6 fold higher at 7-h, 6.9 fold at 14-h, 6.8 fold at 21-h and 5.9 fold at 28-h PIE (*Figure 3.2 B*).

Cytokinin profile of encystation medium-blanks

Due to the relatively high abundance of CKs known to occur in unaltered TYDK, medium-blanks were analyzed at the 0- and 28-h time points for the control culture, whereas for the BAR-supplemented culture, medium-blanks were analyzed at all time points to ensure that the CK profile in the medium never exposed to cells, remain relatively constant throughout incubation.

A total of six CKs were detected in the medium-blanks, including three iP-type CKs: iP, iPR iPRP, three 2MeS-type CKs: 2MeSiP, 2MeSiPR, and 2MeSZR. No differences were observed in the levels of iP-type and 2MeS-type CKs detected in the control medium-blanks between 0 h and 28-h (data not shown) or in the BAR-supplemented medium-blanks at any time points (*Figure S 3.1*). The CK profile of the medium-blanks were dominated by iP-type CKs (iPRP ~ iPR >iP), followed by the three 2MeS-types CKs (< 2 pmol/mL) (*Figure S 3.1 A, B*). Additionally, BAR was detected in the BAR-supplemented medium-blanks and the concentration of BAR was significantly lower at 7 h compared to 0 h but no other derivatives (BA or BARP) were detected, and the level remained stable thereafter (*Figure S 3.1 C*).

Extracellular CK profile during encystation

To profile extracellular CKs, supernatants were collected from the spent medium from the control and BAR-supplemented encysting cultures at 0-, 7-, 14-, 21-, and 28-h. Analysis of culture supernatants revealed that the presence of Giardia resulted in significant changes of most background CKs present in the encystation medium over time. Moreover,

changes of most CKs throughout the time course did not differ significantly between the control and BAR-supplemented culture supernatants with the exception of iP at the 21 h time point and MeSiP at the 14 h time point (*Figure 3.3*). The most prominent extracellular CK changes were decrease of iPR, and an increase of its respective freebase derivative, iP (*Figure 3.3 A*). The levels of iPR decreased from over 150 pmol/mL to a negligible level (< 0.5 pmol/mL) after 21 hours post induction. Inversely, iP levels increased from under 10 pmol/mL up to 190 pmol/mL during the same time course (*Figure 3.3 A*). In parallel, MeSiPR decreased from over 0.1 pmol/mL to undetectable levels at the end of the time course, while the levels of its corresponding freebases, MeSiP increased from under 0.2 pmol/mL up to 0.6 pmol/mL (*Figure 3.3 B*). A similar decreasing pattern was observed for MeSZR, however, the freebase derivative (MeSZ) was not detected (*Figure 3.3 C*). Levels of all CKs detected in the supernatants were significantly different between the 0-h and the end of the time course except for iPRP which fluctuated insignificantly throughout the induction period in both control and BAR-supplemented culture supernatants (*Figure S 3.2*).

In the BAR-supplemented culture supernatants, the most prominent change detected was the decrease of BAR with a simultaneous increase in BA concentration throughout the 28-h incubation period (*Figure 3.4*). The BA increase was not as sharp as the increase of other free bases (iP and MeSiP). The concentration of BA detected at the 28-h time point was approximately half of the BAR concentration at 0-h indicating that much of the BA was likely retained within the encysting cells.

Extracellular metabolite profiles during encystation

To profile extracellular metabolites exchanged by Giardia trophozoites during encystation, supernatants were collected from control and BAR-supplemented cultures at 0-, 7-, 14-, 21-, and 28-h timepoints. Analysis was focused on two metabolite groups found to change prominently during trophozoite growth in Chapter 1: the free amino acids and DNA related metabolites, specifically nucleosides and nucleobases. The amino acids were identified using level 1 accuracy by comparison to labeled internal standards available for quantification while the DNA related metabolites were identified using their unfragmented compound mass which represents compound identification level 3 (see methods).

The DNA related metabolites and free amino acids detected in the supernatants showed changes over time. Of the twenty total amino acids detected, meaningful trends were observed in the three amino acids involved in the energy metabolism involving the arginine dihydrolase pathway (arginine, citrulline and ornithine) and two other amino acids involved in metabolic pathways (serine and alanine). Arginine rapidly decreased to an undetectable level by 14-h PIE while the levels of citrulline and ornithine increased and plateaued at 14-h PIE in both control and BAR-supplemented culture supernatants (*Figure 3.5 A, C*). Similarly, serine decreases, and alanine increases in the supernatants of both control and BAR-supplemented cultures, but the changes are gradual (*Figure 3.5 B, D*).

Within the DNA related metabolite group, nine nucleosides and six nucleobases were detected. Most detected nucleosides (adenosine and deoxy-methylthio adenosine [dMTA], thymidine, uridine, and inosine) decreased gradually over time while some

corresponding nucleobases (adenine, thymine, uracil and hypoxanthine) increased over time in the control and BAR-supplemented culture supernatants (*Figure 3.6*).

Within the detected nucleosides, purines (dMTA, adenosine, and inosine) were gradually depleted from the medium to negligible relative contents by 21-h PIE after which no change was observed, while the pyrimidine nucleosides (thymidine, uridine) decreased sharply until 7-h PIE after which no further decrease was observed (*Figure 3.6 A, C*). Moreover, all nucleosides decrease more gradually in the BAR-supplemented culture compared to the control culture (*Figure 3.6 A, C*). On the other hand, the continued increase of all nucleobases stopped at 14-h PIE in both the control and BAR-supplemented cultures; however, the increases were sharper and higher in the control culture compared to the BAR-supplemented culture up to the 14 h time point (*Figure 3.6 B, D*).

DISCUSSION

This is the first study to characterize the CK and metabolite exchange between Giardia and its medium during the formative process of encystation. The observations of endogenous CK changes during encystation were documented followed by an assessment of the impacts of externally supplied CK (BAR) on the encystation process.

The verification of successful induction of encystation in-vitro in unsupplemented (control) and BAR supplemented Giardia cultures was monitored by IFA through the appearance and localization of Cyst Wall protein 1 (CWP1), which is a widely used marker of the encystation process (*Figure 3.1*). The protein level of CWP1 in the cultures were also determined by western blot analysis (*Figure 3.2*).

Giardia trophozoites must undergo development into cysts to survive outside of the host and to establish new infections. This transition is called encystation, and the cellular changes associated with this process have been well established (Ebneter et al., 2016; Einarsson, Troell, et al., 2016; Frances D. Gillin et al., 1987; Kim et al., 2022; Lujan et al., 1995; Mowatt et al., 1995; Thomas et al., 2021). Soon after the trophozoites receive encystation stimuli in-vitro through an increase in the bile concentration and higher pH, the trophozoites start the synthesis of cyst wall components including cyst wall proteins (CWP-1, 2 and 3) and the carbohydrate polymer ‘giardin’ (Ebneter et al., 2016). After synthesis of CWP1 in the ER, it is packaged in encystation specific vesicles (ESVs), which are gradually trafficked to the cell periphery. At the late stages of encystation, the cyst wall proteins are released from the ESVs to form the protective wall that surrounds the cell. IFA of the BAR-supplemented and control Giardia cultures showed the expected

appearance of CWP1 after the induction of encystation, its initial localization in ESVs at 7 and 12 h PIE, and then its final localization in the cyst wall at 21 h and 28 h PIE (*Figure 3.1*). An increase in the level of CWP1 protein in control and BAR-supplemented cultures was also observed by western blot analysis as encystation progressed *(Figure 3.2)*.

The trophozoite is a tear-drop shaped, motile cell with 4 pairs of flagella and two nuclei which transforms into a circular or oval shaped refractile cyst during encystation (Gillin,' et al., 1989). In the early stages of encystation, the cytoskeleton is disassembled (Morf et al., 2010) which leads to a rounded cell shape during mid encystation. This was also seen in this study at 14-h PIE in the DIC image. Finally, a refractile oval shaped cyst (DIC) with a complete cyst wall (CWP1) was observed in late encystation at 28-h PIE (*Figure 3.1*), consistent with previous reports (Schupp et al., 1988; Thomas et al., 2021). The two nuclei of the trophozoite enclosed in each cyst divide and then undergo DNA replication without cell division to produce a cyst containing four nuclei each containing 4N of DNA each, which results in a 16N cyst (Bernander et al., 2001). Cysts with >2 nuclei/cell were also observed in 21-h and 28-h PIE in this study (*Figure 3.1*), furthering confirming that the induction of encystation was successful.

Strikingly, the BAR-supplemented culture exhibited only half of the fold-increase of CWP1 compared to control culture throughout encystation suggesting that BAR may have an inhibitory effect on encystation (*Figure 3.2*). The application of BAR at the same concentration in trophozoite cultures did not induce any difference in growth or morphology (*Chapter 2, Figure 2.2*). The effects of BA-derivatives on plant growth and differentiation are widely studied (Doležal et al., 2007); however, beyond plants, the most widely known role of BA type CKs is the anticancer and antioxidative properties in human

models (Jabłońska-Trypuć et al., 2016). The anticancer property is proposed to be through the inhibition of various protein kinases that regulate the cell cycle and hinder cell proliferation (Doležal et al., 2007). On the other hand, BAR and BA were found to induce differentiation of human skin fibroblasts and leukemia cell lines again by inhibiting growth (Ishii et al., 2003). In contrast, the BAR supplementation in my experiment seems to inhibit Giardia differentiation into cysts by approximately 50%. How the addition of BAR could inhibit Giardia differentiation but have no effect on the growth of vegetative trophozoites is unknown. However, since this observed reduction of encystation in the BAR spiked culture is based only on a single biological replicate, it is not possible to draw definitive conclusions at this time.

Giardia is an parasite that depends on the exchange of many small molecules for its nutritional needs and for initiating and maintaining infection within a host since it lacks *de novo* synthesis pathways of most essential small molecules (Adam, 2021). The proteins and enzymes in the secretome of Giardia have been characterized to gain insights into its pathogenic mechanisms (Dubourg et al., 2018; Ma'ayeh et al., 2017). However, other small secretory molecules that could serve as a communication signal between Giardia and the host have not been reported. This work is the first to discover the presence of a class of phytohormones called cytokinins (CKs) in Giardia along with capacity of Giardia trophozoites to scavenge and secrete CKs during trophozoite growth and nutrient deprivation (*Chapter 2*). Thus, the aim of this experiment was to identify the nature of exchange of CKs between the medium and Giardia during the crucial transition from trophozoite to its infectious cyst stage. To accomplish this, extracellular medium, also referred to as spent medium, was collected from cultures incubated with encysting

trophozoites. Since the encystation medium already has CKs, an exogenous CK, BAR, was supplemented into the medium to facilitate its clear tracking.

During encystation, a CK profile similar to that of vegetative trophozoites was observed. All riboside CKs (BAR, iPR, MeSZR, and MeSiPR) were present in varying concentrations in the medium initially, but they decreased to undetectable levels by the end of the time course (*Figure 3.3*). However, the decreases of CKs during encystation were more rapid compared to vegetative trophozoite growth and the changes halted by 14- or 21-h PIE in both control and BAR-supplemented encysting cultures. Meanwhile, most corresponding free base CK derivatives (BA, iP, and MeSiP), except MeSZ, increased approximately to a concentration similar to the initial CK-RB levels in the culture medium. This suggest that these CK-RB levels detected at the start of the experiment are converted completely to their free base forms by the end of the 21-h incubation period. Similarly, the level of BAR (another CK-RB) decreased to negligible levels by 21-h PIE. However, the corresponding free base form, BA, only increased only up to half of the initial BAR added to the medium (*Figure 3.4*), which suggested that some of the catabolized BA may retained by the encysting trophozoites.

While CK-RBs levels decreased and are presumed to be up taken by Giardia from the extracellular medium, the nucleotide derivative iPRP did not change within the culture supernatants over time. This observation is consistent with a previous report that indicated that the charge of the nucleotides from their phosphate groups makes them unable to cross the plasma membrane (Pinheiro et al., 2008). Instead, the common purine and pyrimidine nucleotides are catabolized by phosphatases like ATPases, ADPases and ecto-5`-nucleotidase enzymes that are present on the external surface of the cell membrane to

produce nucleosides or nucleobases for uptake by the cell (Pinheiro et al., 2008; Russo-Abrahão et al., 2011). Since the potential substrate specificity of these ecto-enzymes towards CKs is unknown, the results of this study suggest that iPRPs are not suitable substrates for these enzymes, as no substantial change was observed in the extracellular levels during encystation. The extracellular CK profile during encystation closely resembles the extracellular CK changes during vegetative trophozoite growth and during nutrient deprivation (*Chapter 2*). This is consistent with the global transcriptomic and proteomic data showing great similarities between cellular metabolism in uninduced and trophozoites induced to encyst, up until the cyst maturation stage (Einarsson, Troell, et al., 2016; Morf et al., 2010; Rojas-López et al., 2021). Most of the downregulation of metabolic pathways associated with encystation does not occur until the late stages of encystation or until complete cyst maturation (Morf et al., 2010), which would correspond to the 21-h and 28-h timepoints in our study.

The encystation process in Giardia has been widely studied at the transcript and protein level but not in detail at the metabolite level. To address this lack of knowledge, this study examined the exchange of small molecules involved in various metabolic processes between encysting trophozoites and their in-vitro culture medium by metabolomics analysis of the supernatants obtained from the control and BAR-supplemented cultures. Based on the results from Chapter 2, the focus was on free amino acids, nucleosides and nucleobases. Due to its parasitic lifestyle, Giardia depends solely on salvage of amino acids involved in energy metabolism such as the arginine dihydrolase pathway or alanine synthesis pathway (Morrison et al., 2007). During the entire encystation process, there is a requirement of high energy metabolism for successful transition of

trophozoites to cysts (Einarsson et al., 2016). For example, large amounts of cyst wall materials need to be synthesized and exported to the cell surface. Thus, it is expected that the arginine dihydrolase activity for energy production would continue during encystation, potentially at a higher rate than a non-encysting trophozoite culture. This is consistent with the rapid up-take of arginine and secretion of by-products citrulline and ornithine into the encystation medium with no notable difference between the control and BAR-supplemented supernatants (*Figure 3.5*). The exchange of these amino acids was completed within 14-h PIE during encystation while it took 21-h for proliferating trophozoites to utilize all available arginine from the culture medium (*Chapter 2 Figure 2.5*). This result supports the high energy production needed from early to mid encystation (Rojas-López et al., 2021). However, the export of alanine along with the import of serine remained gradual throughout encystation suggesting that alanine import is not as crucial as arginine import for the differentiation of Giardia.

In addition to Giardia's inability to synthesis of some amino acids, Giardia also lost capability for *de novo* synthesis of nucleotides for DNA replication. As a result, Giardia developed a simple salvage pathway to obtain all its raw nucleobases in the form of nucleosides from the host intestinal lumen (Adam, 2021; Morrison et al., 2007). Once nucleosides are imported through broad specificity transporters that recognize the sugar moiety, catabolism of the ribose occurs to obtain a free base (Aldritt et al., 1985; Baum et al., 1993; Wang & Aldritt, 1983). Subsequently, a phosphoribose molecule is added to the free base to create a nucleotide while the excess free bases are discarded to maintain a constant concentration gradient (Ey et al., 1992; Munagala & Wang, 2002; Sarver & Wang, 2002). During encystation, nucleoside salvage continues until mid-to-late encystation in

preparation for DNA replication to occur in late encystation that results in an 16N cyst (Einarsson, Troell, et al., 2016; Rojas-López et al., 2021). This is consistent with my observations whereby uptake of all nucleosides continued or was completed by 21-h PIE and halted thereafter (*Figure 3.6*). While the uptake of nucleosides was irregular in the encysting control culture, the pattern of decrease of nucleosides in the BAR-supplemented culture is likely due to the reduced encystation efficiency in the BAR-supplemented culture. In conjunction with the decrease of nucleosides, the respective free bases continued to be secreted into the culture medium until 21-h PIE which was also consistent with the idea that nucleoside salvage continues until 21-h PIE (Einarsson, Troell, et al., 2016; Sulemana et al., 2014).

Overall, comparing the nucleoside profiles with CK-RBs and the nucleobase profiles with CK-FBs during encystation, it is evident that CK uptake and secretion likely occurs through transporters and enzymes of the nucleoside salvage pathways due to structural similarity. The transport of CKs through common purine transporters is well recognized in planta (Hluska et al., 2021). In non-plant organisms, the notion of CK signaling or role in cell biology is often undermined due to absence of CK-specific receptors or transporters (Hughes & Sperandio, 2008; Sperandio et al., 2003). However, the structural similarity of CKs to adenosine and ATP - one of the most evolutionarily conserved signaling molecules (Verkhratsky & Burnstock, 2014), along with the multi-faceted nature of purine transporters (Hluska et al., 2021) provide a rationale for interkingdom communication.

FIGURES

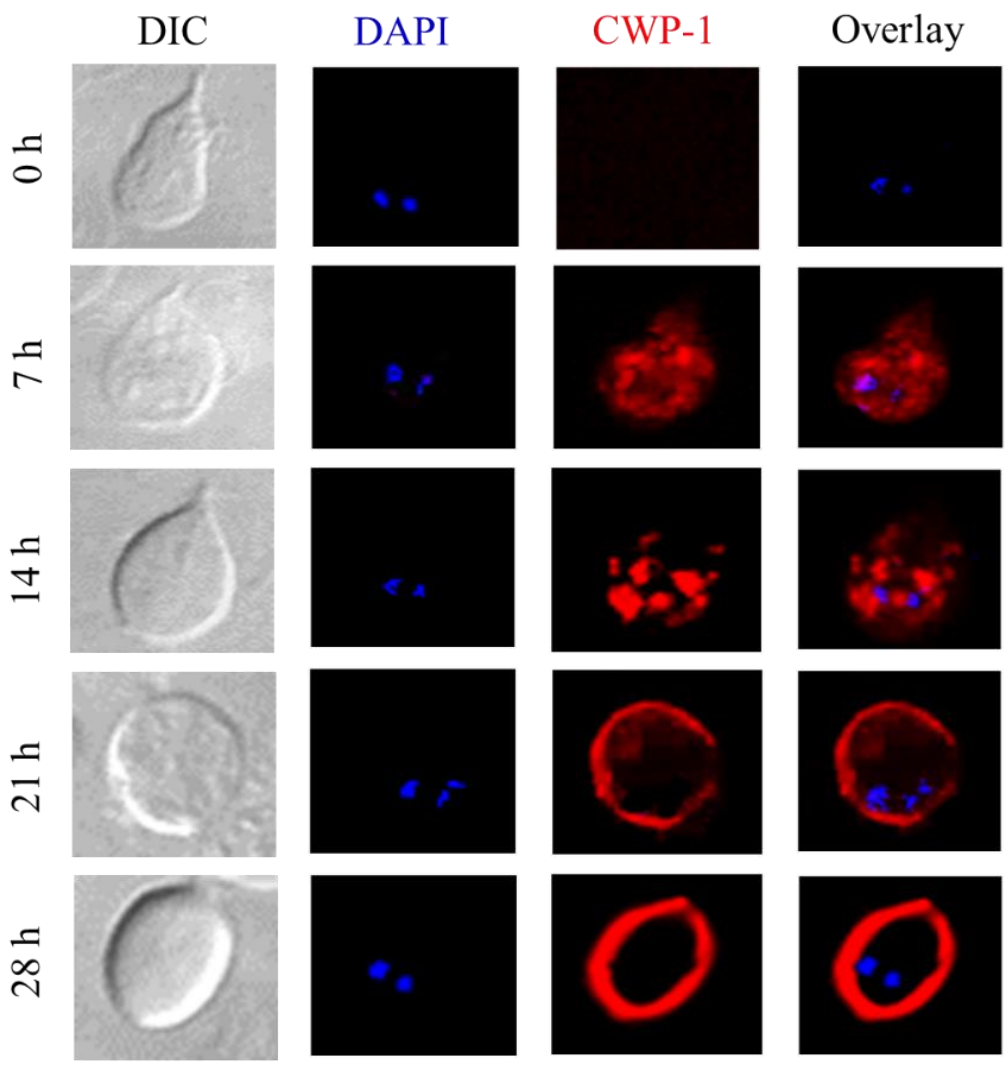

Figure 3.1: *Immunofluorescence assay of encysting cells from the control cultures at 0, 7-, 14-, 21-, and 28-hour post induction. The first column shows differential interference contrast image of encysting trophozoites, second column shows nuclei stained with DAPI, the third column shows CWP1 localization, and the fourth column shows overlay of the DAPI and CWP1 staining. No morphological differences (DIC) or differences in localization of CWP1 were observed in encysting cells obtained from control compared to BAR-supplemented cultures at any time point. At each timepoint, slides were prepared in triplicate and the images shown are cells randomly selected from either of the replicate slides at each time point.*

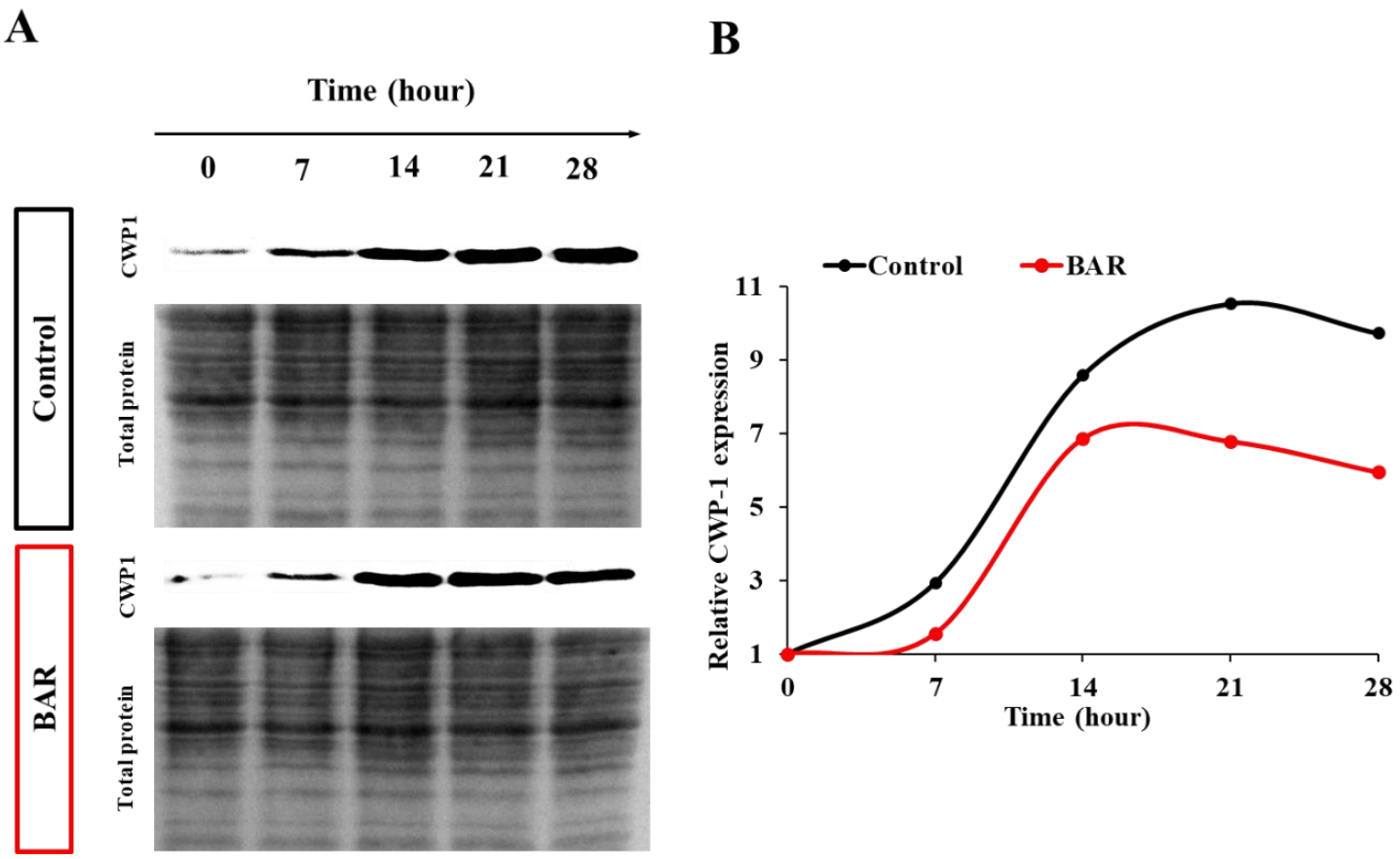

Figure 3.2: *CWP1 protein expression normalized to total protein obtained from cells of the control and BAR-supplemented cultures at 0, 7-, 14-, 21-, and 28-hour post induction. (A) Western blot with CWP1 antibody is shown with the corresponding Ponceau stain of the membrane below. (B) The expression of CWP1 normalized to total protein and relative to 0 h PIE. Each data point is from one cell pellet.*

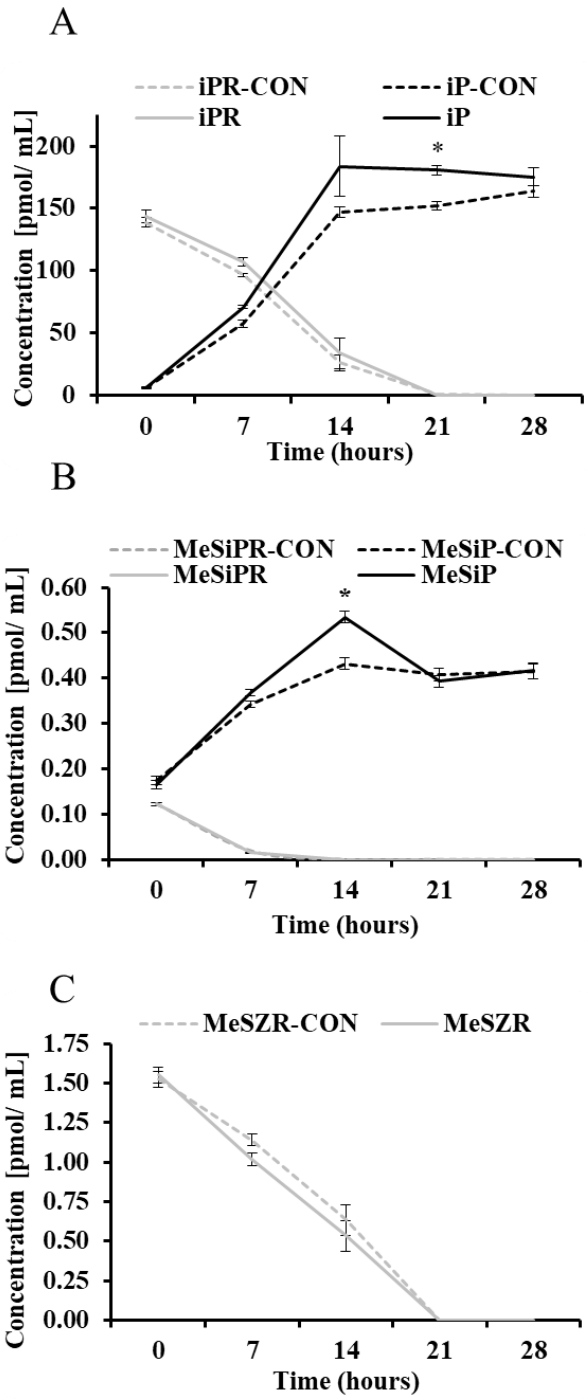

Figure 3.3: *Dynamics of extracellular CKs (iP-type: iPR and iP, A), (2MeS-type: MeSiPR and MeSiP, B; MeSZR, C) detected in the control (dotted lines) and BAR-supplemented (solid lines) culture supernatants over a 28-h encystation induction period. Asterisks show significantly different CK concentration between the control culture compared to the BAR-supplemented culture at a particular time point (Two-way ANOVA, test; Dunnett's post hoc test, $p < 0.05$). Error bars represent standard error (n=3).*

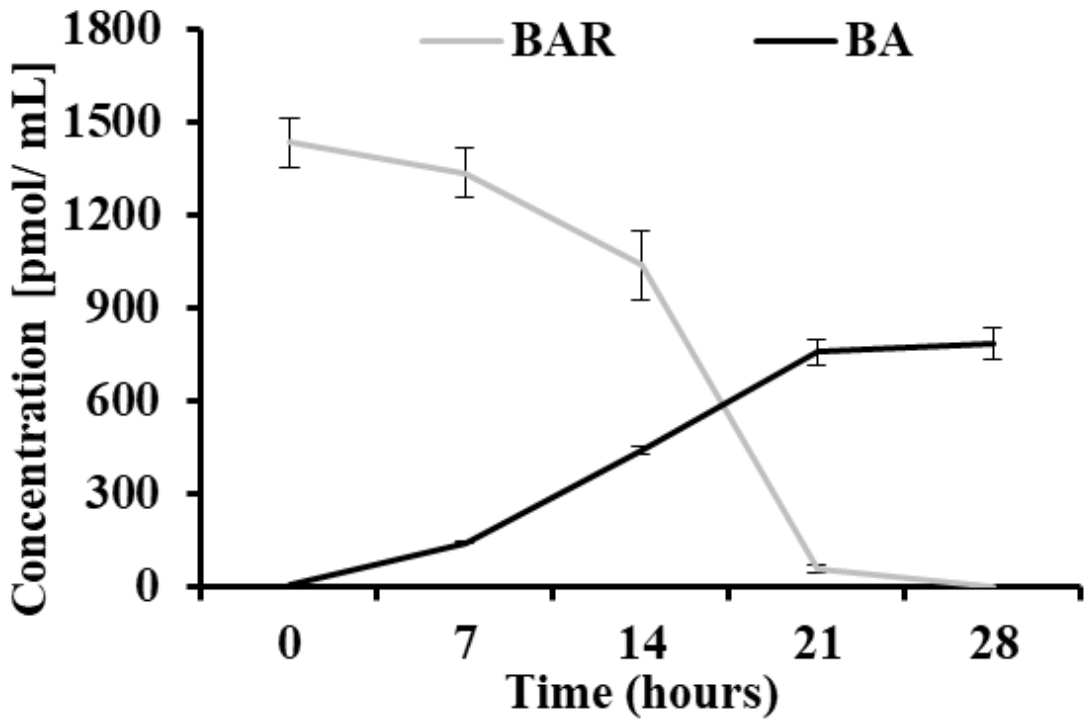

Figure 3.4: *Dynamics of BA-type CKs (BAR and BA) detected in the BAR-supplemented culture over a 28-h encystation induction period. Asterisks show significantly different CK concentrations at each time point (7-, 14-, 21-, and 28-h) compared to the respective CK concentration at the beginning of the time-course (0-h) (One-way ANOVA, Dunnett's post hoc test; $p < 0.05$). Error bars represent standard error (n=3).*

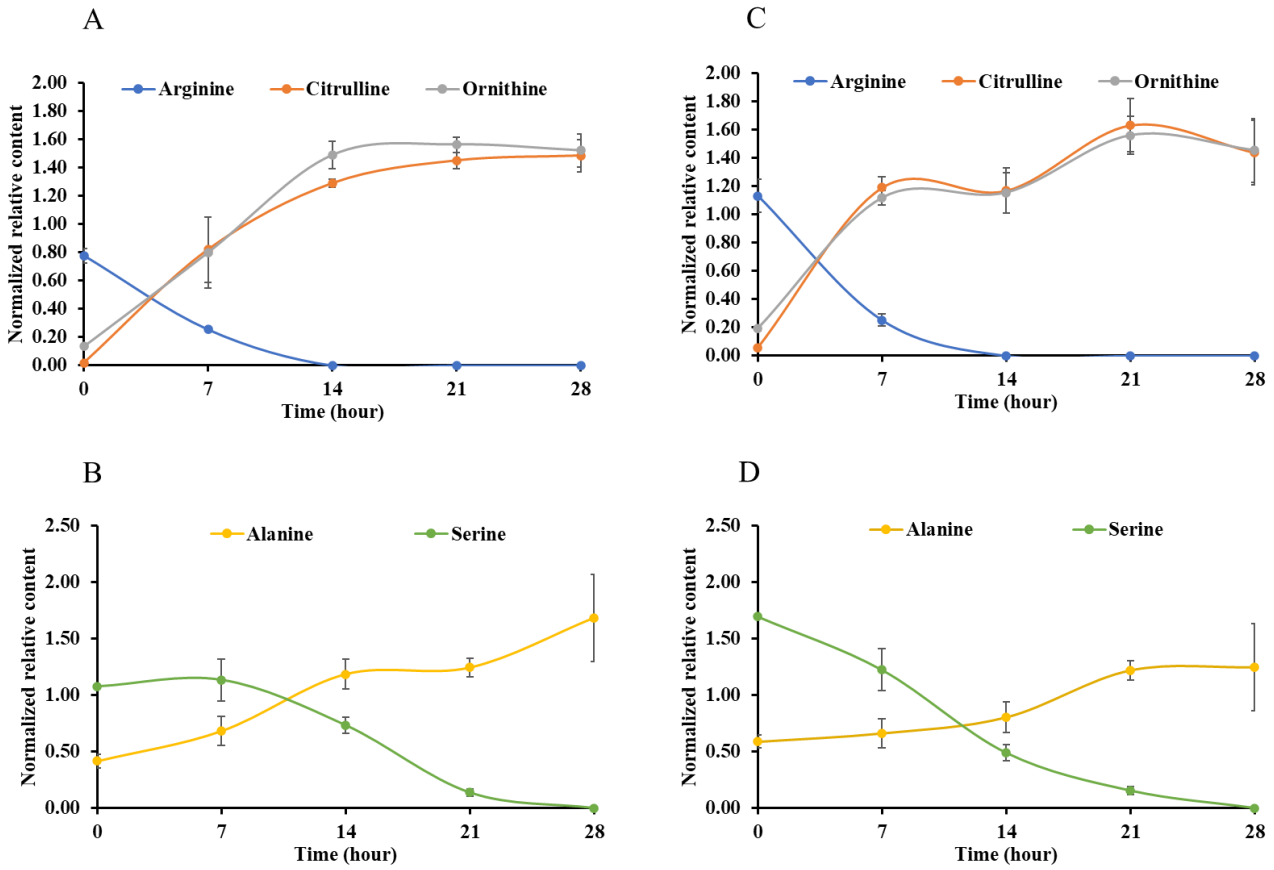

Figure 3.5: *Dynamics of free amino acids involved in the arginine dihydrolase pathway (A, C) and other pathways (B, D) detected in the control culture (A, B) and BAR-supplemented culture supernatants (C, D) over a 28-h encystation induction period. Data points for each compound are a mean of 3 replicates with the error bars showing standard error.*

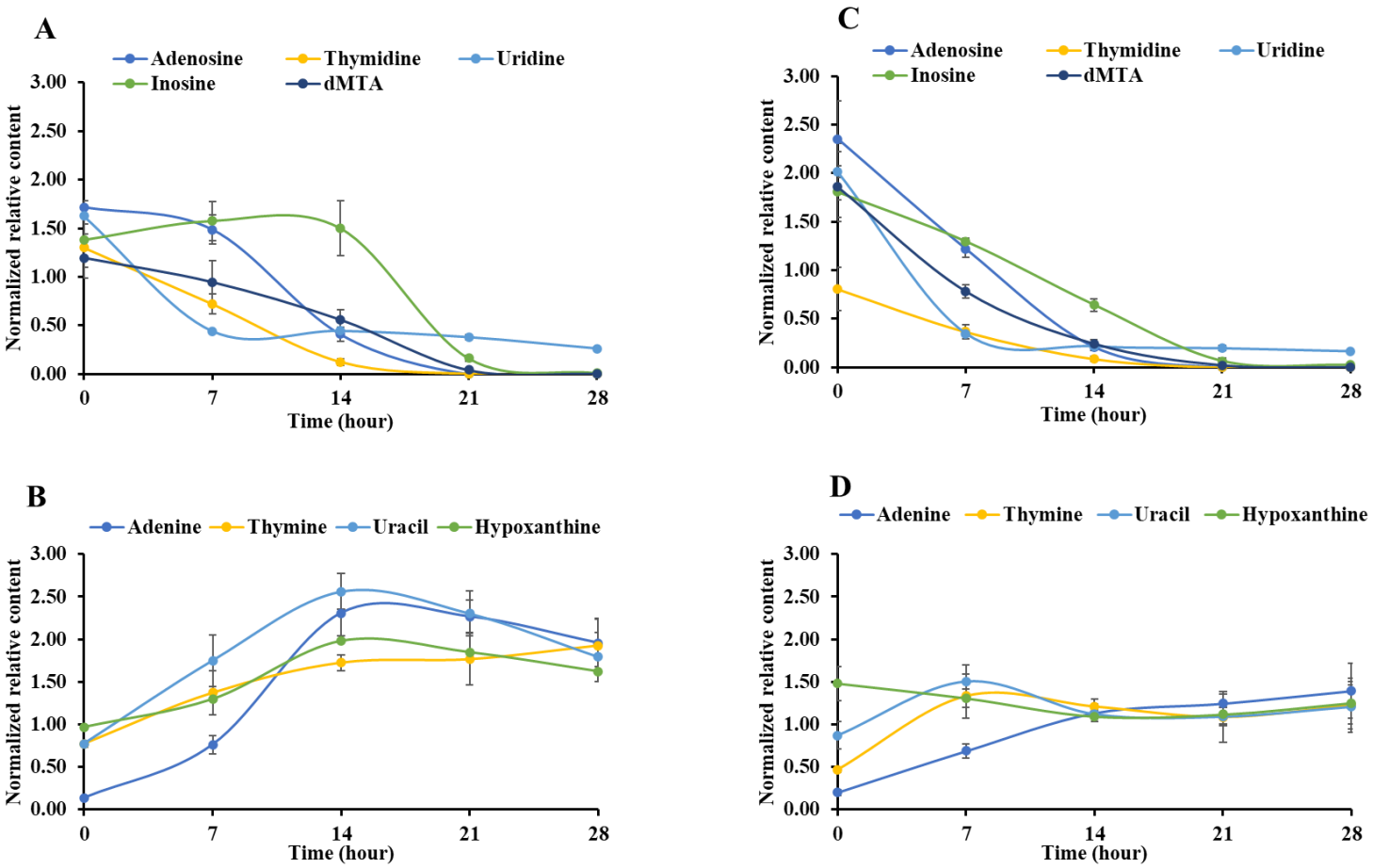

Figure 3.6: *Dynamics of nucleosides (A, C) and nucleobases (B, D) detected in the control culture (A, B) and BAR-supplemented culture supernatants (C, D) over a 28-h encystation induction period. Respective nucleoside-nucleobase pairs are color coded. Data points for each compound are a mean of 3 replicates with the error bars showing standard error.*

SUPPLEMENTARY INFORMATION

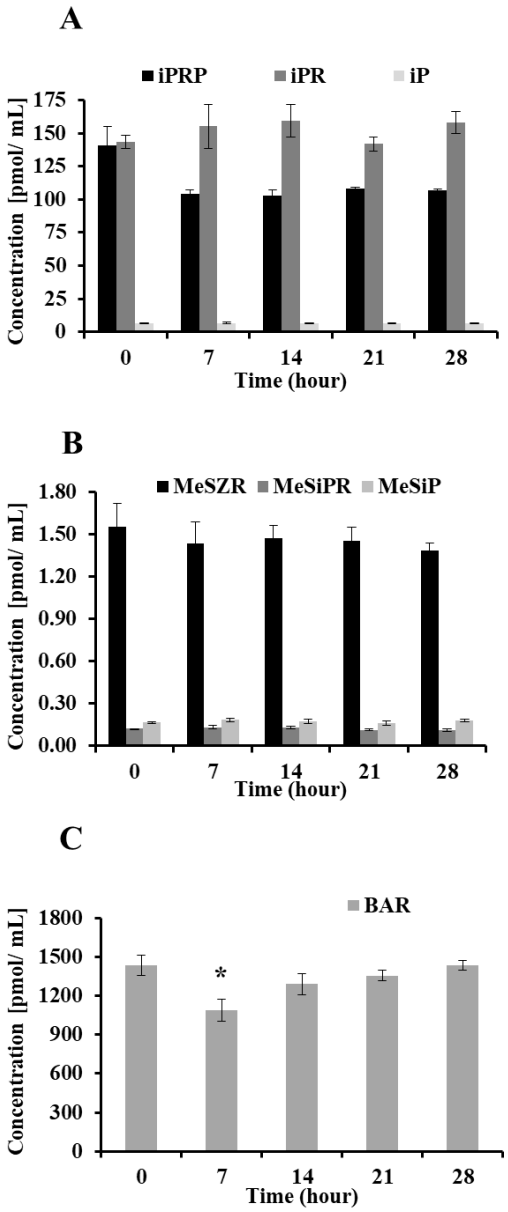

Supplementary figure 3.1*: CKs detected in the BAR-supplemented medium-blanks. No significant differences were observed in the levels of iP-type CKs (iPRP, iPR, iP) (A), and 2-MeS-type CKs (MeSZR, MeSiPR, MeSiP) (B) at any time point (7, 14, 21, and 28 h) compared to 0 hour (one-way ANOVA; $p>0.05$, $n=3$). BAR level was only significantly lower at 7 h compared to 0 h (one-way ANOVA, Duncan's post hoc test; $p<0.05$, $n=3$). Error bars show standard error.*

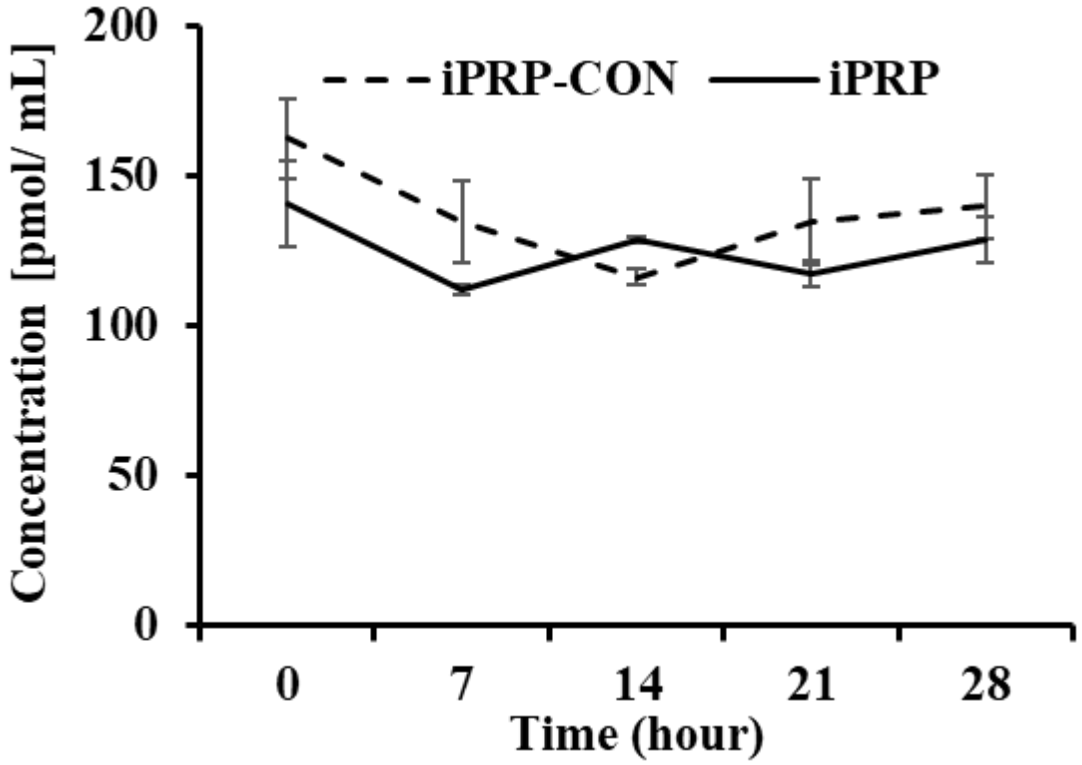

Supplementary figure 3.2: *Dynamics of iPRP detected in the control and BAR-supplemented culture supernatants over a 28-h encystation induction period. No significant differences were observed over time or between control and supplemented cultures (Two-way ANOVA; $p > 0.05$). Error bars represent standard error (n=3).*

CHAPTER 4

General discussion, conclusions, and future directions

CKs in Giardia and metabolism during growth and nutrient deprivation

This is the first report of CK production and the uptake and secretion of extracellular CKs by the protozoan parasite *Giardia intestinalis*. Specifically, I observed the synthesis of iPRP and iP likely originating from the tRNA degradation pathway (*Chapter 2, Figure 2.7*), and the uptake of CK-RBs followed by secretion of CK-FBs (*Chapter 2, Figure 2.3 and 2.4*) during growth and nutrient deprivation conditions. However, Giardia is unable to take up and/or process extracellular CK nucleotides. Since the growth medium of Giardia TYI-S-33 is already relatively CK rich, exogenous CKs (BA, BAR, BARP) normally absent in the medium were used to track the metabolism of extracellular CKs by trophozoites without background interference. Of these applied CKs, only BAR was scavenged. It was then catabolized to BA and secreted. Meanwhile, the exogenous BA and BARP remained unaltered. Of the three aromatic CK derivatives, none affected trophozoite growth. This was also true for the iP-type CKs added to DMEM.

This thesis also examines the metabolites involved in some metabolic pathways of Giardia. Many pathways in Giardia involve the exchange of molecules with the intestinal milieu, such as energy production through arginine uptake and nucleotide synthesis through modification of scavenged nucleosides (Adam, 2001). This is the first HPLC-based metabolomics report of trophozoites cultured in nutrient-rich medium (TYI-S-33) compared to those cultured in the unsupplemented and CK-supplemented nutrient-deprived maintenance medium (DMEM). Overall, a customized processing method of 130

metabolites was created that included many common metabolites involved in various indispensable metabolic processes, and 62 of these were identified in the extracellular extracts of growing trophozoite cultures; while 37 compounds were detected in the supernatants obtained from the nutrient deprived culture. In the TYI-S-33 supernatants, metabolites typical of the arginine dihydrolase activity and nucleoside salvage were detected.

Finally, this thesis shows that CK up-take and secretion likely follows the nucleoside salvage route by highlighting that the transformation patterns of common nucleosides and nucleobases were similar to CK-RBs and CK-FBs respectively (*Chapter 2, Figure 2.9*). This suggests that the purine exchange machinery is used by Giardia for metabolizing CKs. This idea is further supported by the presence of common purine and sugar transporters in plants and humans that perform multiple functions by transporting CKs due to their structural similarities to other purines (Hluska et al., 2021).

Encystation CK and metabolite profile

This is also the first mass spectrometry-based report of the uptake and secretion of extracellular CKs and metabolites by the protozoan parasite *Giardia intestinalis* during the crucial encystation process under the influence of an exogenous CK - BAR. This was achieved by analyzing culture supernatants. Since the encystation medium is already rich in CKs, BAR-supplementation into the culture medium enabled: (1) an analysis of macro-effects of exogenous CKs on encystation through cell morphology and measurement of protein expression levels of the molecular marker CWP1, (2). an analysis of less visible yet impactful effects of exogenous CKs on the extracellular metabolome of the encystation

process. The BAR-supplementation seemed to reduce the encystation efficiency by almost half compared to the control culture; however, more biological replicates would be required to support this observation. BAR-supplementation did not seem to affect the exchange of isoprenoid CKs during encystation; CK-RBs were completely depleted from the culture medium and balanced by the secretion of respective CK-FBs. Interestingly, the BAR-CK added to the medium was depleted from the medium by 21-hours, while the secretion of its FB form BA was impaired. Encysting cells are unable to take up and/or process extracellular CK nucleotides during encystation, which is an observation similar to that seen under growth and nutrient deprivation conditions. On the other hand, notable effects of BAR-supplementation were observed on exchange of extracellular metabolites: the control culture showed more asynchronous nucleoside uptake and nucleobase secretion while the BAR-supplemented culture supernatants had trends similar to growth conditions, likely due to impaired encystation. The metabolism of arginine and alanine were also like growth conditions with no notable differences caused by BAR-supplementation. In addition, this study validates many of the metabolism changes proposed to occur during encystation by previous transcriptomics and proteomics reports (Balan et al., 2021; Rojas-López et al., 2021) by adding a higher-level layer of metabolomics through analysis of the products of cellular metabolism. Finally, the results of this study establish a potential link between the CK exchange during encystation and the nucleoside salvage activities due to structural similarities between CKs and the common nucleosides and nucleobases.

Potential roles of CKs within Giardia

Based on the recent literature that reported roles for CKs in non-phytopathogens, a common theme appears in conjunction with stress response factors. For instance, in the case of *M. tuberculosis* the bacterium uses CK accumulation for protection against oxidative stress imparted by the host cells (Samanovic & Heran, 2015). Giardia trophozoites may also reduce the riboside concentrations from the intestinal milieu due to toxicity of CK-RBs to mammalian cells so the host cells are protected, and the infection can progress to maximum possible capacity (Naseem et al., 2020; Voller et al., 2019). The possibility that CKs are a source of ribose for the trophozoites could be tested using ribose labeled CKs and monitoring the fate of ribose using immunofluorescence assays. In *Chapter 2* of this study, free ribose in the culture medium remained relatively constant while all other molecules containing a ribose ring were consumed from the culture medium. Therefore, an alternate explanation for CK up-take could be the ease of ribose up-take when attachment to an aromatic ring due to abundance of nucleoside transporters in Giardia, compared to the up-take of free ribose.

Future directions

This work is the first to propose CK biosynthesis capability by Giardia trophozoites based on the detected iPRP and iP CKs, typical of tRNA degradation pathway. The presence of a putative tRNA-IPT is reported in some transcriptomics studies earlier but this the activity of this enzyme has not been further characterized (Einarsson, Troell, et al., 2016). Since tRNA-IPT in other organisms is involved in the synthesis of tRNA-bound and free CKs, it is proposed that CKs detected in Giardia originate from tRNA-IPT activity.

The potential absence of adenylate-IPT in Giardia based on homology search with the protein sequence from *D. discoidium* (protist), and *A. thaliana* (planta) as queries, suggest CKs originate in Giardia exclusively through tRNA-IPT. However, the function of tRNA-IPT is also required for modifying tRNA for efficient translation (Dabravolski, 2020; Lamichhane et al., 2011; Nishii et al., 2018), so a knockdown or knockout of tRNA-IPT in Giardia to study the impact of the loss of CKs would likely lead to non-viable Giardia. For this reason, below are a few other ways to study the potential roles of CKs in Giardia.

In the pathway proposed for CK-biosynthesis in Giardia based on the presence of nucleotide and free base CKs, along with the absence of riboside CKs inside cells, the presence of a LOG-like phosphoribohydrolase is suggested. Recently characterized LOG-like enzymes in organisms beyond plants such as *M. tuberculosis* and *B. pertussis* (bacteria), and the protist *D. discoidium* describe the phosphoribohydrolase activity of LOG with CK-NTs and substrates and CK-FBs as products (Aoki, 2023; Moramarco et al., 2019; Zhu & Javid, 2015). Within Giardia, the activity of an adenine phosphoribohydrolase enzyme has been proposed and it is used for the conversion of free adenine base to adenine nucleotides (Sarver & Wang, 2002). In the same study, it is proposed that reverse reaction of this enzyme with the nucleotide as substrate might be possible. If the adenine phosphoribohydrolase has LOG-like activity within Giardia, the enzyme would utilize iPRP as a substrate to produce iP as a product.

The results of this study suggest the involvement of CKs in the biology and metabolism of this unique parasite by identifying links between the dynamics of CKs and metabolites during encystation. Literature on encystation suggests that Giardia trophozoites induced to encyst by cholesterol starvation, were found to increase

transcription of genes involved in the early steps of the cholesterol synthesis pathway (Hernandez & Wasserman, 2006). This upregulation leads to increased production of the isopentenyl chain donor Isopentenyl pyrophosphate (IPP) or the isomer dimethylallyl pyrophosphate (DMAPP) (Hernandez & Wasserman, 2006). Although DMAPP has proven roles in lipid synthesis and protein isoprenylation within Giardia (Lujan, et al., 1995; Yichoy et al., 2011), tRNA-prenylation via the putative tRNA-IPT enzyme is not reported before. For protein isoprenylation and lipid synthesis in Giardia, various downstream modifications are made to IPP/ DMAPP. For instance, in both pathways, IPP is transformed to farnesyl PP which is either converted to geranylgeranyl PP for attachment to proteins (Hoshino & Gaucher, 2018; Lujan et al., 1995) or to squalene to generate lipids (Yichoy et al., 2011). On the other hand, the current work is the first to report the downstream products of tRNA-prenylation. Since the breakdown of prenyl-tRNA likely leads to the synthesis of CKs in Giardia, it is crucial to study this process further to understand the role of generated CKs. If the synthesis of IPP or DMAPP is upregulated during encystation (Hernandez & Wasserman, 2006), the metabolites involved in either protein isoprenylation, lipid synthesis or tRNA-prenylation, would be upregulated. Most of these metabolites can be detected using the methods used in this work (*Chapter 2, Supp. table 2.1*). Thus, performing a metabolomics screening of proliferating or encysting trophozoites can further support the observation and idea that Giardia is capable of CK synthesis despite its genetically minimalist genome.

On the other hand, to understand the CK up-take and secretion mechanisms of Giardia, radiolabeled cytokinins of iP- or BA-type could be used, as in other mammalian studies (Ishii et al., 2003). When radiolabeled BA was added to a human myeloid leukemia

HL-60 cell culture, it was found to be up taken, converted into a nucleotide form, but rather than incorporation into genetic material, they were converted back into a riboside or free base for secretion into the culture medium (Ishii et al., 2003). A similar study for the proliferating or encysting Giardia trophozoites could help decipher the unknown mechanism by which CK-FBs are recognized as modified bases and are exported out of the cell rather than being incorporated into DNA or RNA. To further support this, testing the specificities of common nucleoside and nucleobase transporters against CK-RBs and CK-FBs along with affinities of CKs to the enzymes involved in the nucleoside salvage pathway could strengthen the link between the salvage of common purines and CKs (Baum et al., 1989, 1993; Campagnaro & de Koning, 2020; Munagala & Wang, 2002; Sarver & Wang, 2002; Wang & Aldritt, 1983).

Overall, this study highlights a novel phytohormone-based connection between Giardia and its host with the opportunity for scientists to manipulate the interkingdom molecules to gain a deeper understanding of the parasite, the host or the interaction between the two.

REFERENCES

Adam, R. D. (2001). Biology of Giardia lamblia. In *Clinical Microbiology Reviews* (Vol. 14, Issue 3). https://doi.org/10.1128/CMR.14.3.447-475.2001

Adam, R. D. (2021). Giardia duodenalis: Biology and Pathogenesis. *Clinical Microbiology Reviews*, *34*(4), 1–35. https://doi.org/10.1128/CMR

Aldritt, S. M., Tien, P., & Wang, C. C. (1985). Pyrimidine salvage in Giardia lamblia. *Journal of Experimental Medicine*, *16*(1), 437–445. http://rupress.org/jem/article-pdf/161/3/437/1095088/437.pdf

Anand, G., Gupta, R., Marash, I., Leibman-Markus, M., & Bar, M. (2022). Cytokinin production and sensing in fungi. *Microbiological Research*, *262*. https://doi.org/10.1016/j.micres.2022.127103

Andrabi, S. B. A., Tahara, M., Matsubara, R., Toyama, T., Aonuma, H., Sakakibara, H., Suematsu, M., Tanabe, K., Nozaki, T., & Nagamune, K. (2018). Plant hormone cytokinins control cell cycle progression and plastid replication in apicomplexan parasites. *Parasitology International*, *67*(1), 47–58. https://doi.org/10.1016/J.PARINT.2017.03.003

Andreas, P., Kisiala, A., Neil Emery, R. J., De Clerck-Floate, R., Tooker, J. F., Price, P. W., Miller, D. G., Chen, M. S., & Connor, E. F. (2020). Cytokinins are abundant and widespread among insect species. *Plants*, *9*(2). https://doi.org/10.3390/plants9020208

Aoki, M. M. (2023). *Cytokinins in Dictyostelium discoideum: New insights for extended roles during the life cycle of the social amoeba* (Vol. 334).

Aoki, M. M., Emery, R. J. N., Anjard, C., Brunetti, C. R., & Huber, R. J. (2020). Cytokinins in Dictyostelia – A Unique Model for Studying the Functions of Signaling Agents From Species to Kingdoms. *Frontiers in Cell and Developmental Biology*, *8*(511), 1–16. https://doi.org/10.3389/fcell.2020.00511

Aoki, M. M., Kisiala, A. B., Rahman, T., Morrison, E. N., & Emery, R. J. N. (2021). Cytokinins are pervasive among common in vitro culture media: An analysis of their forms, concentrations and potential sources. *Journal of Biotechnology*, *334*, 43–46. https://doi.org/10.1016/j.jbiotec.2021.05.005

Aoki, M. M., Seegobin, M., Kisiala, A., Noble, A., Brunetti, C., & Emery, R. J. N. (2019). Phytohormone metabolism in human cells: Cytokinins are taken up and interconverted in HeLa cell culture. *FASEB BioAdvances*, *1*(5), 320–331. https://doi.org/10.1096/fba.2018-00032

Balan, B., Emery-Corbin, S. J., Sandow, J. J., Ansell, B. R. E., Tichkule, S., Webb, A. I., Svärd, S. G., & Jex, A. R. (2021). Multimodal regulation of encystation in Giardia duodenalis revealed by deep proteomics. *International Journal for Parasitology*, *51*(10), 809–824. https://doi.org/10.1016/j.ijpara.2021.01.008

Barash, N. R., Nosala, C., Pham, J. K., McInally, S. G., Gourguechon, S., McCarthy-Sinclair, B., & Dawson, S. C. (2017). Giardia Colonizes and Encysts in High-Density Foci in the Murine Small Intestine . *MSphere*, *2*(3). https://doi.org/10.1128/msphere.00343-16

Baum, K. F., Berens, R. L., & Marr, J. J. (1993). Purine Nucleoside and Nucleobase Cell Membrane Transport in Giardia lamblia. *J. Euk. Microbiol*, *40*(5), 643–649.

Baum, K. F., Berens, R. L., Marr, J. J., Harrington, J. A., & Spector, T. (1989). Purine deoxynucleoside salvage in Giardia lamblia. *Journal of Biological Chemistry*, *264*(35), 21087–21090. https://doi.org/10.1016/s0021-9258(19)30049-3

Bernander, R., Palm, J. E. D., & Svärd, S. G. (2001). Genome ploidy in different stages of the Giardia lamblia life cycle. *Cellular Microbiology*, *3*(1), 55–62. https://doi.org/10.1046/j.1462-5822.2001.00094.x

Birkeland, S. R., Preheim, S. P., Davids, B. J., Cipriano, M. J., Palm, D., Reiner, D. S., Svärd, S. G., Gillin, F. D., & McArthur, A. G. (2010). Transcriptome analyses of the

Giardia lamblia life cycle. *Molecular and Biochemical Parasitology*, *174*(1), 62–65. https://doi.org/10.1016/j.molbiopara.2010.05.010

Boucher, S.-E. M., & Gillin, F. D. (1990). Excystation of In Vitro-Derived Giardia lamblia Cysts. *Infection and Immunity*, *58*(11).

Campagnaro, G. D., & de Koning, H. P. (2020). Purine and pyrimidine transporters of pathogenic protozoa – conduits for therapeutic agents. *Medicinal Research Reviews*, *40*(5), 1679–1714. https://doi.org/10.1002/med.21667

Carranza, P. G., & Luján, H. D. (2010). New insights regarding the biology of Giardia lamblia. *Microbes and Infection*, *12*(1), 71–80. https://doi.org/10.1016/J.MICINF.2009.09.008

Dabravolski, S. (2020). Multi-faceted nature of the tRNA isopentenyltransferase. *Functional Plant Biology*, *47*(6), 475–485. https://doi.org/10.1071/FP19255

Davey, R. A., Mayrhofer, G., & Ey, P. L. (1992). Identification of a broad-specificity nucleoside transporter with affinity for the sugar moiety in Giardia intestinalis trophozoites. *Biochimica et Biophysica Acta*, *1109*, 172–178.

Doležal, K., Popa, I., Hauserová, E., Spíchal, L., Chakrabarty, K., Novák, O., Kryštof, V., Voller, J., Holub, J., & Strnad, M. (2007). Preparation, biological activity and endogenous occurrence of N6-benzyladenosines. *Bioorganic & Medicinal Chemistry*, *15*(11), 3737–3747. https://doi.org/10.1016/J.BMC.2007.03.038

Dubourg, A., Xia, D., Winpenny, J. P., Al Naimi, S., Bouzid, M., Sexton, D. W., Wastling, J. M., Hunter, P. R., & Tyler, K. M. (2018). Giardia secretome highlights secreted tenascins as a key component of pathogenesis. *GigaScience*, *7*(3), 1–13. https://doi.org/10.1093/gigascience/giy003

Ebneter, J. A., Heusser, S. D., Schraner, E. M., Hehl, A. B., & Faso, C. (2016). Cyst-Wall-Protein-1 is fundamental for Golgi-like organelle neogenesis and cyst-wall

biosynthesis in Giardia lamblia. *Nature Communications*, *7*. https://doi.org/10.1038/ncomms13859

Einarsson, E., Ma'ayeh, S., & Svärd, S. G. (2016). An up-date on Giardia and giardiasis. *Current Opinion in Microbiology*, *34*, 47–52. https://doi.org/10.1016/j.mib.2016.07.019

Einarsson, E., Troell, K., Hoeppner, M. P., Grabherr, M., Ribacke, U., & Svärd, S. G. (2016). Coordinated Changes in Gene Expression Throughout Encystation of Giardia intestinalis. *PLoS Neglected Tropical Diseases*, *10*(3). https://doi.org/10.1371/journal.pntd.0004571

Ey, P. L., Davey, R. A., & Duffield, G. A. (1992). A low-affinity nucleobase transporter in the protozoan para¢,ite Giardia intestinalis. *Biochimica et Biophysica Acta*, *1109*, 179–186.

Faghiri, Z., & Widmer, G. (2011). A comparison of the Giardia lamblia trophozoite and cyst transcriptome using microarrays. *BMC Microbiology*, *11*. https://doi.org/10.1186/1471-2180-11-91

Faso, C., Bischof, S., & Hehl, A. B. (2013). The proteome landscape of Giardia lamblia encystation. *PLoS ONE*, *8*(12). https://doi.org/10.1371/journal.pone.0083207

Fisher, B. S., Estraño, C. E., & Cole, J. A. (2013). Modeling long-term host cell-Giardia lamblia interactions in an in vitro co-culture system. *PLoS ONE*, *8*(12). https://doi.org/10.1371/journal.pone.0081104

Frances D. Gillin, David S. Reiner, Michael J. Gault, Herndon Douglas, Siddhartha Das, Annette Wunderlich, & Judith F. Sauch. (1987). Encystation and Expression of Cyst Antigens by Giardia lamblia in Vitro. *Science*, *235*, 1040–1043.

Gerwig, G. J., Albert Van Kuik, J., Leeflang, B. R., Kamerling, J. P., Vliegenthart, J. F. G., Karr, C. D., & Jarroll, E. L. (2002). The Giardia intestinalis filamentous cyst

wall contains a novel β(1-3)-N-acetyl-D-galactosamine polymer: a structural and conformational study. *Glycobiology*, *12*(8), 499–505.

Gibb, M., Kisiala, A. B., Morrison, E. N., & Emery, R. J. N. (2020). The Origins and Roles of Methylthiolated Cytokinins: Evidence From Among Life Kingdoms. *Frontiers in Cell and Developmental Biology*, *8*. https://doi.org/10.3389/fcell.2020.605672

Gillin,', F. D., Boucher, S. E., Rossi, S. S., Reiner, D. S., Gillin, F. D., & Giardia, D. S. 1989. (1989). Giardia lamblia: The Roles of Bile, Lactic Acid, and pH in the Completion of the Life Cycle in Vitro. *Experimental Parasitology*, *69*, 164–174.

Hernandez, P. C., & Wasserman, M. (2006). Do genes from the cholesterol synthesis pathway exist and express in Giardia intestinalis? *Parasitology Research*, *98*(3), 194–199. https://doi.org/10.1007/s00436-005-0039-1

Hluska, T., Hlusková, L., & Emery, R. J. N. (2021). The hulks and the deadpools of the cytokinin universe: A dual strategy for cytokinin production, translocation, and signal transduction. *Biomolecules*, *11*(2), 1–40. https://doi.org/10.3390/biom11020209

Horlock-Roberts, K., Reaume, C., Dayer, G., Ouellet, C., Cook, N., & Yee, J. (2017). Drug-Free Approach To Study the Unusual Cell Cycle of Giardia intestinalis. *MSphere*, *2*(5). https://doi.org/10.1128/msphere.00384-16

Hoshino, Y., & Gaucher, E. A. (2018). On the origin of isoprenoid biosynthesis. *Molecular Biology and Evolution*, *35*(9), 2185–2197. https://doi.org/10.1093/molbev/msy120

Hubert, J. (2020). *The identification and characterization of cytokinins in Giardia intestinalis*. Trent University.

Hughes, D. T., & Sperandio, V. (2008). Inter-kingdom signalling: Communication between bacteria and their hosts. *Nature Reviews Microbiology*, *6*(2), 111–120. https://doi.org/10.1038/nrmicro1836

Ishii, Y., Sakai, S., & Honma, Y. (2003). Cytokinin-induced differentiation of human myeloid leukemia HL-60 cells is associated with the formation of nucleotides, but not with incorporation into DNA or RNA. *Biochimica et Biophysica Acta - Molecular Cell Research*, *1643*(1–3), 11–24. https://doi.org/10.1016/j.bbamcr.2003.08.004

Jabłońska-Trypuć, A., Matejczyk, M., & Czerpak, R. (2016). N6-benzyladenine and kinetin influence antioxidative stress parameters in human skin fibroblasts. *Molecular and Cellular Biochemistry*, *413*(1–2), 97–107. https://doi.org/10.1007/s11010-015-2642-5

Jameson, P. E., & Morris, R. O. (1989). Zeatin-Like Cytokinins in Yeast: Detection by Immunological Methods. *Journal of Plant Physiology*, *135*(4), 385–390. https://doi.org/10.1016/S0176-1617(89)80092-6

Jarroll, E. L., Muller, P. J., Meyer, E. A., & Morse, S. A. (1981). Lipid and carbohydrate metabolism of Giardia lamblia. *Molecular and Biochemical Parasitology*, *2*(3–4), 187–196. https://doi.org/10.1016/0166-6851(81)90099-2

Kamada-Nobusada, T., & Sakakibara, H. (2009). Molecular basis for cytokinin biosynthesis. *Phytochemistry*, *70*(4), 444–449. https://doi.org/10.1016/j.phytochem.2009.02.007

Kane, A. V, Ward, H. D., Keusch, G. T., & Pereira, M. E. A. (1991). In vitro Encystation of Giardia lamblia: Large-Scale Production of In vitro Cysts and Strain and Clone Differences in Encystation Efficiency. *The Journal of Parasitology*, *77*(6), 974–981.

Kaur, H., Ghosh, S., Samra, H., Vinayak, V. K., & Ganguly, N. K. (2001). Identification and characterization of an excretory-secretory product from Giardia lamblia. *Parasitology*, *123*(4), 347–356. https://doi.org/10.1017/S0031182001008629

Keister, D. B. (1983). Axenic culture of Giardia lamblia in TYI-S-33 medium supplemented with bile. *Transactions of the Royal Society of Tropical Medicine and Hygiene*, *77*(4), 4–7.

Kendall, M. M., & Sperandio, V. (2016). What a dinner party! mechanisms and functions of interkingdom signaling in host-pathogen associations. *MBio*, *7*(2). https://doi.org/10.1128/mBio.01748-15

Kim, J., Park, E. A., Shin, M. Y., & Park, S. J. (2022). Identification of target genes regulated by encystation-induced transcription factor Myb2 using knockout mutagenesis in Giardia lamblia. *Parasites and Vectors*, *15*(1). https://doi.org/10.1186/s13071-022-05489-z

Kisiala, A., Kambhampati, S., Stock, N. L., Aoki, M., & Emery, R. J. N. (2019). Quantification of Cytokinins Using High-Resolution Accurate-Mass Orbitrap Mass Spectrometry and Parallel Reaction Monitoring (PRM). *Analytical Chemistry*, *91*(23), 15049–15056. https://doi.org/10.1021/acs.analchem.9b03728

Lamichhane, T. N., Blewett, N. H., & Maraia, R. J. (2011). Plasticity and diversity of tRNA anticodon determinants of substrate recognition by eukaryotic A37 isopentenyltransferases. *RNA*, *17*(10), 1846–1857. https://doi.org/10.1261/rna.2628611

Lee, H. Y., Hyung, S., Lee, N. Y., Yong, T. S., Han, S. H., & Park, S. J. (2012). Excretory-secretory products of Giardia lamblia induce interleukin-8 production in human colonic cells via activation of p38, ERK1/2, NF-κB and AP-1. *Parasite Immunology*, *34*(4), 183–198. https://doi.org/10.1111/j.1365-3024.2012.01354.x

Luján, H. D., Mowatt, M. R., Byrd, L. G., & Nash, T. E. (1996). Cholesterol Starvation Induces Differentiation of the Intestinal Parasite Giardia lamblia. *Proceedings of the National Academy of Sciences*, *93*(15), 7628–7633.

Luján, H. D., Mowatt, M. R., Chen, G.-Z., & Nash, T. E. (1995). Isoprenylation of proteins in the protozoan Giardia lamblia. *Molecular and Biochemical Parasitology*, *72*, 121–127.

Lujan, H. D., Mowatt, M. R., Conrad, J. T., Bowers, B., & Nash, T. E. (1995). Identification of a novel Giardia lamblia cyst wall protein with leucine- rich repeats: Implications for secretory granule formation and protein assembly into the cyst wall. *Journal of Biological Chemistry*, *270*(49), 29307–29313. https://doi.org/10.1074/jbc.270.49.29307

Luján, H. D., Mowatt, M. R., & Nash, T. E. (1997). Mechanisms of Giardia lamblia Differentiation into Cysts. *Microbiology and Molecular Biology Reviews* , *61*(3), 294–304.

Luján, H. D., & Svärd, Staffan. (2011). *Giardia : a model organism* (H. D. Lujan & S. Svard, Eds.; 1st ed.). Springer.

Ma'ayeh, S. Y., Liu, J., Peirasmaki, D., Hörnaeus, K., Bergström Lind, S., Grabherr, M., Bergquist, J., & Svärd, S. G. (2017). Characterization of the Giardia intestinalis secretome during interaction with human intestinal epithelial cells: The impact on host cells. *PLoS Neglected Tropical Diseases*, *11*(12), e0006120. https://doi.org/10.1371/journal.pntd.0006120

Martínez-García, M. A., Perpiá-Tordera, M., Vila, V., Compte-Torrero, L., De Diego-Damiá, A., & Macián-Gisbert, V. (2002). Analysis of the stability of stored adenosine 5′-monophosphate used for bronchoprovocation. *Pulmonary Pharmacology and Therapeutics*, *15*(2), 157–160. https://doi.org/10.1006/pupt.2001.0334

Martínez-Gordillo, M. N., González-Maciel, A., Reynoso-Robles, R., Montijo-Barrios, E., & Ponce-Macotela, M. (2014). Intraepithelial Giardia Intestinalis: A case report and literature review. *Medicine (United States)*, *93*(29), e277. https://doi.org/10.1097/MD.0000000000000277

Moramarco, F., Pezzicoli, A., Salvini, L., Leuzzi, R., Pansegrau, W., & Balducci, E. (2019). A lonely guy protein of Bordetella pertussis with unique features is related to oxidative stress. *Scientific Reports*, *9*(1), 1–12. https://doi.org/10.1038/s41598-019-53171-9

Morf, L., Spycher, C., Rehrauer, H., Fournier, C. A., Morrison, H. G., & Hehl, A. B. (2010). The transcriptional response to encystation stimuli in Giardia lamblia is restricted to a small set of genes. *Eukaryotic Cell*, *9*(10), 1566–1576. https://doi.org/10.1128/EC.00100-10

Morrison, H. G., McArthur, A. G., Gillin, F. D., Aley, S. B., Adam, R. D., Olsen, G. J., Best, A. A., Cande, W. Z., Chen, F., Cipriano, M. J., Davids, B. J., Dawson, S. C., Elmendorf, H. G., Hehl, A. B., Holder, M. E., Huse, S. M., Kim, U. U., Lasek-Nesselquist, E., Manning, G., … Sogin, M. L. (2007). Genomic minimalism in the early diverging intestinal parasite Giardia lamblia. *Science*, *317*(5846), 1921–1926. https://doi.org/10.1126/SCIENCE.1143837

Mowatt, M. R., Luján, H. D., Cotten, D. B., Bowers, B., Theodore, N., Yee, J., & Stibbs, H. H. (1995). Developmentally regulated expression of a Giardia lamblia cyst wall protein gene. *Molecular Microbiology*, *5*, 955–963.

Müller, J., Vermathen, M., Leitsch, D., Vermathen, P., & Müller, N. (2020). Metabolomic profiling of wildtype and transgenic Giardia lamblia strains by1H HR-MAS NMR spectroscopy. *Metabolites*, *10*(2), 1–14. https://doi.org/10.3390/metabo10020053

Munagala, N., & Wang, C. C. (2002). The pivotal role of guanine phosphoribosyltransferase in purine salvage by Giardia lamblia. *Molecular Microbiology*, *44*(4), 1073–1079. https://doi.org/10.1046/j.1365-2958.2002.02942.x

Naseem, M., Othman, E. M., Fathy, M., Iqbal, J., Howari, F. M., AlRemeithi, F. A., Kodandaraman, G., Stopper, H., Bencurova, E., Vlachakis, D., & Dandekar, T. (2020). Integrated structural and functional analysis of the protective effects of kinetin against oxidative stress in mammalian cellular systems. *Scientific Reports*, *10*(1). https://doi.org/10.1038/s41598-020-70253-1

Nishii, K., Wright, F., Chen, Y. Y., & Möller, M. (2018). Tangled history of a multigene family: The evolution of isopentenyltransferase genes. *PLoS ONE*, *13*(8). https://doi.org/10.1371/journal.pone.0201198

Oslovsky, V. E., Savelieva, E. M., Drenichev, M. S., Romanov, G. A., & Mikhailov, S. N. (2020). Distinct peculiarities of in planta synthesis of isoprenoid and aromatic cytokinins. *Biomolecules*, *10*(1). https://doi.org/10.3390/biom10010086

Othman, E. M., Naseem, M., Awad, E., Dandekar, T., & Stopper, H. (2016). The plant hormone cytokinin confers protection against oxidative stress in mammalian cells. *PLoS ONE*, *11*(12). https://doi.org/10.1371/journal.pone.0168386

Paget, T., Haroune, N., Bagchi, S., & Jarroll, E. (2013). Metabolomics and protozoan parasites. *Acta Parasitologica*, *58*(2), 127–131. https://doi.org/10.2478/s11686-013-0137-7

Paget, T., Macechko, T., & Jarroll, E. (1998). Metabolic Changes in Giardia intestinalis during Differentiation. *The Journal of Parasitology*, *84*(2), 222–226. http://www.jstor.orgURL:http://www.jstor.org/stable/3284474http://www.jstor.org/stable/3284474?seq=1&cid=pdf-reference#references_tab_contents

Palberg, D., Kisiała, A., Lemes Jorge, G., & Neil Emery, R. J. (2021). A Survey of Methylobacterium Species and Strains Reveals Widespread Production and Varying

Proles of Cytokinin Phytohormones. *BMC Microbiology*, *22*(49), 1–17. https://doi.org/10.21203/rs.3.rs-1034994/v1

Pham, J. K., Nosala, C., Scott, E. Y., Nguyen, K. F., Hagen, K. D., Starcevich, H. N., & Dawson, S. C. (2017). Transcriptomic Profiling of High-Density Giardia Foci Encysting in the Murine Proximal Intestine. *Frontiers in Cellular and Infection Microbiology*, *7*(MAY), 227. https://doi.org/10.3389/FCIMB.2017.00227

Piña-Vázquez, C., Reyes-López, M., Ortíz-Estrada, G., De La Garza, M., & Serrano-Luna, J. (2012). Host-parasite interaction: Parasite-derived and -induced proteases that degrade human extracellular matrix. *Journal of Parasitology Research*, *2012*. https://doi.org/10.1155/2012/748206

Pinheiro, A. A. de S., Cosentino-Gomes, D., Lanfredi-Rangel, A., Ferraro, R. B., Souza, W. De, & Meyer-Fernandes, J. R. (2008a). Giardia lamblia: Biochemical characterization of an ecto-ATPase activity. *Experimental Parasitology*, *119*(2), 279–284. https://doi.org/10.1016/j.exppara.2008.02.006

Pinheiro, A. A. de S., Cosentino-Gomes, D., Lanfredi-Rangel, A., Ferraro, R. B., Souza, W. De, & Meyer-Fernandes, J. R. (2008b). Giardia lamblia: Biochemical characterization of an ecto-ATPase activity. *Experimental Parasitology*, *119*(2), 279–284. https://doi.org/10.1016/j.exppara.2008.02.006

Popruk, S., Abu, A., Ampawong, S., Thiangtrongjit, T., Tipthara, P., Tarning, J., Sreesai, S., & Reamtong, O. (2023). Mass Spectrometry-Based Metabolomics Revealed Effects of Metronidazole on Giardia duodenalis. *Pharmaceuticals*, *16*(3). https://doi.org/10.3390/ph16030408

Powell, A., & Heyl, A. (2023). The origin and early evolution of cytokinin signaling. *Frontiers in Plant Science*, *14*. https://doi.org/10.3389/fpls.2023.1142748

Rahman, T. (2019). *Cytokinins in nematodes: the potential role of cytokinins in soybean (Glycine max) resistance to soybean cyst nematode (Heterodera glycines)*.

Ringqvist, E., Palm, J. E. D., Skarin, H., Hehl, A. B., Weiland, M., Davids, B. J., Reiner, D. S., Griffiths, W. J., Eckmann, L., Gillin, F. D., & Svärd, S. G. (2008). Release of metabolic enzymes by Giardia in response to interaction with intestinal epithelial cells. *Molecular and Biochemical Parasitology*, *159*(2), 85–91. https://doi.org/10.1016/j.molbiopara.2008.02.005

Rodríguez-Fuentes, G. B., Cedillo-Rivera, R., Fonseca-Liñán, R., Argüello-García, R., Muñoz, O., Ortega-Pierres, G., & Yépez-Mulia, L. (2006). Giardia duodenalis: Analysis of secreted proteases upon trophozoite-epithelial cell interaction in vitro. *Memorias Do Instituto Oswaldo Cruz*, *101*(6), 693–696. https://doi.org/10.1590/S0074-02762006000600020

Rojas-López, L., Krakovka, S., Einarsson, E., Ribacke, U., Xu, F., Jerlström-Hultqvist, J., & Svärd, S. G. (2021). A detailed gene expression map of giardia encystation. *Genes*, *12*(12). https://doi.org/10.3390/genes12121932

Romano, M. C., Jiménez, P., Miranda-Brito, C., & Valdez, R. A. (2015). Parasites and steroid hormones: corticosteroid and sex steroid synthesis, their role in the parasite physiology and development. *Frontiers in Neuroscience*, *9*(224), 1–5. https://doi.org/10.3389/fnins.2015.00224

Russo-Abrahão, T., Cosentino-Gomes, D., Daflon-Yunes, N., & Meyer-Fernandes, J. R. (2011). Giardia duodenalis: Biochemical characterization of an ecto-5′-nucleotidase activity. *Experimental Parasitology*, *127*(1), 66–71. https://doi.org/10.1016/j.exppara.2010.06.028

Sáenz, L., Jones, L. H., Oropeza, C., Vláčil, D., & Strnad, M. (2003). Endogenous isoprenoid and aromatic cytokinins in different plant parts of Cocos nucifera (L.). *Plant Growth Regulation*, *39*, 205–215.

Sakakibara, H. (2006). Cytokinins: Activity, biosynthesis, and translocation. *Annual Review of Plant Biology*, *57*, 431–449. https://doi.org/10.1146/annurev.arplant.57.032905.105231

Samanovic, M. I., & Heran, D. K. (2015). Cytokinins beyond plants: Synthesis by Mycobacterium tuberculosis. *Microbial Cell*, *2*(5), 168–170. https://doi.org/10.15698/mic2015.05.203

Samanovic, M. I., Hsu, H. C., Jones, M. B., Jones, V., McNeil, M. R., Becker, S. H., Jordan, A. T., Strnad, M., Xu, C., Jackson, M., Li, H., & Darwin, K. H. (2018). Cytokinin signaling in Mycobacterium tuberculosis. *MBio*, *9*(3). https://doi.org/10.1128/mBio.00989-18

Samanovic, M. I., Tu, S., Novák, O., Iyer, L. M., McAllister, F. E., Aravind, L., Gygi, S. P., Hubbard, S. R., Strnad, M., & Darwin, K. H. (2015). Proteasomal Control of Cytokinin Synthesis Protects Mycobacterium tuberculosis against Nitric Oxide. *Molecular Cell*, *57*(6), 984–994. https://doi.org/10.1016/j.molcel.2015.01.024

Sansom, F. M., Robson, S. C., & Hartland, E. L. (2008). Possible Effects of Microbial Ecto-Nucleoside Triphosphate Diphosphohydrolases on Host-Pathogen Interactions. *Microbiology and Molecular Biology Reviews*, *72*(4), 765–781. https://doi.org/10.1128/mmbr.00013-08

Sarkar, A., Kisiala, A., Adhikary, D., Basu, U., Emery, R. J. N., Rahman, H., & Kav, N. N. V. (2023). Silicon ameliorates clubroot responses in canola (Brassica napus): A "multi-omics"-based investigation into possible mechanisms. *Physiologia Plantarum*, *175*(2). https://doi.org/10.1111/ppl.13900

Sarver, A. E., & Wang, C. C. (2002). The adenine phosphoribosyltransferase from Giardia lamblia has a unique reaction mechanism and unusual substrate binding properties. *Journal of Biological Chemistry*, *277*(42), 39973–39980. https://doi.org/10.1074/jbc.M205595200

Schrimpe-Rutledge, A. C., Codreanu, S. G., Sherrod, S. D., & McLean, J. A. (2016). Untargeted Metabolomics Strategies—Challenges and Emerging Directions. *Journal of the American Society for Mass Spectrometry*, *27*(12), 1897–1905. https://doi.org/10.1007/s13361-016-1469-y

Schupp, D. G., Januschka, M. M., Sherlock, L. A. F., Stibbs, H. H., Meyer, E. A., Bemrick, W. J., & Erlandsen, S. L. (1988). Production of viable Giardia cysts in vitro: Determination by fluorogenic dye staining, excystation, and animal infectivity in the mouse and Mongolian gerbil. *Gastroenterology*, *95*(1), 1–10. https://doi.org/10.1016/0016-5085(88)90283-1

Seegobin, M., Kisiala, A., Noble, A., Kaplan, D., Brunetti, C., & Emery, R. J. N. (2018). Canis familiaris tissues are characterized by different profiles of cytokinins typical of the tRNA degradation pathway. *FASEB Journal*, *32*(12), 6575–6581. https://doi.org/10.1096/fj.201800347

Seng, S., Ponce, G. E., Andreas, P., Kisiala, A., De Clerck-Floate, R., Miller, D. G., Chen, M.-S., Price, P. W., Tooker, J. F., Emery, R. J. N., & Connor, E. F. (2023). Abscisic Acid: A Potential Secreted Effector Synthesized by Phytophagous Insects for Host-Plant Manipulation. *Insects*, *14*(6), 489. https://doi.org/10.3390/insects14060489

Shant, J., Bhattacharyya, S., Ghosh, S., Ganguly, N. K., & Majumdar, S. (2002). A potentially important excretory-secretory product of Giardia lamblia. *Experimental Parasitology*, *102*(3–4), 178–186. https://doi.org/10.1016/S0014-4894(03)00054-7

Šimura, J., Antoniadi, I., Široká, J., Tarkowská, D., Strnad, M., Ljung, K., & Novák, O. (2018). Plant hormonomics: Multiple phytohormone profiling by targeted metabolomics. *Plant Physiology*, *177*(2), 476–489. https://doi.org/10.1104/pp.18.00293

Singer, S. M., Angelova, V. V., DeLeon, H., & Miskovsky, E. (2020). What's eating you? An update on Giardia, the microbiome and the immune response. *Current Opinion in Microbiology*, *58*, 87–92. https://doi.org/10.1016/j.mib.2020.09.006

Spallek, T., Gan, P., Kadota, Y., & Shirasu, K. (2018). Same tune, different song — cytokinins as virulence factors in plant–pathogen interactions? *Current Opinion in Plant Biology*, *44*, 82–87. https://doi.org/10.1016/j.pbi.2018.03.002

Sperandio, V., Torres, A. G., Jarvis, B., Nataro, J. P., & Kaper, J. B. (2003). Bacteria-host communication: The language of hormones. *Proceedings of the National Academy of Sciences of the United States of America*, *100*(15), 8951–8956. https://doi.org/10.1073/pnas.1537100100

Sulemana, A., Paget, T. A., & Jarroll, E. L. (2014). Commitment to cyst formation in Giardia. *Microbiology (United Kingdom)*, *160*(2), 330–339. https://doi.org/10.1099/mic.0.072405-0

Sun, C. H., McCaffery, J. M., Reiner, D. S., & Gillin, F. D. (2003). Mining the Giardia lamblia genome for new cyst wall proteins. *Journal of Biological Chemistry*, *278*(24), 21701–21708. https://doi.org/10.1074/jbc.M302023200

Tejman-Yarden, N., Millman, M., Lauwaet, T., Davids, B. J., Gillin, F. D., Dunn, L., Upcroft, J. A., Miyamoto, Y., & Eckmann, L. (2011). Impaired Parasite Attachment as Fitness Cost of Metronidazole Resistance in Giardia lamblia. *Antimicrobial Agents and Chemotherapy*, *55*(10), 4643–4651. https://doi.org/10.1128/AAC.00384-11

Thomas, E. B., Sutanto, R., Johnson, R. S., Shih, H. W., Alas, G. C. M., Krtková, J., MacCoss, M. J., & Paredez, A. R. (2021). Staging Encystation Progression in Giardia lamblia Using Encystation-Specific Vesicle Morphology and Associating Molecular Markers. *Frontiers in Cell and Developmental Biology*, *9*(662945), 1–10. https://doi.org/10.3389/fcell.2021.662945

Vedanti, G. (2021). *Cytokinins in Giardia intestinalis*. Trent University.

Verkhratsky, A., & Burnstock, G. (2014). Biology of purinergic signalling: Its ancient evolutionary roots, its omnipresence and its multiple functional significance. *BioEssays*, *36*(7), 697–705. https://doi.org/10.1002/bies.201400024

Vermathen, M., Müller, J., Furrer, J., Müller, N., & Vermathen, P. (2018). 1H HR-MAS NMR spectroscopy to study the metabolome of the protozoan parasite Giardia lamblia. *Talanta*, *188*, 429–441. https://doi.org/10.1016/j.talanta.2018.06.006

Voller, J., Béres, T., Zatloukal, M., Džubák, P., Hajdúch, M., Doležal, K., Schmülling, T., & Miroslav, S. (2019). Anti-cancer activities of cytokinin ribosides. *Phytochemistry Reviews*, *18*(4), 1101–1113. https://doi.org/10.1007/s11101-019-09620-4

Wang, C. C., & Aldritt, S. (1983). Purine salvage networks in Giardia Lamblia. *Journal of Experimental Medicine*, *158*, 1703–1712.

Xu, F., Jex, A., & Svärd, S. G. (2020). A chromosome-scale reference genome for Giardia intestinalis WB. *Scientific Data*, *7*(1). https://doi.org/10.1038/s41597-020-0377-y

Yichoy, M. (2009). *Lipid Uptake and Metabolism in the Parasitic Protozoan Giardia lamblia.* https://digitalcommons.utep.edu/open_etd/387

Yichoy, M., Duarte, T. T., De Chatterjee, A., Mendez, T. L., Aguilera, K. Y., Roy, D., Roychowdhury, S., Aley, S. B., & Das, S. (2011). Lipid metabolism in Giardia: A post-genomic perspective. *Parasitology*, *138*(3), 267–278. https://doi.org/10.1017/S0031182010001277

Zhu, J. H., & Javid, B. (2015). Tuberculosis: Hey There, Lonely Guy! *Molecular Cell*, *57*(6), 951–952. https://doi.org/10.1016/j.molcel.2015.03.004